2013

Defining neurochemical properties and functions of primary sensory neurons in the rat trigeminal ganglion

Triner, Joceline Clare

Copyright Statement

Defining neurochemical properties and functions of primary sensory neurons in the rat trigeminal ganglion

by

JOCELINE CLARE TRINER

A thesis submitted to the University of Plymouth

in partial fulfilment for the degree of

DOCTOR OF PHILOSOPHY

School of Biomedical and Biological Sciences

Faculty of Science and Technology

April 2013

Abstract

Joceline Clare Triner

Defining neurochemical properties and functions of primary sensory neurons in the rat trigeminal ganglion

The trigeminal ganglion (TG) is a complex sensory structure and multiple lines of evidence suggest that significant differences exist in anatomical, neurochemical and physiological properties between it and its equivalent structure in the somatosensory system, the dorsal root ganglion (DRG). This is likely to be a reflection, first on the unique areas of tissue innervation of the TG and second, on the unusual responses to injury which give rise to distinct pain symptoms such as toothache, migraine and temporomandibular joint disorders. In an attempt to address this disparity in knowledge, we have carried out an in-depth *in vivo* study investigating neurochemical populations and cell size distributions of sensory neurons within the rat TG. We have performed a detailed analysis of expression patterns for receptor components of important inflammatory mediators, NGF (TrkA), TNFα (p55) and IL-6 (gp130), along with the thermo-transducers TRPV1 and TRPM8. For each analysis we have compared our findings with those of the rat DRG.

We have shown a significantly larger population of NF200+ neurons within the TG (51%) compared to the DRG (40%), and most interestingly, the majority of NF200+ neurons in the TG were within the small to medium cell size range, conferring a nociceptive phenotype. We have for the first time, determined expression of p55 and gp130 protein levels within neurochemically defined subpopulations of the TG. We show that a large proportion (33%) of TG neurons, in particular 27% of NF200+ neurons co-express p55, and thereby have the potential to respond directly to TNFα. Furthermore, we have observed gp130 protein expression to be ubiquitous within the TG, suggesting all neurons, including non-nociceptors, could respond to IL-6.

In addition, we have utilised biochemical and electrophysiological techniques *in vitro* to measure the functional outcome of exposure of TG neurons to IL-6. We have demonstrated that IL-6 activates the JAK/STAT signalling pathway, preferentially within NF200+ neurons. Furthermore, we have shown that IL-6 sensitises the response of TG neurons to the TRPV1 agonist capsaicin, altering the gating properties and prolonging the opening time of the channel.

Taken together, our findings support the emerging picture of a complex combinatorial pattern of co-expression of sensory neurochemicals, transducers and receptor components that help to define TG neuronal modality and function. We would advocate caution in making generalisations across sensory ganglia in particular in extrapolating data from the DRG to the trigeminal ganglion.

List of Abbreviations

CAPS	Capsaicin
CGRP	Calcitonin gene related peptide
CNS	Central nervous system
DAPI	4’,6-diamidino-2-phenylindole
DRG	Dorsal root ganglion
EIA	Enzyme immunoassay
Gab1	Grb2-associated binder-1
Gp130	Glycoprotein 130
HBSS	Hank’s Balanced Salt Solution
HE-TRPV1	High Expressing TRPV1
IB4	Isolectin B4
IL-6	Interleukin 6
IL-6Rα	Interleukin 6 receptor alpha
NF200	Neurofilament 200
NGF	Nerve growth factor
P55	High affinity receptor for TNFα
pA	Picoampere
PBS	Phosphate buffered saline
pF	Picofarad
PKCδ	Protein kinase C-delta
PNS	Peripheral nervous system
pSTAT3	Phosphorylated STAT3
STAT3	Signal transducer and activator of transcription 3
TG	Trigeminal ganglion

TN	Trigeminal nerve
TNFα	Tumour necrosis factor-alpha
TrkA	Tropomyosin-related kinase A
TRPM8	Transient receptor potential melastatin type 8
TRPV1	Transient receptor potential vanilloid 1
TRPV2	Transient receptor potential vanilloid 2
V1	Ophthalmic branch of the trigeminal nerve
V2	Maxillary branch of the trigeminal nerve
V3	Mandibular branch of the trigeminal nerve
VBSNC	Trigeminal brainstem sensory nuclear complex

List of Contents

List of Figures and Tables

Acknowledgements

First and foremost, I would like to thank my primary supervisor **Dr Stephen Thompson**, for all his support and guidance over the past few years and for his great sense of humour which has helped to keep me (almost) sane throughout this episode of my life!

To my second supervisor, **Dr Jon Bennett**, I would like to thank for all his support and encouragement during the last few years and for his calming influence in times of stress.

To **Dr Kathryn Yuill**, thank you for being my long-suffering guru in the 'world' of e-phys – thank goodness for Crunchie bars!

To **Holly Hardy** for her great work on TRPM8 and for her dedication and enthusiasm – thank you.

I must also thank **Lynne Cooper**, who has been a life saver during my harrowing days of primary cell culture – for all her snippets of advice whilst waiting for the kettle to boil!

To my **friends** on the 4th and 8th floor of Davy – thank you for your help, friendship, cakes and for just being there during this rollercoaster of a journey.

And, last but by no means least, to **my family**. You have all been amazing and have always been there for me, encouraging and supporting. I could not have done this without you all – my eternal thanks.

Author's declaration

At no time during the registration for the degree of Doctor of Philosophy has the author been registered for any other University award without prior agreement of the Graduate Committee.

No work submitted for a research degree at Plymouth University may form part of any other degree either at the University or at another establishment.

This study was financed by the University of Plymouth and the Peninsula Dental School.

A programme of advanced study was undertaken, and all work presented in this thesis was carried out by Joceline Clare Triner.

Publications and presentations:

November 2010	Poster presentation at Society for Neuroscience conference, USA
December 2010	Oral presentation at Peninsula Dentistry School Research Day, UK
March 2011	Oral presentation at Peninsula College of Medicine and Dentistry conference, UK
April 2011	Oral presentation at Centre for Research in Translational Biomedicine Research Day, UK
August 2011	Oral presentation at Life Beyond the PhD conference, UK
September 2011	Oral presentation for the Senior Colgate Prize at the British Society for Oral and Dental Research conference, UK
December 2011	Oral presentation and workshop for the Peninsula Dentistry School, UK

Conferences Attended:

August 2010	International Association for the Study of Pain, Montreal, Canada
November 2010	Society for Neuroscience, San Diego, USA
March 2011	Peninsula College of Medicine and Dentistry, Torquay, UK
August 2011	Life Beyond the PhD, Windsor, UK
September 2011	British Society for Oral and Dental Research, Sheffield, UK

Word count of main body of thesis: 42,974

Signed: ……

Date: ……

1. Introduction

1.1. Encoding senses

The environment around us is constantly providing all our senses with a diverse range of stimuli and the question of how this information is integrated and interpreted has long been a fascination to many scientific disciplines. Our ability to sense stimuli from the surrounding environment as well as to monitor internal parameters is fundamentally important to our survival (Lechner and Siemens, 2011). Selective evolutionary pressure has therefore driven the acuity of the sensory nervous system towards accurately discriminating between diverse types of sensation (see Frings, 2009). This has led to the existence of phenotypically and functionally specialised sensory neurons which are finely tuned to respond to specific sensory modalities (Frings, 2009, Lallemend and Ernfors, 2012).

Over the past 130 years, two main theories have been proposed to explain how the sensory nervous system encodes environmental stimuli into a final perceived sensation. In the late 19th century three scientists, Magnus Blix, Alfred Goldscheider and Henry Donaldson put forward their specificity theory suggesting a direct relationship between the stimulus, receptor, afferent nerve and the percept, with each sensory modality being processed along specific labelled lines (see Norrsell *et al.*, 1999). Secondly, the pattern theory, as exemplified in the gate control theory of pain, proposed that afferent fibres respond to a host of stimulus modalities and that the final percept depends upon the summation of inputs from various primary sensory afferents together with the brains interpretation and modulation of these patterns of activity (Melzack and Wall, 1962, 1965).

Over the past few decades, great progress has been made in understanding how distinct modalities are encoded. The theory of population coding is now emerging which encompasses elements from both the specificity and pattern theories (Ma, 2010). The population coding theory hypothesises that different modalities are selectively processed along specific labelled lines, but in addition, that crosstalk, which can often be antagonistic, occurs between labelled lines within the CNS (Craig, 2003, Ma, 2010, Prescott and Ratté, 2012). Moreover, an important feature of this theory is that activation of a nerve fibre by a particular stimulus may not necessarily correlate with the sensation perceived (see Ma, 2010). This paradox between stimulus and percept is exemplified during the processing of nociceptive information, as outlined below, and gives weight to the theory of population coding.

1.2. Nociception and pain

The term nociception was first used at the beginning of the 20th century by Charles Sherrington (1906) who suggested that any stimuli capable of injuring tissue be labelled 'noxious' and devised the terms 'nociception' and 'nociceptor' to define unique activity by selective afferents (see Perl, 2011). Since this time, the nociceptive system has been recognised as a discrete system responsible for the processing of noxious information and for the perception of pain (see Norrsell *et al.*, 1999). However, to this day, pain perception remains an enigma, differing from the other senses, not only due to the particularly labile nature of the nociceptive system, but also as a result of the emotional component involved in the processing of nociceptive information (Craig, 2003, Colvin, 2006).

Under normal circumstances, the sensory experience of pain is the expected outcome following activation of nociceptors by high threshold mechanical and

thermal stimuli and by algesic chemical modulators. The experience of pain under normal conditions serves a useful biological function. Short term sensitisation of nociceptors may result in physiological enhancement of pain perception enabling the injured part to be protected and allowing time for the healing process (Colvin, 2006). However, if sensitisation is prolonged, the plasticity of the nociceptive system can lead to pathological chronic pain conditions offering no biological advantage, and increasing suffering (see Woolf and Mannion, 1999(b)). Furthermore, mechanisms distinguishing the transition from acute to chronic pain are presently poorly understood. Currently chronic pain is often diagnosed based on temporal cut-offs, however, clinical experience suggests the transition is more accurately defined by an uncoupling between the observed pathology and the perceived pain, and decreased responsiveness to acute pain therapy (see Reichling and Levine, 2009). One of the central goals in the study of pain mechanisms therefore is to understand how chronic pain is maintained or persists (see Costigan and Woolf, 2000).

Following injury, the inflammatory process produces profound changes to the chemical milieu surrounding the peripheral terminals of nociceptors. Inflammatory mediators such as cytokines, chemokines, kinins, purines, protons and neurotrophins are released from injured tissue, activated nociceptors or non-neural cells such as immune cells and keratinocytes. Nociceptors express transducer proteins at their peripheral terminals which are gated by specific noxious temperatures, chemicals or mechanical forces. Inflammatory mediators can act either directly or indirectly to sensitise nociceptors via these transducer proteins (see Basbaum *et al.*, 2009).

Sensitisation may occur via reductions in the threshold for activation of membrane transducers resulting in an increase in the excitability of the terminal membrane or by the increased expression of transducer proteins or both (see Basbaum *et al.*, 2009).

Subsequent to sensitisation, nociceptors change from being exclusive detectors of noxious stimuli to being detectors of innocuous stimuli (see Woolf and Ma, 2007). Furthermore, activity evoked by nociceptors can induce a state of central sensitisation within the spinal cord whereby aberrant processing of sensory information can underlie such clinical states as hyperalgesia (an exaggerated or prolonged response, disproportionate to the noxious stimuli), and allodynia (pain in response to a previously innocuous stimuli) (see Coutaux *et al.*, 2005). These key mechanisms of neuronal plasticity in response to tissue damage are now well established and have been extensively reviewed over the past 20 years (Woolf and Costigan, 1999(a), Hill, 2001, Lewin *et al.*, 2004, Woolf, 2004, Coutaux *et al.*, 2005, Woolf and Ma, 2007, Basbaum *et al.*, 2009, Ringkamp and Meyer, 2009, Woolf, 2011, Sandkühler and Gruber-Schoffnegger, 2012).

In summary, the schematic in Figure 1-1 illustrates the key mechanisms of peripheral and central sensitisation as follows: (A) Peripheral sensitisation (PS) – (1) Injury to and inflammation of tissue results in profound changes to the chemical milieu surrounding the peripheral terminals of nociceptors. Inflammatory mediators such as NGF, TNFα and IL-6, are released from injured and inflammatory cells and bind to their cognate receptors on the peripheral terminals of nociceptors. (2) Inflammatory mediator-initiated signalling leads to post-translational changes to pre-existing transducer proteins and ion channels on the nociceptor terminal. For example, activation of TrkA by NGF activates the PLC/PKC signalling pathway resulting in the phosphorylation and sensitisation of TRPV1 to subsequent stimuli. In addition, activation of TrkA leads to an increase in TRPV1 expression via the PI3K/PKC signalling pathway. (3) The sensitisation and increased expression of TRPV1 augments the inward sodium current in the nociceptor terminal such that a depolarising stimulus produces greater excitation, thereby lowering the activation

threshold of these neurons. (3) These changes produce a state of heightened sensitivity within the nociceptor terminal such that further noxious or innocuous stimuli now produce exaggerated or prolonged responses. (4) PS manifests as hyperalgesia at the site of injury (primary hyperalgesia).

(B) Central sensitisation (CS): (1) Afferent peripheral sensory neurons terminate on wide dynamic range cells (WDRC) within the CNS. Following PS, WDRCs receive enhanced input from sensitised nociceptors. (2) Enhanced nociceptor input triggers the recruitment of ionotropic *N*-methyl-D-aspartate (NMDA) receptors, leading to temporal summation and the phenomenon of windup within the WDRC. This results in a progressively increasing output during the course of a train of identical stimuli. In addition, enhanced nociceptor input increases α-amino-3-hydroxy-5-methyl-4-isoxazolepropionic acid (AMPA) receptor conductance and enhances levels of AMPA receptor expression. These modifications result in an increase in synaptic efficacy lasting long after the end of the conditioning stimuli (long term potentiation (LTP)). (3) Inflammatory mediator-initiated signalling results in an elevated release of synaptic modulators such as neuropeptides, which contribute to the sustained depolarisation of WDRCs. (4, 5) The majority of synaptic input to neurons is sub-threshold, acting subliminally either because the synaptic input is too weak or that membrane excitability is controlled by inhibitory inputs. However, following PS and CS, the increase in membrane excitability of WDRCs means that normally sub-threshold inputs can be brought to threshold, such that previously innocuous, light touch, input from Aβ-fibers is now perceived as pain. (6) CS manifests as secondary hyperalgesia (hyperalgesia at the site of injury and outside of the site of injury) and allodynia.

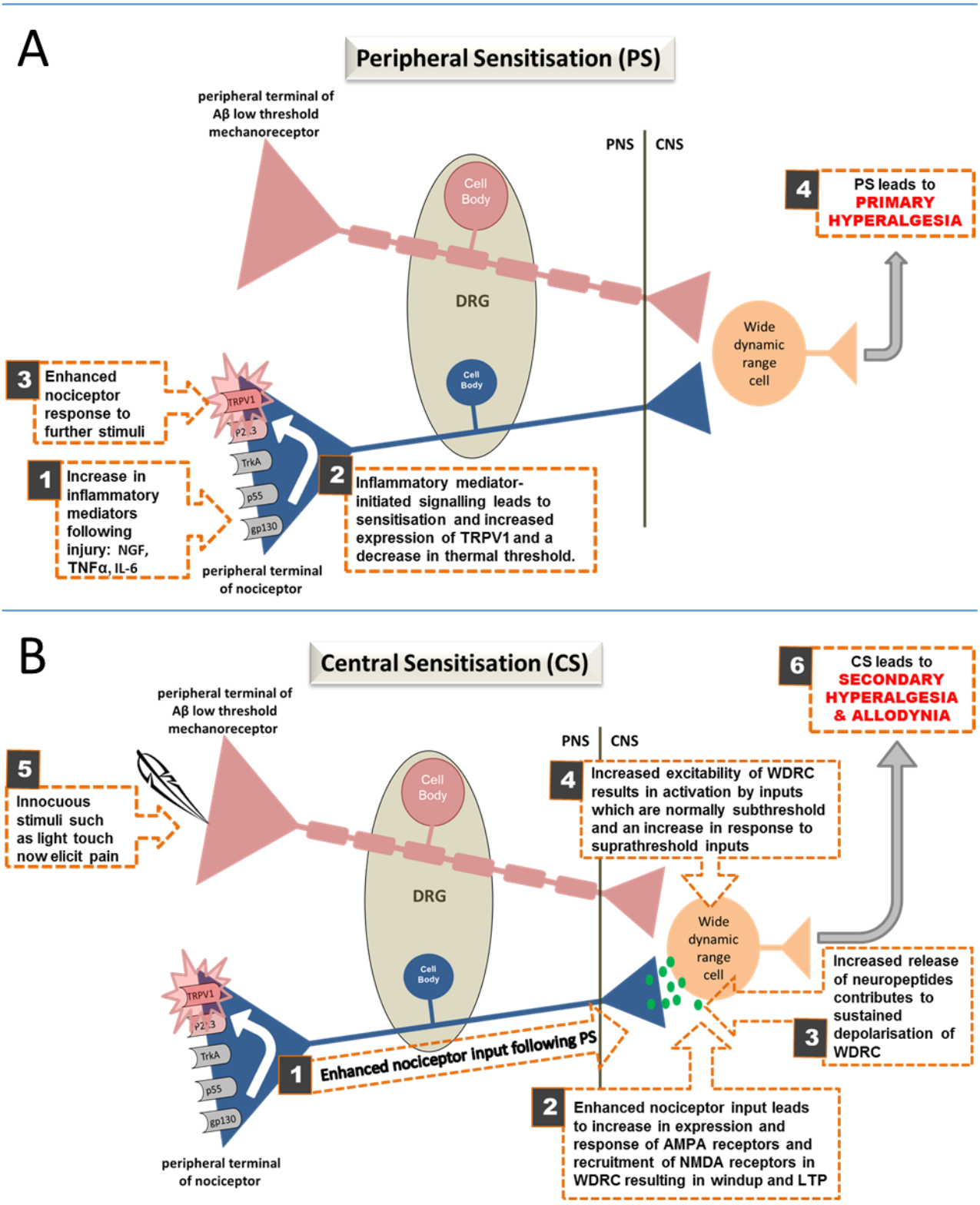

Figure 1-1: Schematic illustrating (A) peripheral sensitisation and (B) central sensitisation (see text for further details). AMPA – α-amino-3-hydroxy-5-methyl-4-isoxazolepropionic acid receptor; CNS - central nervous system; CS - central sensitisation; DRG - dorsal root ganglion; LTP – long term potentiation; NMDA – *N*-methyl-D-aspartate receptor; PNS - peripheral nervous system; PS - peripheral sensitisation; WDRC - wide dynamic range cell.

Hypersensitivity may not always resolve itself, and pain may continue to be intense and often unremitting, becoming physiologically and psychologically debilitating. Under these circumstances, pain, as an acute warning and protective mechanism, has outlived its usefulness (see Basbaum *et al.*, 2009). A recent review by Tracey *et al*. (2009) used neuroimaging studies to investigate chronic pain. Not only do they highlight the huge financial burden to society due to chronic pain, estimated at over €200 billion per annum in Europe and $150 billion per annum in the USA, but also suggest that chronic pain could be a disease state in its own right. White *et al.* (2005) suggest that chronic pain is one of the most intractable and widespread conditions in addition to having a low treatment success. Furthermore, they highlight the role of cytokines and chemokines involved in the inflammatory process as an important mechanism in the development of chronic pain.

The vital role of inflammatory mediators in establishing many chronic pain conditions has also been recognised in recent epigenetic studies. Histone deacetylase (HDAC) inhibitors have been shown to significantly improve symptoms of certain inflammatory diseases (Chung *et al.*, 2003, Leoni *et al.*, 2005, Glauben *et al.*, 2006). The effects of these inhibitors are believed to be mediated through suppression of crucial pro-inflammatory cytokines such as TNFα (Leoni *et al.*, 2002). Indeed, the levels of inflammatory mediators such as TNFα, have been found to correlate with pain severity in patients with chronic pain conditions (see Reichling and Levine, 2009), and TNFα has been linked to neuropathic pain (Moalem and Tracey, 2006, Calvo *et al.*, 2012). Interestingly, the constitutively expressed TNFα receptor, p55, was demonstrated to have a major role in the development of chronic hyperalgesia (Sommer *et al.*, 1998). In addition, patients suffering from complex regional pain syndrome are shown to have significantly increased levels of both TNFα and IL-6 in blister fluid from affected areas (Heijmans-Antonissen *et al.*, 2006). Moreover, IL-6

has been shown to contribute significantly towards the pathogenesis of chronic pain (Zanjani *et al.*, 2010).

Another important inflammatory mediator is now known to be nerve growth factor (NGF) and its mode of action typifies the mechanism of sensitisation of peripheral nociceptor terminals. NGF is a member of the neurotrophin family of proteins, originally identified as promoters of neuronal development and survival (Reichardt, 2006). However, NGF expression continues into adulthood and is now thought to contribute to the expression of a normal neuronal phenotype (Ritter *et al.*, 1991). In addition, it is considered to have a direct role as a mediator of peripheral sensitisation in chronic inflammatory states (Dmitrieva and McMahon, 1996) and an indirect role via mast cell degranulation (De Simone *et al.*, 1990). The interest in NGF as a key inflammatory mediator has grown. Several studies have demonstrated increased levels of NGF upon inflammation and its contribution to inflammatory pain (Woolf *et al.*, 1994, Lowe *et al.*, 1997, Halliday *et al.*, 1998, Kasai *et al.*, 1998, Oddiah *et al.*, 1998).

Furthermore, disruption within the central nervous system (CNS) such as deficiencies in noradrenergic inhibitory pathways have been linked with pain chronicity (Baron *et al.*, 2012), along with the activation of microglia, suggested to be the driving force of chronic pain (see Guo and Schluesener, 2007). Indeed, the important role of non-neuronal cells in pain processing within the CNS is becoming widely recognised. For instance, activated microglia release inflammatory mediators such as TNFα and IL-6, which induce a state of hyperexcitability within the CNS pain signalling pathways (see McMahon and Malcangio, 2009). However, the importance of ongoing peripheral input to the maintenance of chronic pain is also widely recognised (see Gold and Gebhart, 2010), hence the continuing emphasis on the peripheral nervous

system for the development of drug strategies (Liu *et al.*, 2011a). Nevertheless, evidence suggests that peripheral and central mechanisms of persistent pain are intrinsically linked. For instance, in a model of masseter muscle inflammation, activation of NMDA receptors on central terminals of TG neurons and resultant hyperalgesia, was dependent on glial cell activation and subsequent release of pro-inflammatory cytokines (Guo *et al.*, 2007). Since NMDA receptors are fundamental to activity-dependent synaptic plasticity and persistent pain (see Thompson, 2009), this would suggest that both peripheral and central mechanisms are required for the maintenance of chronic pain. Furthermore, the labile nature of the nociceptive system highlights the complication of attempting to apply theories of encoding to sensory neurons. Under normal conditions, a line-labelled system may well function, however the diverse responses by sensory neurons to inflammatory mediators, would negate the idea of a line-labelled system, and offer support to the theory of population coding (Craig, 2003, Ma, 2010).

Much of our understanding on the mechanism of pain has been derived from studies on somatic nociceptors whose somata lie within the dorsal root ganglia (DRG). Therefore, an extremely well established characterisation of the neuronal phenotype within the DRG now exists (see Basbaum *et al.*, 2009). Nociceptive information from the face and oral tissues is relayed to the central nervous system via sensory neurons within the trigeminal ganglia (TG). In contrast to the somatosensory system, there is relatively less information regarding sensory neuron properties and their responses within the trigeminal system (Sessle, 2005). This relative lack of knowledge has been exacerbated by the fact that chronic craniofacial pain models have been slow to appear (Sessle, 2005). However, although there are similarities between the DRG and the TG, emerging evidence appears to be highlighting differences in anatomical, physiological and neurochemical properties.

Moreover the orofacial region is the site of some of the most common pains in the body and is also an area with special emotional and psychological meaning to the patient, making effective treatment of pain difficult (Sessle, 2000). Furthermore, there are particular structures within the oral cavity, such as the tooth pulp, that have unique developmental and innervation properties (Sessle, 2005). In addition there are a number of painful chronic oral conditions such as atypical trigeminal neuralgia, malignant neoplasms and burning mouth syndrome (Scully, 2008). These relatively common conditions, with a population prevalence reported to be between 4.5% - 15% (Bergdahl and Bergdahl, 1999; LeResche and Drangsholt, 2008), can only be effectively treated once the mechanisms underlying orofacial pain are fully understood (Woolf *et al.*, 1998).

1.3. Classification of sensory neurons

In an attempt to specify a line-labelling system of primary afferent neurons, it has been the tradition in the field of sensory neurobiology to classify sensory neurons into functional sub-populations by the use of certain phenotypic, neurochemical and physiological characteristics (Priestley, 2009). Various attributes such as extent of myelination, cell body size, conduction velocity (CV), electrophysiological responses, neurochemical phenotype and neurotrophin receptor expression have been used to describe functionally distinct subpopulations of sensory neurons (Zotterman, 1939, Harper and Lawson, 1985, Lawson and Waddell, 1991, Mense, 2009, Ringkamp and Meyer, 2009). More recent advances in molecular studies and transgenic technology have provided further data that strongly support the presence of modality-specific sets of sensory neurons (see Liu *et al.*, 2011a). Axon diameter and extent of myelination was first recognised as being of physiological importance in the early

1930's when it was found that nerve fibres fell into size groups and displayed different physiological characteristics (see Duncan, 1934). It is now known that the extent of myelination determines the nerve's CV (see McGlone and Reilly, 2010) and several classes of sensory afferent nerves are now recognised. These are (in rat): Aα fibres which are thickly myelinated (20 μm diameter) and have the fastest CV (70-120 m/s); Aβ fibres which are less thickly myelinated (10 μm diameter) and have a fast CV (35-75 m/s); Aδ fibres which are thinly myelinated (2.5 μm diameter) and have an intermediate CV (4-30 m/s); and C fibres which are unmyelinated (1 μm diameter) and have a slow CV (0.3-1.5) (Coutaux *et al.*, 2005) (see Table 1-1).

With the use of additional anatomical, physiological and neurochemical data, four general functional sub-populations of sensory neurons within the DRG have now been described. Approximately 40% of the DRG neurons conduct in the Aα/β range, are thickly myelinated, with the majority having medium to large sized cell bodies (>500 μm²), and have been physiologically classified as low threshold mechanoreceptors or proprioceptors. These neurons are neurochemically distinguished by their expression of the phosphorylated heavy chain (200kDa) neurofilament (NF200) (Michael and Priestley, 1999). A further 40% of DRG neurons constitutively express neuropeptides and are identified by their expression of calcitonin gene-related peptide (CGRP). The majority of these have small cell body size (<500 μm²), are mostly unmyelinated C fibre nociceptors and are termed peptidergic nociceptors (Price and Flores, 2007). A group of neurons overlap with the previous two groups with regard to their neurofilament and neuropeptide properties. These neurons express NF200 and CGRP, are thinly myelinated with small-to-medium sized cell bodies (<1100 μm²), and are mostly Aδ high threshold mechanoreceptors (see McMahon and Priestley, 2005). A final 30% of DRG neurons are identified for their binding of isolectin-B4 (IB4) from the plant *Griffonia*

simplicifolia. The majority do not express neuropeptides, have small cell body size and are mostly unmyelinated C fibre nociceptors, termed non-peptidergic nociceptors (Fang *et al.*, 2006). However, approximately 10% of this group overlaps that of the peptidergic nociceptors by expressing low levels of neuropeptides (McMahon and Priestley, 2005).

Table 1-1: Classification of cutaneous somatosensory neurons in rat into functional sub-populations based on extent of myelination, conduction velocity and cell body size.

Class	Axonal diameter (μm)	Conduction velocity (m/s)	Cell body size (μm²)	Modality
Myelinated				
Aβ	6-12	35-75	Large >1100	Low-threshold mechanoreceptors
Aδ Type I	1-5	4-30	Medium 500-1100	Mechanically sensitive, cold, noxious, thermal, gentle cooling
Aδ Type II	1-5	4-30	Medium 500-1100	Mechanically insensitive, cold, noxious, thermal, gentle cooling
Unmyelinated				
C-pain	0.3-1.5	0.4-2	Small <500	Noxious, heat, thermal
C-tactile	0.3-1.5	0.4-2	Small <500	Light stroking, gentle touch
C-warm/cool	0.3-1.5	0.4-2	Small <500	Gentle warming or cooling

Further distinction can be made when examining the expression of neurotrophin receptors and transducer proteins. For instance, neurotrophin receptor expression within peptidergic and non-peptidergic populations is strikingly different. The majority of peptidergic neurons express trkA, the receptor for NGF, and approximately 20% of these also express NF200 and are thought to correspond to the population of Aδ high threshold mechanoreceptors. Non-peptidergic neurons however, respond to glial cell line-derived neurotrophic factor (GDNF) by the expression of its receptor components GFRα1 and GFRα2 along with its co-receptor molecule Ret (McMahon and Priestley,

2005). Expression of one or more of the thermo-sensitive family of transient receptor potential ion channels (TRPV1, TRPV2, TRPA1) may also confer certain functional distinctions to neuronal populations. TRPV1 is gated in response to noxious heat (>43°C), capsaicin and protons (Caterina and Julius, 2001), and TRPA1 by noxious cold (<18°C) and pungent isothiocyanate compounds (Huang *et al.*, 2006b). TRPA1 is frequently co-expressed with TRPV1 in both peptidergic and non-peptidergic nociceptors (Guo *et al.*, 1999, Michael and Priestley, 1999, Kobayashi *et al.*, 2005) conferring a polymodal function to these nociceptors. Such co-expression may explain the paradoxical burning sensation of extreme cold (Tominaga and Caterina, 2004, Huang *et al.*, 2006b). The high threshold vanilloid receptor homologue (TRPV2) gated by temperatures above 52°C, is expressed on a population of Aδ high threshold mechanoreceptors co-expressing NF200, CGRP and trkA (Caterina *et al.*, 1999) again conferring a polymodal function to this population of nociceptors.

However, using such classifications as a way of conferring modality specificity to neuronal sub-populations is now becoming recognised as a considerable oversimplification. For instance, in the rat, about 20% of fibres conducting in the Aα/Aβ range are nociceptors (Djouhri and Lawson, 2004). Conversely, cutaneous non-nociceptors conduct across all CV ranges (Perl, 1992, Lawson, 2002). Indeed, in studies on rat DRG, 19% and 12% of cells conducting in the Aδ and C ranges respectively were non-nociceptors (Fang *et al.*, 2005). The use of cell body size alone as an indicator of function can also be misleading. Although small cell size indicates a higher probability of nociceptive function, some neurons within the large cell size range are nociceptive (Harper and Lawson, 1985). A significant number of C-fibres have been found to express markers for both peptidergic and non-peptidergic populations and are responsive to NGF and GDNF (Bennett *et al.*,

1998(b), Michael and Priestley, 1999, Fang *et al.*, 2006). Furthermore, a large number of so-called non-peptidergic sensory neurons identified by their binding of IB4, express trkA and neuropeptides (Kashiba *et al.*, 2001).

TRPA1, which was originally described as being only present in TRPV1 expressing neurons, is now accepted as being more widely distributed with 40% of total rat DRG profiles showing expression of TRPA1 (Kobayashi *et al.*, 2005). However, with only 7-25% of neurons responding to temperatures below the activation threshold for this transducer, it has been suggested that additional mechanisms may be involved in the transduction of cold stimuli including the possibility of inhibitory modulation (Reid and Flonta, 2001). Alternatively, there may be a requirement for the combinatorial co-expression of ion channels and transducers, in order for response to cold stimuli to occur (see Belmonte and Viana, 2008).

TRPM8 belongs to the thermo-sensitive family of transient receptor potential ion channels and is activated by cooling (<25°C). TRPM8 and TRPA1 are purported to be major ion channels sensing cool and cold temperatures respectively (Huang *et al.*, 2006b). The controversy over the expression of TRPA1 has raised the question of organ-specific differences in TRP-mediated detection of cold, with the suggestion that TRPM8 is responsible for this function within the somatosensory system, whilst the vagal system uses TRPA1 to report cold temperatures (see Lechner and Siemens, 2011). The role of TRPA1 in cold sensation has been further questioned in a study using selective blockade of TRPA1 channels (Chen *et al.*, 2011). They found that noxious cold sensation was unaffected under normal conditions and suggest distinct roles for TRPA1 in physiological and pathological states. This confirms the findings of a previous study that suggested TRPA1 is a mediator of cold hypersensitivity only under pathological conditions (del Camino *et al.*, 2010).

What appears to be emerging from the literature is that the perception of a single stimulus may require the expression of several transduction mechanisms or the combinatorial co-expression of receptors, transducers and ion channels, which together confer specificity (see Belmonte and Viana, 2008, Liu *et al.*, 2011a). A common feature found in sensory neurons of different modalities is the formation of a transduction complex by the co-assembly of a large number of transducer proteins. These transduction complexes confer considerable plasticity to the sensory neuron which may contribute towards differences seen in adaptation and response mechanisms depending on target innervation (see Frings, 2009). Indeed, an hypothesis is now emerging, that of peripheral regulation of neuronal phenotype (see Hargreaves, 2011). This is supported by recent studies identifying phenotypic differences in sensory neurons depending on their target tissue (see Frings, 2009, Kiasalari *et al.*, 2010, Hargreaves, 2011). Finally, a new concept is developing regarding the role of epithelial cells in sensory transduction and whether their expression of TRP channels can contribute towards the transduction of physical stimuli (Lumpkin and Caterina, 2007).

A further point to consider when applying generalisations regarding functional modalities to neuronal populations and their ultimate extension to human studies, is the variation between species in levels of expression and co-expression of molecules and transducer proteins. For example, in rats a large proportion of both peptidergic and non-peptidergic neurons express TRPV1, whilst in mice, only a minority of non-peptidergic neurons are found to express TRPV1 (see Ringkamp and Meyer, 2009). Furthermore, in mice, the distinction between peptidergic and non-peptidergic neurons is clear, whereas in rats, this distinction is more complex (Price and Flores, 2007). In studies examining the proportion of nociceptors conducting in the Aβ fibre range, values ranged from 18% - 65% depending on the species being investigated

(cat, guinea pig, monkey, mouse, rat) (see Lawson, 2002, Djouhri and Lawson, 2004). Expression of certain transducer proteins also appear to be different between species. For instance, expression of TRPA1 and TRPM8 mRNA in rat DRG was shown to be 30% and 23% respectively (Kobayashi *et al.*, 2005), however in mice DRG, it was 4% and 5-10% respectively (Peier *et al.*, 2002, Story *et al.*, 2003). Different methodologies can also lead to variations in results between studies. Of particular interest are the findings of one study investigating the variations in expression of glutaminase, TRPV1 and the voltage-gated sodium channel $Na_v1.8$ in rat DRG. Their results showed that increasing the concentration of fixative from 0.25% - 4%, significantly reduced the levels of expression in all three markers. In addition, increasing antibody incubation times from 2 h to 192 h significantly increased levels of expression in all three markers (Hoffman *et al.*, 2010). A criticism has also been made on the explosion of nucleic acid studies, focussing on mRNA expression, which often ignore the fact that sensory neurons are primarily made of protein and that the main method of communication is via electrical impulses (Costigan, 2012). The promise of quantitative peptide analysis *en masse* using mass spectrometry however, should hopefully provide us with a clearer picture of the *in vivo* state (Costigan, 2012).

It is clear from the above, that the functional classification of sensory neurons is a far more complex and perplexing process than originally thought. Much of our understanding of transduction and encoding of stimuli within the sensory nervous system is derived from studies on populations of somatosensory neurons. However, the trigeminal nervous system displays distinct organisational characteristics and unique areas of innervation which may confer distinct response mechanisms. Moreover, a more complex picture is emerging with regard to the functional classification of sensory neurons, that of a characteristic combinatorial expression

pattern of a number of receptors, transducers and ion channels, which together confer modality specificity (Belmonte and Viana, 2008). In light of these considerations, the necessity for further molecular studies on sensory neurons within the trigeminal nervous system is even greater.

1.4. Trigeminal nerve anatomy

The trigeminal nerve is the largest and most extensively distributed of the cranial nerves. It is a mixed sensory-motor nerve, transmitting sensory information from the orofacial region and motor innervation to the muscles of mastication (Norrsell *et al.*, 1999). The trigeminal nerve projects to three sensory nuclei and from one motor nucleus which extend through much of the brainstem. Central processes of the trigeminal nerve carrying sensory information enter the brainstem, synapsing on second-order neurons within the trigeminal brainstem sensory nuclear complex (VBSNC). The VBSNC extends from the midbrain to medulla with the mesencephalic nucleus within the midbrain, main sensory nucleus within the pons and spinal tract nucleus within the medulla. The spinal tract nucleus is further split into three sub-nuclei, namely oralis, interporalis and caudalis (Sessle, 1986, Lumpkin and Caterina, 2007). The main sensory nucleus mediates the tactile sensation of light touch and pressure. The mesencephalic nucleus mediates proprioceptive information controlling the strength of the bite and the spinal tract nucleus conveys sensation of pain and temperature (Colvin, 2006). The smaller motor root of the trigeminal nerve originates from cell bodies within the motor nucleus located in the upper pons, medial to the main sensory nucleus which receives sensory proprioceptive input from the mesencephalic nucleus (Lumpkin and Caterina, 2007, Mense, 2009, Fernandes *et al.*, 2012). Afferent fibres of the mesencephalic nucleus convey proprioceptive

information from the teeth, palate and temporomandibular joint to motor neurons within the motor nucleus which convey impulses to control bite force and mastication (Lechner and Siemens, 2011).

Sensory neurons throughout the VBSNC project to higher CNS centres such as the thalamus, cerebellum, superior colliculus, periaqueductal grey, reticular formation and pontine parabrachial nucleus (Sessle *et al.*, 2008). More specifically, proprioceptive and low threshold sensory information is carried to the ventral posteromedial nucleus of the thalamus via the trigeminal lemniscus, whereas nociceptive sensory information reaches the intralaminar nuclei (mediodorsalis, centralis lateralis and parafascicularis nuclei) of the contralateral thalamus via the trigeminothalamic tract. From the thalamus, trigeminal sensory information travels via the posterior limb of the internal capsule to the lateral region of the postcentral gyrus of the primary sensory cortex (Belmonte *et al.*, 1996).

Extra-cranially, the sensory component of the trigeminal nerve trunk expands forming the trigeminal ganglion (TG) which contains the cell bodies of the trigeminal sensory first-order neurons with the exception of proprioceptive afferents. Cell bodies of proprioceptive afferents are contained within the mesencephalic nucleus and are considered to be primary sensory neurons which have been retained within the central nervous system (Melzack and Wall, 1965, Siemionow *et al.*, 2011, Liu and Ma, 2011b, Fernandes *et al.*, 2012). Indeed, the mesencephalic nucleus is the only known nucleus within the CNS that contains the cell bodies of primary afferent neurons (Michael and Doufexi, 2000, Benarroch, 2011). Distal to the TG, the trigeminal nerve trifurcates to form three main branches, ophthalmic (V1), maxillary (V2) and mandibular (V3). The motor root of the trigeminal nerve bypasses the TG then re-unites with the sensory component of V3. The three main branches split to

form smaller branches as follows: V1 divides forming the frontal, lacrimal, nasociliary, tentorial and dural nerves innervating the eye, nose, paranasal sinuses and upper face; V2 divides forming the infraorbital, zygomatic, greater and lesser palatine, posterior superior alveolar and meningeal nerves innervating the middle third of the face and upper teeth; V3 divides forming five sensory branches, meningeal, lingual, auriculotemporal, inferior alveolar and buccal and five motor branches, masseteric, deep temporal, medial pterygoid, lateral pterygoid and mylohyoid. Sensory V3 nerves innervate the lower third of the face, tongue, jaw and lower teeth while motor V3 nerves innervate muscles of mastication (Norrsell *et al.*, 1999, Colvin, 2006, Lumpkin and Caterina, 2007, Lechner and Siemens, 2011, Liu and Ma, 2011b, Fernandes *et al.*, 2012). The schematic in Figure 1-2 illustrates areas of peripheral innervation, branches and central projections of the trigeminal nerve.

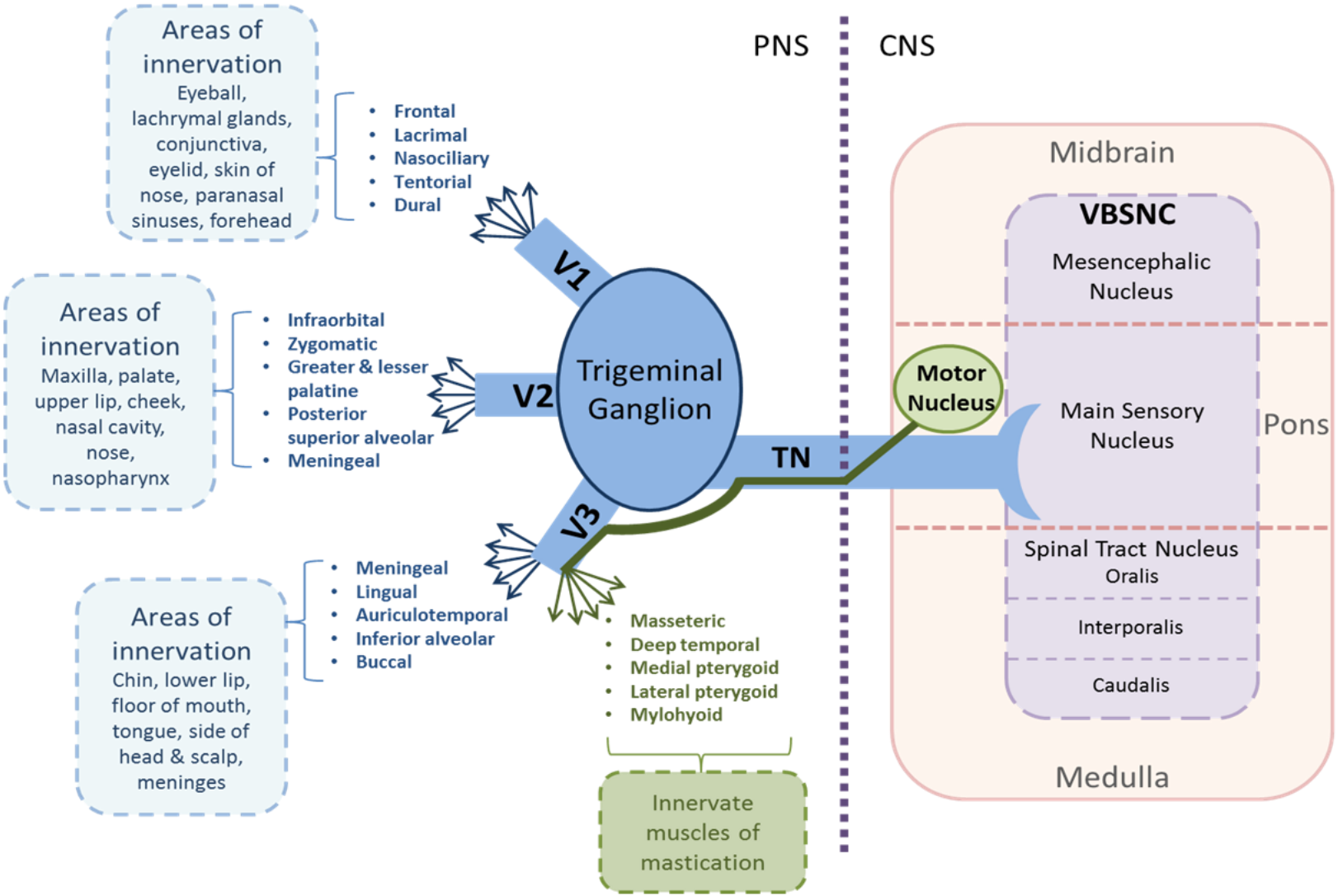

Figure 1-2: Schematic of trigeminal nerve illustrating peripheral and central projections and areas of innervation. VBSNC - Trigeminal brainstem sensory nuclear complex; TN – Trigeminal nerve; V1 – Ophthalmic branch; V2 – Maxillary branch; V3 – Mandibular branch.

1.5. Trigeminal sensory neurons

Despite awareness of the functional complexity of the trigeminal nervous system in comparison to spinal nerves (Kruger and Young, 1981), our understanding of trigeminal pain mechanisms has often relied on analogies from the spinal sensory system. There are however, a number of considerations why such mechanisms should not be extrapolated directly to the orofacial sensory system. For instance, the trigeminal nervous system displays some distinct embryonic origins and organisational characteristics along with several unique areas of innervation which will be discussed in more detail below (Bereiter *et al.*, 2009). In addition, there is growing evidence that the properties of TG nociceptors and their responses to peripheral injury are distinct from those of the DRG (Sessle, 2005, Hargreaves, 2011). Previous studies for example have suggested that the cell-size correlation (Matsuo *et al.*, 2001, Price and Flores, 2007) and expression of certain nociceptive-specific markers (Mosconi *et al.*, 2001, Kobayashi *et al.*, 2005, Price and Flores, 2007) observed in DRG nociceptors, may not be reflected in TG nociceptor populations.

The development of the sensory ganglia involves migration of precursor cells to the site of ganglion formation and differentiation of sensory neurons. There is a significant difference however, between the development of sensory neurons in DRG compared to TG. DRG sensory neurons are derived from neural crest cells whilst the majority of TG sensory neurons are derived from the neurogenic placodes (D'Amico-Martel and Noden, 1983, Lazarov, 2002). A further distinction is the lack of progenitor cells within the forming TG. Progenitor cells are found within developing DRGs allowing them to retain a degree of plasticity, however, TG progenitor cells

differentiate during migration and enter the forming TG as post-mitotic neurons (Blentic *et al.*, 2010). Furthermore, the TG as opposed to the DRG shows distinct somatotopic organisation whereby cell bodies of the mandibular nerve are located in the postero-lateral part of the ganglion, those of the ophthalmic nerve antero-medially, and those of the maxillary nerve between these two locations (Shellhammer *et al.*, 1984).

Nociceptors from the DRG terminate within the dorsal horn of the spinal cord. Peptidergic C fibres terminate superficially within lamina I and II outer. Non-peptidergic C fibres terminate within Lamina II inner, and finely myelinated Aδ fibres terminate within lamina I, lamina II outer and lamina V (see Basbaum *et al.*, 2009). TG nociceptors terminate within the brainstem in the VBSNC, more particularly within the most caudal region of the Vc, as previously described. The Vc is a laminated structure which resembles the dorsal horn, with nociceptor terminals most densely located within laminae I and II (see Sessle, 2000). However, the clear laminar delineations of terminals seen within the DRG are less well defined within the TG. The Vc displays a broader density of non-peptidergic C fibres which cross laminae I, II outer and II inner and overlap the terminal regions of peptidergic C fibres (see Bereiter *et al.*, 2000). Furthermore, there are unique structures within the VBSNC where nociceptor terminals have been located, namely the paratrigeminal islands. These are small nuclei located within the dorsal lateral medullary spinal trigeminal tract. These, paratrigeminal terminating nociceptors have been implicated in inflammation induced pain (Yamazaki *et al.*, 2008). A further inconsistency exists between the DRG and TG in that nociceptors also terminate within the Vi/Vc transition region, which is not a laminated structure and which has been implicated as a critical region for the processing of craniofacial pain (Bereiter *et al.*, 2000). Furthermore, a distinctive feature of the trigeminal system is the dual representation

of specialised craniofacial tissues innervated by the ophthalmic division of the trigeminal nerve. Such tissues are represented discontinuously within the Vi/Vc transition zone and Vc, in contrast to spinal nerves which project to a dominant segment (Molander and Grant, 1990, Bullitt, 1991, Bereiter *et al.*, 2000). It has been suggested that dual representation allows for parallel or redundant processing and may ensure the faithful encoding of critical sensory information.

Perhaps most importantly, the orofacial region has specialised peripheral structures such as meningeal membranes, oral mucosal tissues, cornea and tooth pulp. These structures are densely innervated by small diameter trigeminal afferents and show a marked sensitivity to chemical irritants (see Bereiter *et al.*, 2000, Sessle, 2005). Furthermore, the face has been reported to be the area with the highest distribution of sensory neurons with free nerve endings (Kawakami *et al.*, 2001). Pain is the predominant sensation evoked by stimuli to tooth pulp, an area richly innervated by Aδ- and C-fibre afferents most of which are deemed to be polymodal. Being within a highly vascular area, they would be very susceptible to sensitisation via inflammatory mediators (see Sessle, 2005). Paradoxically, although tooth pulp is richly innervated by nociceptors, stimulation can be either extremely intense, or pulpal inflammation can proceed to total necrosis without any painful symptoms being present (Narhi *et al.*, 1994).

1.6. Aim of research

Chronic orofacial pain conditions are among the commonest in the Western world (Sessle, 2000), with a prevelance in the UK of around 7% (Zakrezewska, 2010). In order to better manage orofacial pain conditions, it is important to more fully understand mechanisms of sensitisation and hyperalgesia within the trigeminal

system. Full clarification of neurochemically defined populations of TG neurons together with the pattern of distribution of inflammatory mediator receptors that form key components of the sensitisation pathway is a priority in order that defined physiological roles are ascribed to these cells.

1.7. Research objectives

- Using indirect fluorescence immunohistochemistry, to perform an in-depth analysis of neuronal populations within the TG in naïve rat using the neurochemical markers NF200, CGRP and IB4.

- Using indirect fluorescence immunohistochemistry, to perform an in-depth analysis of cell size distributions across the entire TG and within each neurochemical population in naïve rat.

- Using indirect fluorescence immunohistochemistry to perform a detailed analysis of the expression patterns of receptor components for several important inflammatory mediators, namely, NGF, TNFα and IL-6 across the entire TG in naïve rat. We will analyse the combinatorial co-expression of these receptor components within each neurochemical population in TG.

- Using indirect fluorescence immunohistochemistry to perform a detailed analysis of the expression patterns of the thermo-transducers, TRPV1 and TRPM8 across the entire TG in naïve rat. We will analyse the combinatorial co-expression of these thermo-transducers within each neurochemical population in TG.

- For each analysis we will make direct equivalent comparison with the naïve rat DRG.

- To perform *in vitro* analysis of the functional competency of the IL-6 receptor component gp130 in cultured rat TG neuronal cells by investigating the activation and phosphorylation of the downstream signalling molecule STAT3.

- Using immunocytochemistry, to examine the activation status of STAT3 in TG neuronal cells following exposure to IL-6.

- To quantify any changes in STAT3 phosphorylation in TG neuronal cells following exposure to IL-6 by Western blot analysis.

- To determine whether IL-6 was preferentially activating a specific neurochemical sub-population of TG neuronal cells.

- Using biochemical and electrophysiological outcomes we will explore mechanisms by which activation of gp130 by IL-6 might lead to the sensitisation of the thermo-transducer TRPV1 *in vitro* in rat TG neuronal cells.

- Using a CGRP-release enzyme immunoassay, to determine whether exposure of TG neuronal cells to IL-6 resulted in a change in CAPS-evoked CGRP release.

- Using whole-cell patch-clamp electrophysiological analysis to determine whether exposure of TG neuronal cells to IL-6 resulted in any change to CAPS-evoked responses.

2. Molecular biology of the trigeminal ganglion
Part 1: Neurochemistry

2.1. Introduction

Understanding the mechanisms involved in encoding somatosensory stimuli has long been a major goal in the field of neurobiology. To this end, many studies have been undertaken on sensory neurons whose somata lie within the DRG, to the extent that a well-established characterisation of neuronal phenotype now exists within this system (see Basbaum *et al.*, 2009). Traditionally, neurons have been divided into subpopulations based on their anatomy, neurochemistry and physiology as a way of assigning a specific function to a population of sensory neurons and to aid understanding of response mechanisms and the subsequent encoding of specific stimuli (see Priestley, 2009).

The neurochemical marker NF200 (phosphorylated heavy chain (200 kDa) neurofilament), has been traditionally used to identify sensory neurons which are thickly myelinated and conduct in the Aα/β fibre range with a non-nociceptive phenotype. A further neurochemical marker, CGRP (calcitonin gene-related peptide) has been used to identify sensory neurons with a nociceptive phenotype and which are classed as peptidergic and conduct within the Aδ/C fibre range. Binding of IB4 (isolectin-B4 from the plant *Griffonia simplicifolia*) identifies a third population of sensory neurons as non-peptidergic nociceptors, conducting within the C fibre range (McMahon and Priestley, 2005). In addition to these neurochemical markers, soma size has been used as a means of identification of neuronal subpopulations, such that in rat, neurons considered to have a nociceptive function generally have small

(<500 μm²) to medium (500-1100 μm²) sized cell bodies, and those with a large (>1100 μm²) soma size are generally considered to have a non-nociceptive function (Wotherspoon and Priestley, 1999).

Using these conventions of classification, it is now widely accepted that cell size distribution of DRG neurons ranges from approximately 75 μm² to 4,500-5,500 μm² (Pover *et al.*, 1992, Bosco *et al.*, 2010). Around 40% of DRG neurons are low-threshold, Aα/β fibre non-nociceptive proprioceptors or mechanoreceptors (Michael and Priestley, 1999) and a further 40% are high-threshold peptidergic Aδ/C fibre nociceptors (Price and Flores, 2007). Approximately 10% of DRG neurons co-express both NF200 and CGRP and are classified as mostly Aδ fibre high threshold mechanoreceptors (see McMahon and Priestley, 2005). A final 30% are classified as non-peptidergic nociceptors, although there is some degree of overlap with peptidergic nociceptors by the expression of low levels of neuropeptides (McMahon and Priestley, 2005).

As mentioned in Chapter 1, in contrast to the somatosensory system, there is relatively less information regarding the properties of sensory neurons and their response mechanisms within the TG (Sessle, 2005). Indeed, much of our understanding on TG sensory mechanisms has relied on extrapolating data from studies on the DRG. However, although there are similarities between the two systems, growing evidence suggests there are distinct properties and response mechanisms within the trigeminal sensory system (Sessle, 2005, Price and Flores, 2007, Hargreaves, 2011). Studies on the TG investigating phenotypic and cell size populations have been unsuccessful in agreeing with the established data for the DRG, moreover many researchers have shown contrasting results when comparing their outcomes to similar studies on the TG.

For instance, in their study on rat TG, Cho *et al.* (2009a) showed that 58.2% of TG neurons were NF200+, with CGRP+ and/or IB4+ neurons making up a smaller population of 37.2%. This was compared to their results on the DRG where 40% were NF200+ and 58% were CGRP+ and/or IB4+, in line with the accepted proportions mentioned previously. With regard to expression of CGRP in TG neurons, previous studies have shown widely differing data. For example, populations of CGRP+ neurons in rat TG have been reported as 16% (Price and Flores, 2007), 22% (Nagamine *et al.*, 2006) and 44% (Lennerz *et al.*, 2008) across the entire TG; whilst studies investigating specific subpopulations within the rat TG have reported 5% (Mosconi *et al.*, 2001), 33% (Yang *et al.*, 2006), 40% (Mori *et al.*, 1990) and 72% (Ichikawa *et al.*, 2006) in tooth pulp; 40% (Mori *et al.*, 1990) in buccal mucosa; 50% (Ichikawa *et al.*, 2006) in facial skin and 40% (Nagamine *et al.*, 2006) within the TG maxillary region. Furthermore, populations of IB4+ rat TG neurons have been reported as approximately 19% (Cho *et al.*, 2009a) and 23% (Price and Flores, 2007). These data are summarised in Table 2-1.

Cell size data for TG neurons has also proved inconsistent. For example, cell size distribution over the entire rat TG has been reported to range from 75-2800 μm² (Wotherspoon and Priestley, 1999), ~50-1800 μm² (Paik *et al.*, 2009) and 75-2550 μm² (Lennerz *et al.*, 2008); with peak frequencies between 200-400 μm² (Ichikawa *et al.*, 2006), 400-500 μm² (Wotherspoon and Priestley, 1999), 200-300 μm² (Paik *et al.*, 2009) or 314-491 μm² (Lennerz *et al.*, 2008) (see Table 2-1). Furthermore, cell size distributions for neurons innervating sub-populations of rat TG range widely and are summarised in Table 2-1 (Sugimoto *et al.*, 1988, Mori *et al.*, 1990, Wotherspoon and Priestley, 1999, Mosconi *et al.*, 2001, Fristad *et al.*, 2006, Ichikawa *et al.*, 2006, Nagamine *et al.*, 2006, Yang *et al.*, 2006, Price and Flores, 2007, Lennerz *et al.*, 2008, Cho *et al.*, 2009a, Paik *et al.*, 2009).

Therefore, in order to better understand sensory mechanisms within the trigeminal nervous system, we have conducted an in-depth study adopting conventional methods to classify neurons first of all on the basis of neurochemistry. Results on DRG from our study have concurred with the generally accepted proportions showing approximately 40% NF200+, 32% CGRP+ and 40% IB4+ neurons. We have also examined co-expression of these factors and compared our findings to established functional subgroupings within the DRG. In addition, we have determined cell size distribution profiles for all neurons within the TG and have determined neurochemical phenotypic distribution across these size distribution ranges, comparing our findings to established distribution profiles in DRG. Here again, our results on the DRG concur with those established findings. Of particular note is that our study has found significant differences in the proportions of these neuronal subpopulations and in cell size distributions within the TG compared to the DRG.

Table 2-1: Summary of NF200, CGRP and IB4 expression and cell size data in adult rat TG from previous research studies.

% Neuronal expression over entire TG	% Expression within neuronal sub-population	Cell size data over entire TG or within neuronal sub-population	Reference
58% NF200+ 37% CGRP+ and IB4+ combined			(Cho *et al.*, 2009)
16% CGRP+ 23% IB4+			(Price and Flores, 2007)
22% CGRP+	40% CGRP+ (Maxillary region)		(Nagamine *et al.*, 2006)
44% CGRP+		75-2550 μm² Peak frequency between 314-491 μm²	(Lennerz *et al.*, 2008)
	5% CGRP+ (Incisor pulp)		(Mosconi *et al.*, 2001)
	33% CGRP+ (Molar pulp)	491-2836 μm² (Molar pulp) Peak frequency between 1257-1590 μm² (Molar pulp)	(Yang *et al.*, 2006)
	40% CGRP+ (Incisor pulp) 40% CGRP+ (Buccal mucosa)		(Mori *et al.*, 1990)
	72% CGRP+ (Molar pulp) 50% CGRP+ (Facial skin)	Peak frequency between 200-400 μm² 234-1440 μm² (Molar pulp) Peak frequency between 600-800 μm² (Molar pulp) 105-1959 μm² (Facial skin) Peak frequency between 200-400 μm² (Facial skin)	(Ichikawa *et al.*, 2006)
		75-2800 μm² Peak frequency between 400-500 μm²	(Wotherspoon and Priestley, 1999)
		~50-1800 μm² Peak frequency between 200-300 μm² 50-1796 μm² (Molar pulp) Peak frequency between 400-500 μm² (Molar pulp) 67-1486 μm² (Incisor pulp) Peak frequency between 300-400 μm² (Incisor pulp)	(Paik *et al.*, 2009)
		143-2729 μm² (Molar pulp) Peak frequency between 700-900 μm² (Molar pulp)	(Fristad *et al.*, 2006)
		131-1673 μm² (Molar pulp) Peak frequency between 500-600 μm² (Molar pulp)	(Sugimoto *et al.*, 1988)

2.2. Methods

2.2.1. Animals

Experiments were conducted on eight adult naive male Sprague Dawley rats ranging from 220-250 g body weight (Charles River, Margate, UK). All procedures were conducted in accordance with the UK 1986 Animals (Scientific Procedures) Act. Animals were housed in a temperature controlled room on a 12:12 h light/dark cycle, food and water was available *ad libitum*. Following Schedule 1 killing, animals were transcardially perfused with 0.01 M phosphate-buffered saline (PBS, pH 7.4), followed by fixation with 4% paraformaldehyde in 0.2 M phosphate buffer (pH 7.4).

TG and DRG (lumbar 4 and 5) were rapidly dissected and postfixed for 2 h in 4% paraformaldehyde in 0.2 M phosphate buffer (pH 7.4), followed by overnight cryoprotection in 20% sucrose. Tissues were blocked in OCT mounting media (Tissue-Tek), snap-frozen in liquid nitrogen and stored at -80°C until required. The tissue was then cut into 8 µm sections on a Leica cryostat (CM1100), sequentially thaw-mounted onto SuperFrost Plus slides (VWR) and stored at -20°C in cryoprotection solution (30% sucrose, 30% ethylene glycol, PBS) until use. Sequential sectioning was carried out in order to eliminate biasing of counts and to ensure that sections from across the entire ganglion were represented on each slide. Figure 2-1 illustrates the process as follows: slides are labelled from 1 – 18. Section one is thaw-mounted onto slide 1, section two is thaw-mounted onto slide 2 etc. until slide 18 is reached. Section 19 is then thaw-mounted onto slide 1 and the process is repeated until slide 18. Therefore, once all sections have been cut from the TG or DRG, the sections on each slide represent areas throughout the entire ganglia.

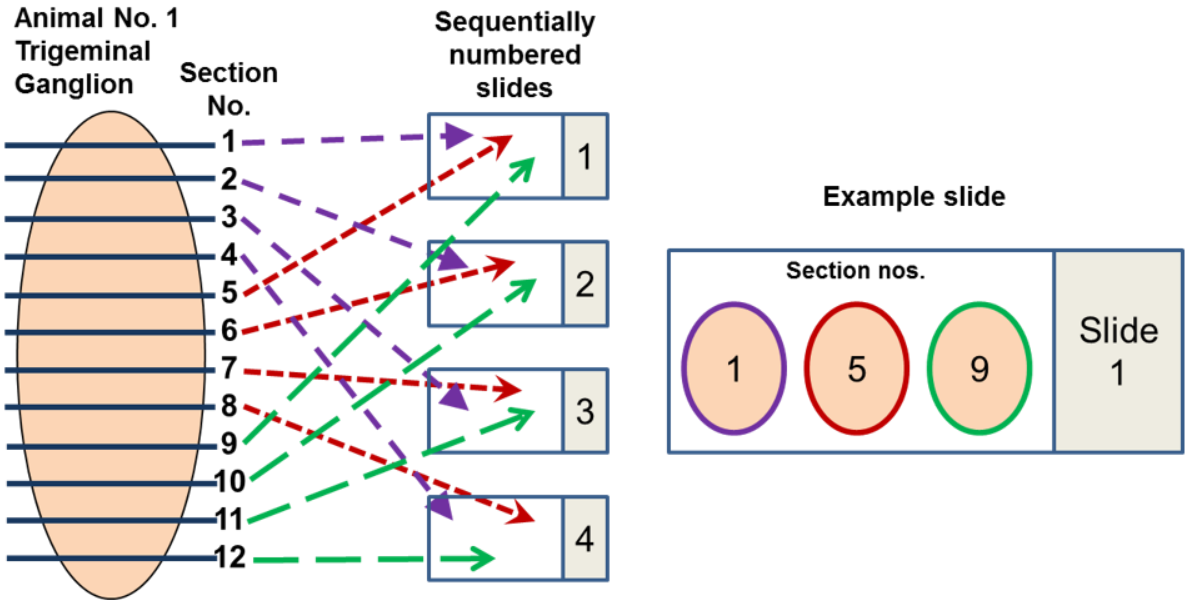

Figure 2-1: TG and DRG were fixed and blocked in mounting media and stored at -80°C. 8 µm sections were cut and sequentially thaw-mounted onto slides to ensure sections from across the entire ganglion were represented on each slide as follows: slides are labelled from 1 – 18. Section one is thaw-mounted onto slide 1, section two is thaw-mounted onto slide 2 etc. until slide 18 is reached. Section 19 is then thaw-mounted onto slide 1 and the process is repeated until slide 18.

Table 2-2: Antibodies and lectin for standard neurochemical markers used to determine neurochemical phenotypic populations in TG and DRG.

Antigen	Lectin	Host	Species reactivity	Manufacturer	Dilution used	Secondary Antibody used
NF200		Mouse	Wide range	Sigma (#N0142)	1:4,000	DαM-FITC (1:200) or DαM-AF555 (10 µg/ml)
CGRP		Sheep	Rat, human	Enzo Life Sciences (#CA 1137)	1:300	DαS-FITC (1:200) or DαS-AF555 (10 µg/ml)
	IB4-FITC			Sigma (#L2895)	10 µg/ml	n/a

2.2.2. Antibody characterisation

Table 2-2 describes the primary and secondary antibodies used in this study. The NF200, CGRP and IB4 antibodies used have been widely characterised in a number of previous studies (Wotherspoon and Priestley, 1999, Hwang *et al.*, 2005, Eftekhari *et al.*, 2010, Kiasalari *et al.*, 2010). Specificity for secondary antibodies was

confirmed by omitting primary antibodies from immunohistochemical protocols. No labelling was observed under these conditions.

2.2.3. Immunohistochemistry

Indirect dual immunofluorescence was performed using NF200, CGRP and IB4 to determine levels of expression and co-expression of these neurochemical phenotypic markers. The sources, characteristics and dilutions of the primary and secondary antibodies used are listed in Table 2-2. All antibodies were made up in 5% donkey serum (Sigma (#D9663)) in 0.01 M PBS (Sigma (#P4417)) / 0.2% Triton X-100 (Sigma (#T8787)) / 0.1% Azide (Sigma (#S2002)). All experiments were carried out in at least 3 animals, and were duplicated concurrently under identical conditions in both TG and DRG. The slides were placed in a Coplin jar on an orbital shaker and washed 3 X 10 min in PBS. A well was formed around tissue sections using a PAP pen (Sigma (#Z377821)). Slides were then placed in a humidity chamber at room temperature and blocked for 1 h in 10% donkey serum (in 0.01 M PBS/0.2% Triton X-100/0.1% Azide). The slides were washed 3 X 10 min in PBS, placed in a humidity chamber, incubated with primary antibodies and left overnight at room temperature. Following this, the slides were again washed 3 X 10 min in PBS, placed in a humidity chamber, incubated with secondary antibodies and left for 3 h at room temperature. Slides were then washed 3 X 10 min in PBS, placed in a humidity chamber and stained with DAPI (Sigma (#32670)) (100 ng/ml, in 0.01 M PBS) for 1 h at room temperature in order to stain nuclei. The slides were washed 1 X 10 min in PBS then coverslipped with the use of FluorSave mounting media (Calbiochem, VWR (#345789-20)) and left in dark to dry overnight. The slides were then sealed using nail varnish and stored at 4°C.

2.2.4. Image acquisition and analysis

Images were acquired with the use of a Nikon Eclipse 80i epifluorescence microscope equipped with a Nikon DS-Qi1Mc camera using NIS-Elements Software (BR 3.0, Nikon). All images were taken at X20 magnification. For expression levels, 3 images were taken from each of the eight sections per slide from TG and DRG and from at least three animals. For cell size distribution, images were taken covering the entire eight sections on each slide from TG and DRG from three animals. Counting and measuring were carried out using NIS elements Software including only those neuronal profiles with visible nuclei DAPI staining. Profile area values were binned to create neuron size frequency profiles. Expression and co-expression data are expressed as mean ± SEM. Statistical differences in proportions of cells expressing markers or cells within size ranges between TG and DRG were assessed on raw data using a 2-sample T-test. Significance was set at p=<0.05. * p=<0.05; ** p=<0.01; *** p=<0.001.

2.3. Results

2.3.1. Expression of phenotypic markers in TG and comparison with expression patterns in DRG

In order to determine proportions of functional sub-populations of neurons within TG and DRG, the technique of indirect dual immunofluorescence was used to detect a range of neurochemical phenotypic markers considered indicative of functional sub-groups. In order to avoid bias, expression levels were determined using sections from throughout the entire TG and DRG. Expression of the phosphorylated heavy chain (200kDa) neurofilament (NF200) was used to distinguish a sub-population of low threshold Aβ-fibre mechanoreceptors. Expression of the neuropeptide calcitonin gene-related peptide (CGRP) and binding of the lectin *Griffonia simplicifolia* IB4 were used to distinguish sub-populations of Aδ- or C-fibre peptidergic and non-peptidergic nociceptors respectively (see Priestley, 2009). Figure 2-2 shows photomicrographs of immunoreactivity ('+') for NF200, CGRP and IB4, expressed by sensory neurons in transverse sections of the TG.

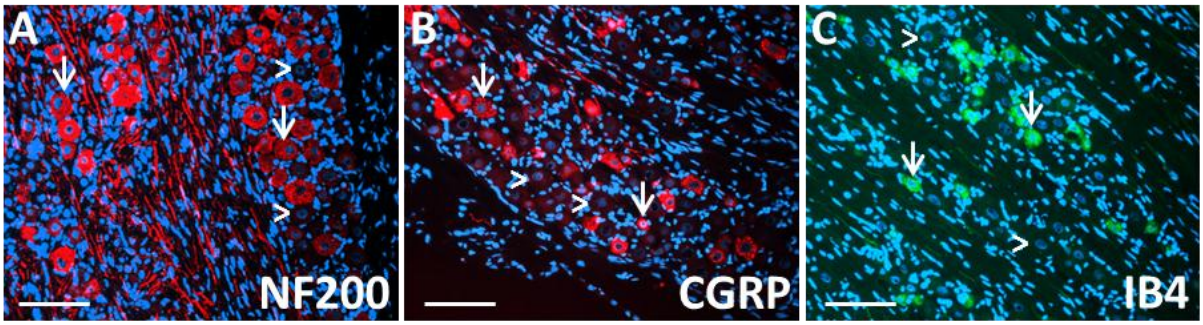

Figure 2-2: Indirect fluorescence immunohistochemistry was used to determine functional sub-populations within TG. **A-C** Photomicrographs of adult naive rat TG demonstrating immunoreactivity for NF200, CGRP and IB4 respectively with DAPI staining showing cell nuclei. Positive profiles (arrows), negative profiles (arrowheads). Scale bars 100μm.

The proportion of neuronal profiles which were NF200+, CGRP+ and IB4+ within the TG compared to the DRG was 50.78±0.7% (n=5) vs. 40.08±0.9% (n=5); 18.65±1.1% (n=5) vs. 31.64±1.9% (n=5) and 26.25±1.2% (n=6) vs. 39.61±1.2% (n=6) respectively (Figure 2-3, Table 2-3 A). These data indicate a significantly higher proportion of neuronal profiles are NF200+ in TG compared to DRG (p=<0.001 t-test) and a significantly lower proportion of neuronal profiles are CGRP+ (p=<0.01 t-test) and IB4+ (p=<0.001 t-test) in TG compared to DRG (Figure 2-4, Table 2-3 A).

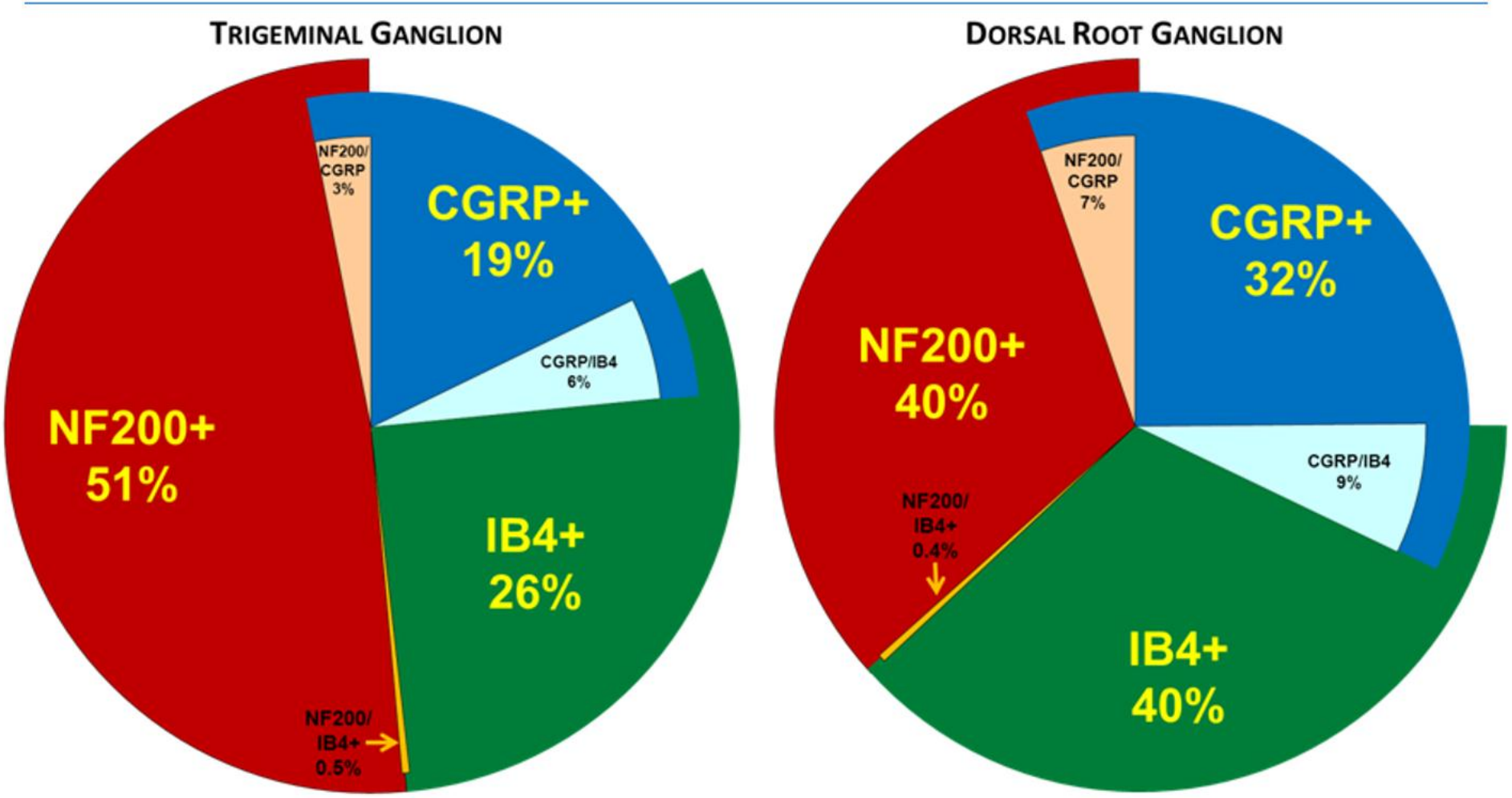

Figure 2-3: Pie-charts summarising the proportional distribution of TG and DRG neurochemical phenotypes. There was a significant difference between proportions of neuronal profiles expressing NF200 (p=<0.001), CGRP (p=<0.01) and IB4 (p=<0.001) in TG compared to DRG. See text and Table 2-3 for specific values.

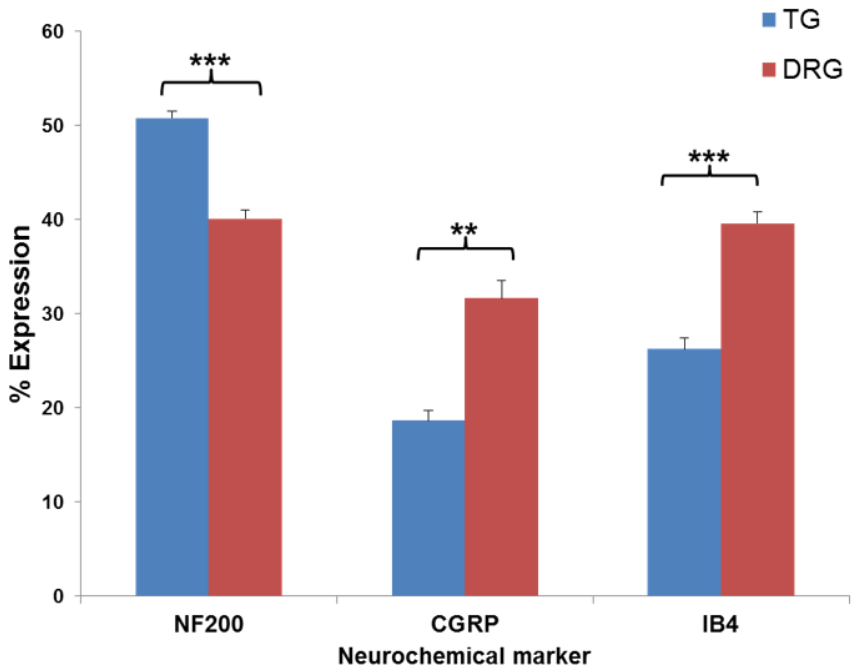

Figure 2-4: Mean % expression of NF200+, CGRP+ and IB4+ neuronal profiles in TG vs. DRG. There was a significantly larger population of NF200+ neurons in TG compared to DRG (p=<0.001) and significantly smaller populations of CGRP+ (p=<0.01) and IB4+ (p=<0.001) neurons in TG compared to DRG. Bars = +SEM

Previous data from the DRG has also shown a small degree of co-expression of these standard neurochemical markers. We have therefore assessed percentage co-expression within the TG. Within the TG, 6.27±2.0% (n=5) of NF200+ neuronal profiles were CGRP+ compared to 18.17±2.8% (n=4) within the DRG. Co-expression of these two markers has previously been suggested to constitute a population of Aδ TRPV2+ nociceptors (high threshold mechanoreceptors) (Priestley, 2009). Our data show a significantly lower proportion of NF200+ neuronal profiles co-expressing CGRP in TG compared to DRG (p=<0.001 t-test) which would suggest a significantly smaller population of Aδ TRPV2+ nociceptors are present within the TG. Within the TG 1.07±0.4% (n=3) of NF200+ neuronal profiles were IB4+ compared to 1.08±0.5% (n=3) within the DRG. No significant difference was found between these values (Table 2-3 B).

Within the TG, 18.14±4.36% (n=4) of CGRP+ neuronal profiles were NF200+ compared to 19.24±4.38% within the DRG. Within the TG, 29.79±2.76% (n=3) of CGRP+ neuronal profiles were IB4+ compared to 28.12±2.19% (n=3) within the DRG. These data were not significantly different between TG compared to DRG (Table 2-3 B). Within the TG, 3.01±1.15% (n=3) of IB4+ neuronal profiles were NF200+ compared to 1.47±0.78% (n=3) within the DRG. Within the TG, 23.82±0.54% (n=3) of IB4+ neuronal profiles were CGRP+ compared to 24.21±0.06% within the DRG. These data show a significantly higher proportion of IB4+ neuronal profiles co-expressing NF200 in TG compared to DRG (p=<0.05 t-test) (Table 2-3 B).

These data can also be expressed as a percentage of total neuronal profiles across the entire TG and DRG, representing 3.2% of TG and 7.3% of DRG are NF200+/CGRP+, 0.5% of TG and 0.4% of DRG are NF200+/IB4+ and 5.56% of TG and 8.9% of DRG are CGRP+/IB4+ (Figure 2-3).

Overall, these data show a much larger proportion of the TG is made up of NF200+ neurons with correspondingly smaller populations of CGRP+ and IB4+ neurons when compared to the DRG. However, despite the larger population of NF200+ neurons within the TG, a smaller proportion of this population appear to co-express CGRP in comparison to the DRG. In addition, although the TG appears to have a much smaller population of IB4+ neurons, a larger proportion of this population appear to co-express NF200 than in the DRG.

In addition, it is noteworthy that our results for expression levels within the DRG concur with those from research undertaken over the past few decades (for review

see Priestley, 2009), and can therefore serve as a further mechanism of control for interpreting our results from the TG.

Table 2-3: **A**) Proportion of neuronal profiles in TG and DRG which were NF200+, CGRP+ or IB4+. **B**) Proportion of neuronal profiles co-expressing neurochemical phenotypic markers in TG and DRG.

A

	% expression in TG and DRG (positive neuronal profiles/total counted)		
	NF200	CGRP	IB4
TG	**50.78±0.7%** (15,570/30,481) (n=5)	**18.65±1.1%** (4,701/25,654) (n=5)	**26.25±1.2%** (7,556/28,523) (n=6)
	***** (*p*=<0.001)**	**** (*p*=<0.01)**	***** (*p*=<0.001)**
DRG	**40.08±0.9%** (4,644/11,556) (n=5)	**31.64±1.9%** (3,259/10,410) (n-5)	**39.61±1.2%** (5,830/14,796) (n=6)

B

	% NF200 expressing other		% CGRP expressing other		% IB4 expressing other	
	CGRP	IB4	NF200	IB4	NF200	CGRP
TG	**6.27±2.0%** (295/5,428) (n=5)	**1.07±0.4%** (27/2,534) (n=3)	**18.14±4.4%** (295/1,834) (n=4)	**29.79±2.8%** (211/700) (n=3)	**3.01±1.2%** (27/924) (n=3)	**23.82±0.5%** (211/879) (n=3)
	*** (*p*=<0.05)**				*** (*p*=<0.05)**	
DRG	**18.17±2.8%** (151/840) (n=4)	**1.08±0.5%** (13/1,214) (n=3)	**19.24±4.4%** (151/831) (n=4)	**28.12±2.2%** (176/629) (n=3)	**1.47±0.8%** (13/1,036) (n=3)	**24.21±0.1%** (176/727) (n=3)

2.3.2. Cell size distribution

Within the somatic distribution of the somatosensory system, it is generally accepted that somal size is an indicator of functional modality. Under these circumstances somal size is considered directly proportional to axon calibre, myelination status, conduction velocity and ultimately functional modality (Duncan, 1934, Mense, 2009). Within the DRG, neurons considered to have a nociceptive function generally have a mean neuronal cross-sectional profile area <1100 µm² and are classified as small (< 500 µm²) or medium (500 – 1100 µm²) sized cells. Those cell profiles with a cross-

sectional profile area >1100 µm² are classified as large and generally considered to have a non-nociceptive function (Wotherspoon and Priestley, 1999).

A total of 3,700 (TG) and 1,756 (DRG) neuronal profiles were measured across entire sections taken from throughout the TG and DRG from three animals. Neuronal profiles were manually outlined and areas calculated. Only profiles containing visible nuclei were included. Values ranged from 79.17 - 2,703.96 µm² for TG (median value 1,164.39 µm²; 3,700 profiles) and 85.39 - 4,596.07 µm² for DRG (median value 589.01 µm²; 1,756 profiles). The proportional distribution for all neuronal profiles in both TG and DRG are shown in Figure 2-5A represented as proportions within each cell size bin. DRG profile distribution shows a bi-modal distribution with peaks at 500 µm² and 1,700 µm². The TG profile distribution shows a uni-modal distribution with a single peak at 400 µm². These data show that the TG has a relative absence of larger neuronal profiles ranging above 1,800 µm² and a relative increase in neuronal profiles in the region 700 – 1,300 µm². These data show a significant difference between mean values for overall neuronal profile distributions in TG compared with DRG (p=<0.001 t-test).

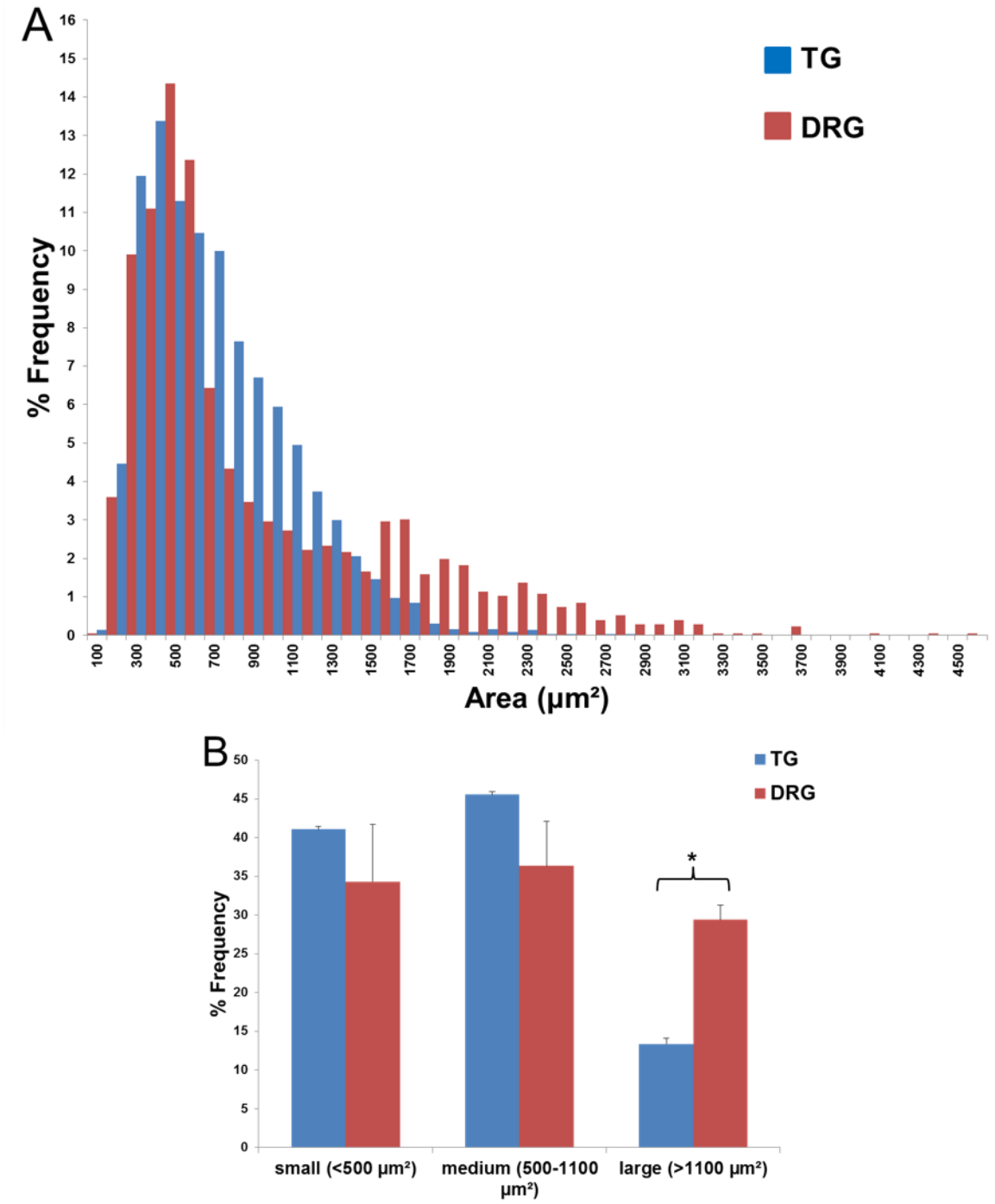

Figure 2-5 – **A**) Total neuronal profile distribution in TG and DRG. Cell size distribution ranged from 79 - 2,703 µm² for TG (3,700 profiles) and 85- 4,596 µm² for DRG (1,756). DRG shows a bi-modal distribution with peaks at 500 µm² and 1,700 µm², and median value 589µm². TG shows a uni-modal distribution peaking at 400 µm² and median value 1,164 µm². TG has almost complete absence of larger neuronal profiles (1,800 – 4,600 µm²) and increase in neuronal profiles in region of 700 – 1,300 µm². There was a significant difference between mean values for neuronal profile distributions in TG and DRG (p=<0.001). **B**) % frequency of neuronal profiles within small (<500 µm²), medium (500-1100 µm²) and large (>1100 µm²) cell size ranges in TG (blue) and DRG (red). There was a significant difference in proportions of large cells (p=<0.05) between TG and DRG. Bars = +SEM

As mentioned previously, cells were divided into 3 size groups (small, medium, large) according to criteria of Wotherspoon and Priestley (1999). Over the whole ganglia neuronal profiles were distributed within cell size groups in TG and DRG as follows: small 41.07% vs. 34.3%, medium 45.56% vs. 36.36%, large 13.36% vs. 29.39% respectively (Figure 2-5 B). These data show a significantly lower proportion of cells within the large size group in TG compared to DRG (p=<0.05 t-test).

Previous studies within the DRG have shown differential expression of neurochemical markers across all cell size groups. Hence the majority of NF200+ neurons are generally considered to fall within the large cell size group, give rise to axons of large calibre with fast conduction velocities. In contrast, the majority of CGRP+ and IB4+ neurons are considered to lie within the small/medium cell size groups, give rise to axons of small calibre with low conduction velocities. We have further analysed the cell size distribution of neuronal profiles from each neurochemical sub-population within the TG and compared these to the DRG from the same animals.

In TG, the overall cell size distribution for NF200+ neuronal profiles ranged from 300 – 2,200 µm² (median value of 913 µm²; 2,508 profiles) with a peak value of 900 µm². In DRG, cell size range was 300 – 3,600 µm² (median value 1,437 µm²; 1,766 profiles) with a peak value of 1,500 µm² (Figure 2-6 A-B). There was a significant difference between mean cell size values for NF200+ profiles in TG and DRG (p=<0.001 t-test)**.** These data indicate a mean smaller overall size of NF200+ neurons in TG compared to DRG. Furthermore, NF200+ profiles were distributed within cell size groups in TG and DRG as follows: small 5.98% vs. 1.96%, medium 64.27% vs. 26.43%, large 29.75% vs. 71.61% respectively (Figure 2-7 A). These data confirm our overall findings and show that for NF200+ profiles there were a

significantly higher proportion in the small and medium cell size groups (p=<0.05 and p=<0.001 t-test) and a significantly lower proportion in the large cell size group in TG compared to DRG (p=<0.001 t-test) (Figure 2-7 A).

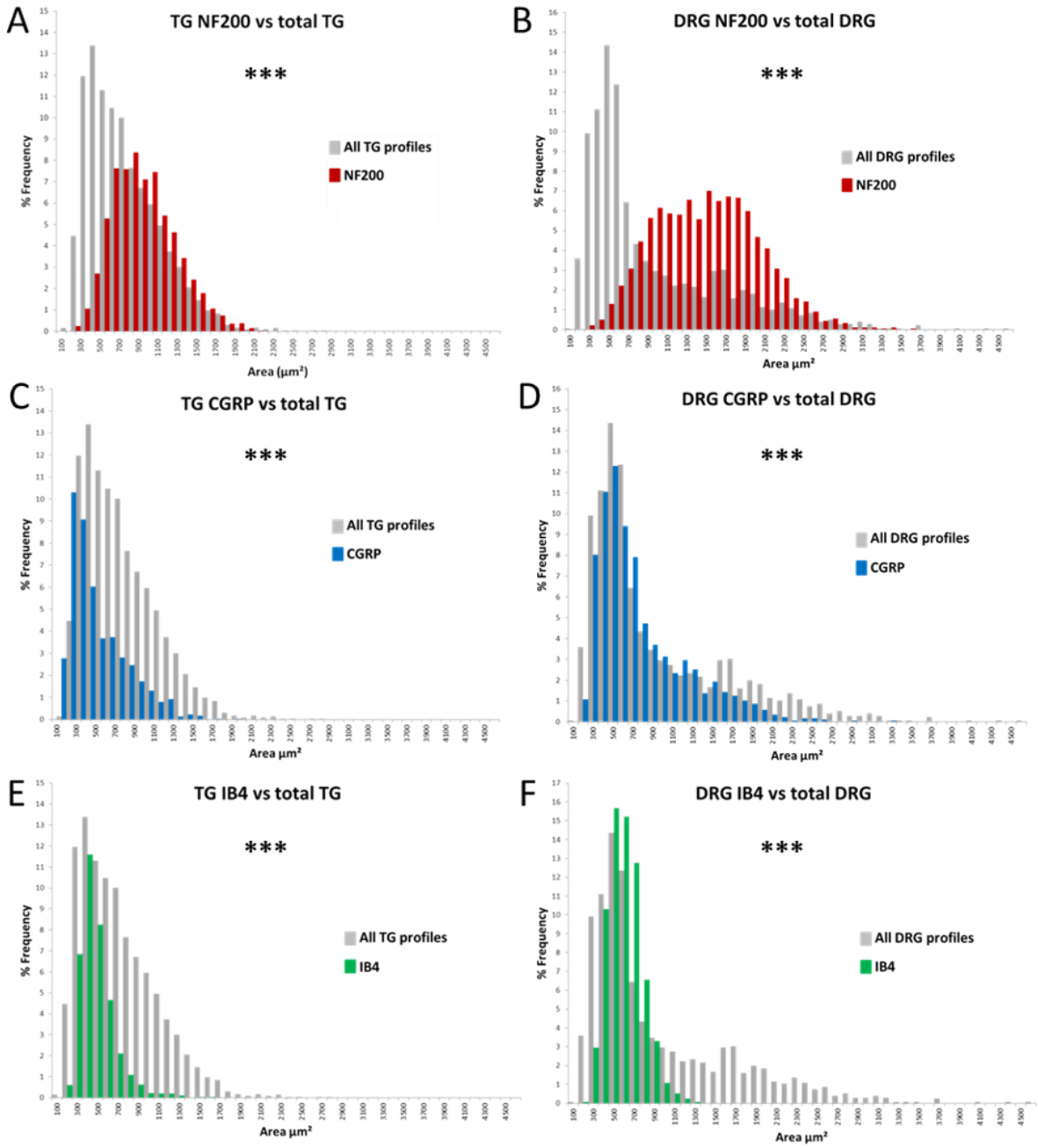

Figure 2-6: Cell size distribution in TG and DRG for profiles expressing standard phenotypic markers illustrated as proportional representation within cell size bins. (**A, C, E**) TG cell size distribution of NF200, CGRP and IB4 against total TG. (**B, D, F**) DRG cell size distribution of NF200, CGRP and IB4 against total DRG. There were significant differences between mean values for overall neuronal profile distributions for NF200, CGRP and IB4 expressing neurons in TG compared to DRG (p=<0.001, p=<0.001, p=<0.001 respectively).

In TG, the overall cell size distribution for CGRP+ neuronal profiles ranged from 200 – 1,600 µm² (median value 416.68 µm²; 1,708 profiles) with a peak value of 300 µm². In DRG, cell size range was 200 – 3,300 µm² (median value 568.78 µm²; 1,383 profiles) with a peak value of 500 µm² (Figure 2-6 C-D). There was a significant difference between mean cell size values for CGRP+ profiles in TG and DRG (*p*=<0.001 t-test). CGRP+ profiles were distributed within cell size groups in TG and DRG as follows: small 60.54% vs. 39.8%, medium 34.36% vs. 40.62%, large 5.09% vs. 19.58% respectively (Figure 2-7 B). These data show that for CGRP+ profiles there was a significantly higher proportion in the small cell size group (*p*=<0.01 t-test) and a significantly lower proportion in the large cell size group in TG compared to DRG (*p*=<0.05 t-test) (Figure 2-7 B).

In TG, the overall cell size distribution for IB4+ neuronal profiles ranged from 200 – 1,300 µm² (median value 393 µm²; 1,350 profiles) with a peak value of 400 µm². In DRG, cell size range was 200 – 1,300 µm² (median value 531 µm²; 1,206 profiles) with a peak value of 500 µm² (Figure 2-6 E-F). There was a significant difference between mean cell size values for IB4+ profiles in TG and DRG (*p*=<0.001 t-test). IB4+ profiles were distributed within cell size groups in TG and DRG as follows: small 74.99% vs. 41.9%, medium 24.19% vs. 57.7%, large 0.82% vs. 0.44% respectively (Figure 2-7 C). These data show that for IB4+ profiles there was a significantly higher proportion in the small cell size group (*p*=<0.01 t-test) and a significantly lower proportion in the medium cell size group in TG compared to DRG (*p*=<0.01 t-test) (Figure 2-7 C). Data for cell size distributions are summarised in Table 2-4.

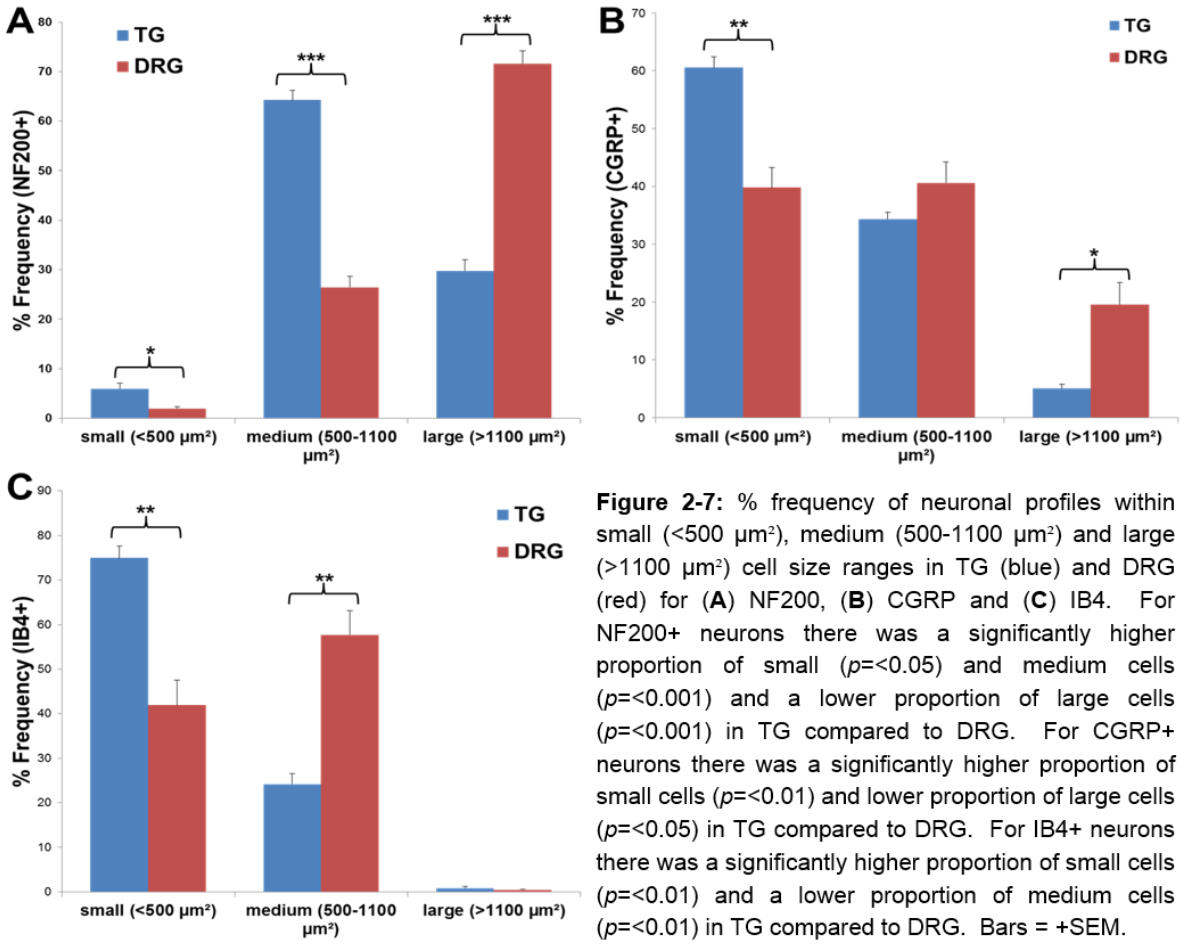

Figure 2-7: % frequency of neuronal profiles within small (<500 µm²), medium (500-1100 µm²) and large (>1100 µm²) cell size ranges in TG (blue) and DRG (red) for (**A**) NF200, (**B**) CGRP and (**C**) IB4. For NF200+ neurons there was a significantly higher proportion of small (*p*=<0.05) and medium cells (*p*=<0.001) and a lower proportion of large cells (*p*=<0.001) in TG compared to DRG. For CGRP+ neurons there was a significantly higher proportion of small cells (*p*=<0.01) and lower proportion of large cells (*p*=<0.05) in TG compared to DRG. For IB4+ neurons there was a significantly higher proportion of small cells (*p*=<0.01) and a lower proportion of medium cells (*p*=<0.01) in TG compared to DRG. Bars = +SEM.

Table 2-4: Summary of cell size distribution data

	Neuronal Profile range (µm²)	Median value (µm²)	*P*=	Modal Peak value(s) (µm²)	% small <500 µm²	*P*=	% medium 500-1100µm²	*p*=	% large >1100 µm²	*P*=	No. profiles measured
Total TG	79.17-2702.96	1164.39	<0.001	400	41.07	n/s	45.56	n/s	13.36	<0.05	3700
Total DRG	85.39-4596.07	589.01		500 & 1700	34.3		36.36		29.39		1756
NF200											
TG	300-2200	912.70	<0.001	900	5.98	<0.05	64.27	<0.001	29.75	<0.001	2508
DRG	300-3600	1437.61		1500	1.96		26.43		71.61		1766
CGRP											
TG	200-1600	416.68	<0.001	300	60.54	<0.01	34.36	n/s	5.09	<0.05	1708
DRG	200-3300	568.78		500	39.8		40.62		19.58		1383
IB4											
TG	200-1300	393.08	<0.001	400	74.99	<0.01	24.19	<0.01	0.82	n/s	1350
DRG	200-1300	531.345		500	41.9		57.7		0.44		1206

2.3.3. Summary of results

- There was a significantly larger population of NF200+ neurons in TG and significantly smaller populations of CGRP+ and IB4+ neurons in TG compared to DRG (Figures 2-3 and 2-4, Table 2-3 A).

- Levels of NF200/CGRP co-expression were significantly lower in TG compared to DRG. Furthermore, a significantly larger proportion of IB4+ neurons co-express NF200 in TG compared to DRG (Table 2-3 B).

- The overall cell size distribution within the TG is significantly skewed towards the smaller size ranges with results showing a distinct lack of large cells in TG compared to DRG (Figure 2-5 A-B, Table 2-4).

- The majority of NF200+ neurons were within the small and medium cell size groups in TG whereas in the DRG, the majority of NF200+ neurons are within the large cell size group (Figure 2-7 A, Table 2-4).

- The majority of CGRP+ neurons were within the small cell size group in TG whereas CGRP+ neurons in the DRG are more evenly distributed across all cell size groups (Figure 2-7 B, Table 2-4).

- The majority of IB4+ neurons were within the small cell size group in TG whereas IB4+ neurons in the DRG are evenly distributed across the small and medium cell size groups (Figure 2-7 C, Table 2-4).

2.4. Discussion

A major goal in the field of neurobiology has been to understand the mechanisms involved in encoding sensory information from afferent neurons within the peripheral nervous system. With the use of certain anatomical, neurochemical and physiological markers, neurons in the DRG have been classified into well-established functional subpopulations. It is now widely accepted that around 40% of DRG neurons are Aα/β fibre non-nociceptors, having large sized cell bodies and identified by their expression of NF200 (see Michael and Priestley, 1999). Neurons with small-medium sized cell bodies have generally been divided into two main subgroups of which around 50% are Aδ/C fibre peptidergic nociceptors, identified by their expression of CGRP, and approximately 50% are C fibre non-peptidergic nociceptors, identified by their binding of IB4, with some degree of overlap between these three populations (see McMahon and Priestley, 2005). More recently, these two main subgroups of nociceptors have been further sub-divided using the co-expression of additional markers as a means of classification. Consequently, CGRP expressing nociceptors have been further sub-divided into those co-expressing NF200 and TRPV2 making up a smaller population of Aδ fibre nociceptors, and a larger population of C fibre nociceptors co-expressing TRPV1, TRPA1 and TrkA. The majority of the C fibre IB4 expressing neurons are believed to co-express TRPV1, TRPA1, and the purinoceptor, $P2X_3$ (see Priestley, 2009).

In contrast to the DRG, there is relatively less information regarding the properties of sensory neurons within the TG (Sessle, 2005). Indeed, prudence has been suggested when extrapolating data from studies on the DRG and applying these to the TG, as there is growing evidence for distinct properties and response

mechanisms within the trigeminal sensory system (Sessle, 2005, Price and Flores, 2007, Hargreaves, 2011). Therefore, in order to better understand sensory mechanisms within the trigeminal nervous system we have performed an in-depth study making direct comparisons between TG and DRG using established neurochemical markers and cell size distributions to determine functional sub-populations of neurons within the TG.

2.4.1. Expression of neurochemical markers and cell size distribution: a direct comparison between TG and DRG

In the current study, we have adopted traditional conventions to classify neurons on the basis of neurochemistry. It is noteworthy that our results for neurochemical populations within the DRG concur with the well-established and accepted proportions mentioned previously. We found approximately 40% of DRG neurons were NF200+, 32% CGRP+ and 40% IB4+. Levels of co-expression are also within accepted limits such that approximately 7% of DRG neurons were NF200+/CGRP+, 9% were CGRP+/IB4+ and 0.4% NF200+/IB4+ (Figures 2-3 and 2-4, Table 2-3) (see also Priestley, 2009). Our results for the TG were significantly different for all three neurochemical populations. We found a significantly higher proportion of NF200+ neurons (51%, p=<0.001) along with significantly lower proportions of both CGRP+ (19%, p=<0.01) and IB4+ (26%, p=<0.001) in TG compared to DRG. In addition, we found discrepancy in the levels of co-expression of markers between ganglia, with a larger population of IB4+/NF200+ neurons and smaller population of NF200+/CGRP+ neurons in the TG (Figures 2-3 and 2-4, Table 2-3). As far as we are aware, only one other study to date has carried out a similar direct comparison between rat TG and DRG using standard neurochemical markers to determine expression over the entire ganglia (Cho *et al.*, 2009b). Unfortunately in this study, the same secondary

antibody chromophore was used for both CGRP+ and IB4+ neurons, hence the authors were unable to distinguish between these two cell populations. However, our results concur with their study in that they found a significantly larger population of NF200+ neurons in TG along with a smaller population of CGRP+ and/or IB4+ neurons when compared to their data on DRG.

As mentioned earlier, there are a number of studies which have examined expression of one or more neurochemical markers in TG only, without a direct comparison being carried out with the DRG. These studies however, have produced inconsistent results for example, levels of CGRP expression have ranged from 16% to 44% across the entire TG (Nagamine *et al.*, 2006, Price and Flores, 2007, Lennerz *et al.*, 2008) and from 5% to 72% in sub-populations of TG neurons (Mori *et al.*, 1990, Mosconi *et al.*, 2001, Ichikawa *et al.*, 2006, Nagamine *et al.*, 2006, Yang *et al.*, 2006). Due to the lack of direct comparison to the DRG in previous research and for reasons of variability amongst studies mentioned in Chapter 1, it is difficult to use these data to make a valid comparison between earlier data and the results from our study.

Using data generated within this study therefore, there are several important functional implications that can be drawn. Traditionally, the marker NF200 has been used to define a population of neurons with a non-nociceptive function that conduct in the Aα/β fibre range and have large sized cell bodies (Michael and Priestley, 1999). Our data show that there are significantly more NF200+ neurons in the TG than DRG. These data are surprising at a number of levels. First, considering the lack of proprioceptive neurons within the TG, whose cell bodies are located within the mesencephalic nucleus (see Bereiter *et al.*, 2009), we would have expected to see significantly fewer NF200+ neurons in the TG than the DRG. Second, our data showed these NF200+ neurons to be enriched within the small to medium cell size

range with an almost complete absence of larger neuronal cells >1800 µm² in the TG. Whilst this is in line with the lack of proprioceptive neurons and in agreement with several previous studies (Wotherspoon and Priestley, 1999, Ichikawa *et al.*, 2004, Ichikawa *et al.*, 2006) the implication may be that many of these small to medium NF200 expressing neurons could be nociceptors. This hypothesis could possibly be supported by our finding of an increase in the frequency of cells within the 700 – 1,300 µm² range within the TG, possibly Aδ fibre, nociceptors. The hypothesis could be that these may account for the larger population of NF200 expressing neurons. In order to test this, we carried out further analysis of cell size distribution within each neurochemical population.

As mentioned earlier, there was a significant shift towards the smaller cell sizes in the TG for all three neurochemical populations compared to the DRG. Again, this would be somewhat expected, due to the lack of proprioceptors in the TG (Figure 2-6, Table 2-4). To further quantify these findings, the cells were divided into 3 size groups, small (<500 µm²), medium (500-1100 µm²) and large (>1100 µm²). With the small-medium sizes assuming to be a nociceptive phenotype and large, a non-nociceptive phenotype (Harper and Lawson, 1985, Lawson and Waddell, 1991). Of particular interest were the results for NF200+ neurons. Here we found significantly larger NF200+ populations in the small and medium size groups in TG compared to DRG, and most interestingly, the majority (64%) of NF200+ TG neurons were in the medium cell size group, whereas the majority (72%) of NF200+ DRG neurons were in the large cell size group (Figure 2-7, Table 2-4). These data therefore, initially suggest that the TG contains significantly more neurons than the DRG which fall within the small to medium cell size range and which are NF200+. The functional implication here is that the TG is potentially enriched with small diameter, NF200+ nociceptors.

These data however, need to be viewed alongside that from further analysis of the other neurochemical markers. In the TG, the majority of CGRP+ and IB4+ cells fell within the small size group, whereas in the DRG, both groups were more evenly distributed across all cell size groups (see Figure 2-7, Table 2-4). These data do agree with previous studies for the TG whereby CGRP and IB4 expression was found predominantly within the small cell size group. For instance, CGRP+ rat TG neurons showed peak frequency between 314-491 μm² (Lennerz *et al.*, 2008) and a mean soma size of 325 μm² (Price and Flores, 2007). In addition, the mean soma size for IB4+ rat TG neurons has been reported as 366 μm², significantly smaller than corresponding cells within the DRG (Price and Flores, 2007).

From our previous assertion that because the TG appears to be enriched with NF200 expressing neurons within the smaller cell size ranges and may therefore be nociceptors, it follows that we may find higher levels of co-expression of NF200 with either CGRP or IB4 within these size brackets in the TG compared to the DRG. This could possibly support the hypothesis that these small NF200+ neurons were nociceptors. However, our data showed significantly less co-expression of NF200 and CGRP within the TG compared to the DRG, which would imply that these smaller NF200+ TG neurons are not the CGRP/NF200/TRPV2 expressing nociceptor population as described earlier. Nonetheless, our data did show significantly higher co-expression of NF200 within the IB4+ population of neurons in the TG compared to the DRG. Although only accounting for a small proportion of the total neuronal populations in both ganglia, our data appear to describe a novel neuronal population of IB4/NF200/$P2X_3$ expressing nociceptors which are enriched within the TG. The function of IB4 expressing neurons is largely unknown and it has been suggested that they signal different types of pain to those expressing CGRP (see Priestley, 2009). Indeed, IB4+ DRG neurons have been shown to terminate less superficially

(within lamina II inner), than those expressing CGRP (within lamina 1 and II outer), and are believed to be responsible for mediating acute thermal and mechanical nociception (Vulchanova *et al.*, 2001, Zylka *et al.*, 2005). Of particular interest is the suggestion that non-peptidergic nociceptors may innervate different central pathways to those of peptidergic nociceptors and are primarily responsible for conveying the affective rather than sensory component of pain (see Priestley, 2009). Thus, this small, but enriched population of neurons within the TG may help to explain the difficulties encountered in treating pain within the orofacial region due to its being an area with special emotional and psychological meaning to patients (see Sessle, 2000).

Since pain is the predominant sensation evoked by pulpal stimuli, and tooth pulp is rich in unmyelinated nerve fibres, it has generally been accepted that these pulpal fibres give rise to small diameter nociceptive neurons that conduct in the C fibre range (Brashear, 1935, Anderson *et al.*, 1970, Mumford and Bowsher, 1976, Johnsen and Johns, 1978, McGrath *et al.*, 1983, Sessle, 1986, Narhi *et al.*, 1994, Nair, 1995, Orchardson and Cadden, 2001, Narhi, 2005). However, studies are now suggesting that many of the unmyelinated axons within tooth pulp originate from myelinated parent axons which have tapered terminal segments within the pulp (Orchardson and Cadden, 2001). For instance, Ichikawa *et al.* (2006) found that tooth pulp neurons had larger cell bodies than those of cutaneous TG neurons. Sugimoto *et al.* (1988) showed that the majority (64%) of pulpal neurons had cell bodies over 500 μm^2, namely within the medium cell size range. A more recent study concurs with these findings, where the majority of parent axons innervating tooth pulp were found to be small myelinated fibres, namely Aδ fibres with correspondingly medium size cell bodies (Paik *et al.*, 2009). In agreement with these studies, physiological experiments have also showed that pulpal axons increase their

conduction velocity as they leave the pulp and enter the alveolar nerve (for reviews see Hildebrand *et al.*, 1995, Lazarov, 2002, Fried *et al.*, 2011). As fibre type would strongly influence the characteristic quality of the pain perceived following activation of pulpal nociceptors, it is therefore important to determine the relative contribution of pulpal innervation from sensory neurons that give rise to either unmyelinated or myelinated parent axons (Henry *et al.*, 2012).

The dense innervation of the tooth pulp, and the fact that these neurons are being shown to have myelinated parent axons, may help to explain our results. We know that the TG lacks proprioceptors, therefore the lack of large cells is somewhat expected. In addition, we found an over-representation of NF200+ neurons, the majority of which had medium sized cell bodies. These neurons may possibly contribute towards the population of Aδ fibre, tapering neurons that innervate the tooth pulp. Furthermore, the current study has demonstrated some key differences between the neurochemical and cell size distribution patterns in the TG compared to the DRG, which likely reflect functional differences in response mechanisms between the ganglia. In addition, we have identified populations of TG neurons with unusual phenotypes, and would therefore agree with previous researchers who dictate prudence when extrapolating data from the DRG and applying it to the TG.

3. Molecular biology of the trigeminal ganglion Part 2: Neurotrophin receptor, cytokine receptor and thermo-transducer protein expression

3.1. Introduction

An understanding of the sensory processes responsible for pain and the factors that can modify these response mechanisms is important for the effective management of orofacial pain (Cadden and Orchardson, 2001). Moreover, treatment of orofacial pain is more complex owing to a lack of discrimination making it difficult for some patients to locate the exact source of intraoral pain conditions (Weigelt *et al.*, 2010). Inflammatory mediators, such as neurotrophins and cytokines, released following injury, form what is more commonly referred to as the "inflammatory soup" and have the effect of profoundly changing the chemical milieu surrounding the peripheral terminals of sensory neurons (see Basbaum *et al.*, 2009). By expression of specific receptor components on the terminals of sensory neurons, these inflammatory mediators can have a direct effect on neuronal response mechanisms. In addition, sensory neurons express transducer proteins, which can be sensitised indirectly via post-translational mechanisms initiated by inflammatory mediators. The resulting sensitisation of sensory neurons, leads to such states as thermal and mechanical hyperalgesia (as explained in Chapter 1). Furthermore, this form of hypersensitivity may be unresolved, resulting in chronic and debilitating pain conditions (see Basbaum *et al.*, 2009).

Clinical biopsy studies and pre-clinical animal studies have shown that some of the most potent mediators present within the inflammatory milieu are nerve growth factor

(NGF) (see Pezet and McMahon, 2006), tumour necrosis factor alpha (TNFα) (Miller *et al.*, 2009) and interleukin 6 (IL-6) (Andratsch *et al.*, 2009). NGF activates cells by binding to a high affinity tropomyosin-related kinase receptor, TrkA. In the somatosensory system TrkA is specifically expressed by populations of nociceptor-specific neurons expressing CGRP or co-expressing NF200 (Lewin and Mendell, 1993, Averill *et al.*, 1995). Activation of TrkA on these sensory neurons underlies nociceptor activation and sensitisation to algogenic stimuli such as heat and noxious chemicals and is considered a major mechanism underlying some persistent inflammatory pain states (Dmitrieva and McMahon, 1996, Lowe *et al.*, 1997, Halliday *et al.*, 1998, Gould *et al.*, 2000, Pezet and McMahon, 2006). Indeed, the use of antibodies to sequester NGF has given effective and sustained relief from clinical pain (Lane *et al.*, 2010). Furthermore, it has been suggested that local availability of NGF may be a crucial factor in altering nociceptor phenotype and lowering threshold levels (Bennett *et al.*, 1998(a), Obreja *et al.*, 2011).

Overall expression of TrkA in DRG is generally accepted to be around 40-45% (Averill *et al.*, 1995, Kobayashi *et al.*, 2005, McMahon and Priestley, 2005). There is extensive overlap between TrkA expressing cells and those expressing CGRP (McMahon, 1996), indeed, Averill *et al.* (1995) showed that 90% of peptidergic nociceptors co-expressed TrkA in DRG. Furthermore, approximately 25% of NF200+ neurons co-express TrkA (McMahon and Priestley, 2005) and around 6-12% of IB4+ neurons co-express TrkA (Averill *et al.*, 1995, McMahon, 1996) in DRG. Reported expression levels of TrkA in rat TG have varied greatly from 38% to 78% between studies and depending on the type of tissue innervated (Wetmore and Olson, 1995, Jacobs and Miller, 1999, Pan *et al.*, 2000, Yang *et al.*, 2006, Gaspersic *et al.*, 2007, Svensson *et al.*, 2010). These previous studies highlight a discrepancy between the

DRG and TG in relation to the potential for TG cells to respond to an important inflammatory mediator.

TNFα is a potent pro-inflammatory cytokine which is rapidly produced by a wide range of immune cells in response to inflammatory stimuli (Verri *et al.*, 2006a). TNFα interacts with target cells through two structurally related high-affinity receptors p55 (TNFR1, CD120a) and p75 (TNFR2, CD120b) both able to activate pro-inflammatory signalling pathways (Caminero *et al.*, 2011). Within the DRG, the proportion of neurons which display p55 protein expression have been reported as 13% (Sakuma *et al.*, 2007) and 15%, mainly in C fibres (Xu *et al.*, 2006). Increased levels of TNFα have been correlated with a number of painful inflammatory conditions (Lindenlaub and Sommer, 2003), complex regional pain syndrome (see Calvo *et al.*, 2012) rheumatoid arthritis, Crohn's disease (see Coutaux *et al.*, 2005) and neurodegenerative disorders (see Mc Guire *et al.*, 2011). Furthermore, TNFα produces ectopic activity and sensitisation of nociceptors (Sorkin *et al.*, 1997, Sabsovich *et al.*, 2008, Schäfers *et al.*, 2008) and plays a pivotal role in the development of inflammatory hyperalgesia (Cunha, 1992, Cunha *et al.*, 2008). Of particular interest is that the constitutively expressed receptor p55 has been demonstrated to be key in the development of hyperalgesia and allodynia (Sommer *et al.*, 1998, Moalem and Tracey, 2006, Schäfers *et al.*, 2008). In addition, TNFα has been shown to enhance capsaicin sensitivity and increase levels of TRPV1 expression (Nicol *et al.*, 1997, Khan *et al.*, 2008, Spicarova and Palecek, 2010) thus demonstrating a link between TNFα signalling and TRPV1 sensitisation.

Studies on rat TG have again shown equivocal results. For example, it is known that TNFα enhances capsaicin sensitivity and significantly increases TRPV1 expression (Khan *et al.*, 2008). Of interest here was their finding that >90% of TRPV1+ neurons

co-expressed p55. In contrast however, Zhang *et al*. (2011) found increased TNFα plasma levels during migraine attacks, but were unable to locate p55 on neuronal cells and only observed expression on non-neuronal dural endothelial vascular cells and macrophages. Bowen *et al.* (2005) observed p55 expression almost exclusively on CGRP+ neuronal cells, and Hakim *et al*. (2009) found that 29% of masseter neuronal cells were positive for p55. We will attempt a further detailed analysis of the expression of p55 in sensory neurons under normal conditions in the rat TG.

TNFα has been shown to activate sensory neurons directly initiating a cascade of inflammatory reactions and resulting in production of further cytokines such as IL-6 (see Dray, 2005). IL-6 is a predominantly pro-inflammatory cytokine released by a variety of cell types including immune, neuronal and glial cells (Verri *et al.*, 2006a, Austin and Moalem-Taylor, 2010). IL-6 is a member of the neuropoietic cytokine family which share the transmembrane signal transducing receptor component gp130 (see Scheller *et al.*, 2011(b)). Elevated levels of IL-6 have been linked to several chronic inflammatory diseases such as rheumatoid arthritis and burning mouth syndrome (see Gadient and Patterson, 1999, Suh *et al.*, 2009). Indeed it is now being recognised that IL-6 may contribute to the development and progression of certain chronic inflammatory conditions (see Gadient and Patterson, 1999, Rincon, 2012) along with having a key role in the development of hyperalgesia (see Verri *et al.*, 2006a), mechanical allodynia (Anderson and Rao, 2001) and chronic neuropathic pain (Arruda *et al.*, 1998). For instance, patients with complex regional pain syndrome have displayed elevated levels of both IL-6 and TNFα (Heijmans-Antonissen *et al.*, 2006) whilst upregulation of IL-6 has been shown in patients with temporomandibular disorder (Wang *et al.*, 2009b). Moreover, injury-induced upregulation of IL-6 has been positively correlated to pain intensity and the onset of

acute inflammatory pain (Wang *et al.*, 2009c). In addition, IL-6 has been linked to the pathogenesis of migraine headache (Yan *et al.*, 2012).

Gp130 has previously been reported to be expressed on neuronal cells, albeit in MAH cells (immortalised sympathoadrenal progenitor cell line) (Ip *et al.*, 1992), and within the CNS in rat brain, including the trigeminal sensory nuclei (Watanabe *et al.*, 1996). However, a more recent study on the somatosensory system has demonstrated ubiquitous expression of gp130 on DRG neurons (Gardiner *et al.*, 2002). Of particular interest was a study by Quarta *et al.* (2011) who termed gp130 a 'chronification factor' and found it to be essential for the long-term potentiation of mechanical hypersensitivity associated with inflammation, cancer and nerve injury. To date, only one other study has examined localisation of gp130 within the trigeminal nervous system, where gp130 mRNA was shown to be expressed in >90% of trigeminal neurons (Mizuno *et al.*, 1997). Therefore, as far as we are aware, ours is the first study to demonstrate localisation of gp130 protein within the TG.

Major sensitisation effects within DRG sensory neurons occur through local signalling, leading to post-translational changes to pre-existing proteins. One such important substrate protein is TRPV1 (transient receptor potential vanilloid 1) (Nicholas *et al.*, 1999, Shu and Mendell, 1999, 2001, Bonnington and McNaughton, 2003b, Amaya *et al.*, 2004, Lewin *et al.*, 2004, Zhang *et al.*, 2005, Huang *et al.*, 2006a, Zhu and Oxford, 2007). TRPV1 is a polymodal transducer channel, gated in response to noxious heat, capsaicin and protons and is a member of the thermo-TRP subfamily of the TRP superfamily (Caterina and Julius, 2001). Whilst debate remains over the role of TRPV1 in transducing acute thermal stimuli there is now a consensus regarding its central role in mediating thermal hyperalgesia (Rueff and Mendell, 1996, Bennett *et al.*, 1998(a), Caterina *et al.*, 2000, Shu and Mendell, 2001, Bonnington

and McNaughton, 2003b, Lewin *et al.*, 2004, Woodbury *et al.*, 2004, Pogatzki-Zahn *et al.*, 2005, Zhang *et al.*, 2005, Yu *et al.*, 2008, Walder *et al.*, 2012, Barcena de Arellano *et al.*, 2013). Within the TG, a significant increase in NGF levels and subsequent increase in TRPV1 expression has been found in patients with burning mouth syndrome (BMS) (Yilmaz *et al.*, 2007, Jääskeläinen, 2011). In addition, NGF-mediated TRPV1 sensitisation has been linked to ectopic orofacial pain (Shinoda *et al.*, 2011).

In the DRG around 50% of neurons are TRPV1+ (Guo *et al.*, 1999, Kobayashi *et al.*, 2005, Kiasalari *et al.*, 2010). Approximately 65% of peptidergic nociceptors and 75% of non-peptidergic nociceptors co-express TRPV1 (see Guo *et al.*, 1999, McMahon and Priestley, 2005) and only 3% of NF200+ neurons co-express TRPV1 (see Priestley *et al.*, 2002). Previous data have estimated the proportion of TRPV1 expressing neurons in the TG to be between 16% to 50% (Ichikawa and Sugimoto, 2001, Bae *et al.*, 2004, Kobayashi *et al.*, 2005, Tanimoto *et al.*, 2005, Nagamine *et al.*, 2006, Simonetti *et al.*, 2006, Pei *et al.*, 2007, Price and Flores, 2007, Kiasalari *et al.*, 2010, Gibbs *et al.*, 2011). Moreover, studies investigating sub-populations of rat TG neurons have also varied from 8% to 35% depending on the target tissue being innervated (Ichikawa and Sugimoto, 2001, Stenholm *et al.*, 2002, Murata and Masuko, 2006, Gibbs *et al.*, 2011, Saloman *et al.*, 2013). We have therefore further analysed TRPV1 expression in TG neurons.

TRPM8 (transient receptor potential melastatin 8) was first reported around a decade ago as a specific marker for prostate cancer (Knowlton and McKemy, 2011) and is now known to be activated by gentle cooling, menthol, eucalyptol and icilin (see Latorre *et al.*, 2007). Interestingly, TRPM8 can be activated by both innocuous and noxious temperatures ranging from 28 to <5 °C (McKemy *et al.*, 2002, Knowlton and

McKemy, 2011) and may likely be involved in thermal nociception (Tominaga and Caterina, 2004). The sensory discrimination between innocuous and noxious cold by TRPM8 may be due to its co-expression with either tetrodotoxin-sensitive (TTXs) or TTX-resistant (TTXr) voltage gated Na+ channels, with TTXs inferring a non-nociceptive phenotype, and TTXr a nociceptive phenotype (Sarria *et al.*, 2012). The role of TRPM8 in inflammatory pain is still under debate, although functional modulation of TRPM8 by pro-inflammatory mediators such as NGF has been reported (see Babes *et al.*, 2011). Indeed a recent study using TRPM8-ablated and knockout mice showed significant attenuation of cold pain associated with inflammation and nerve injury (Knowlton *et al.*, 2013). Studies on rat DRG have reported the proportion of neurons expressing TRPM8 to be between 6% and 23% and in rat TG between 12% and 35% (Peier *et al.*, 2002, Abe *et al.*, 2005, Kobayashi *et al.*, 2005, Su *et al.*, 2011).

Since the trigeminal system plays a major role in the detection of noxious chemicals via transducer channels located on nociceptor terminals within the oral and nasal mucosa (Gerhold and Bautista, 2009), and given the role played by many of these underlying neuronal sensitisation, elucidating expression patterns and proportions of transducer channels within the TG would appear to be a priority. Moreover, commensal microbiota, which is abundant within the oral mucosa, has been shown to enhance the development of inflammatory hyperalgesia (Amaral *et al.*, 2008). In addition, the successful development of novel analgesics is contingent upon the correct target molecule being selected which can only happen once we have a thorough understanding of transducer receptor distribution and mechanisms of sensitisation (Hughes *et al.*, 2012).

To provide greater insight into the functional roles of TG neurons we have made a detailed examination of the distribution of key receptor and transducer molecules known to be important for the induction of peripheral sensitisation or as potential downstream targets for post-translational modifications. We have examined the distribution of the high affinity NGF receptor, TrkA, along with receptor components for two further major inflammatory mediators TNFα and IL6 (p55 and gp130 respectively). In addition, we have examined patterns of expression for the thermo-transducer proteins TRPV1 and TRPM8 and compared our findings for all markers to patterns of expression within the DRG, in order to establish a basis for dynamic plasticity of the TG nociceptive system. Furthermore, we have compared co-localisation of each of these receptor components and transducer proteins with standard neurochemical markers in both TG and DRG. Finally, we have determined the neuronal cell size profile distributions for each molecular marker and compared distributions between TG and DRG.

3.2. Methods

3.2.1. Animals

Experiments were conducted on adult naive male Sprague Dawley rats ranging from 220-250 g body weight (Charles River, Margate, UK). All procedures were conducted in accordance with the UK 1986 Animals (Scientific Procedures) Act. Animals were housed in a temperature controlled room on a 12:12 h light/dark cycle, food and water was available *ad libitum*. Following Schedule 1 killing, animals were transcardially perfused, dissected and the tissue was snap-frozen and stored at -80°C. The tissue was cut into 8 µm sections and thaw-mounted onto SuperFrost Plus slides as previously described in Chapter 2.

3.2.2. Antibody characterisation

Table 3-1 describes the primary and secondary antibodies used in this study. The NF200, CGRP and IB4 antibodies used have been widely characterised as described in Chapter 2. Antibodies for markers of interest have previously been characterised as follows: TrkA (Drummond *et al.*, 2006), p55 (Xu *et al.*, 2006), gp130 (Gardiner *et al.*, 2002), TRPV1 (Kiasalari *et al.*, 2010, Harrington *et al.*, 2011) and TRPM8 (Harrington *et al.*, 2011). Specificity for secondary antibodies was confirmed by omitting primary antibodies from immunohistochemical protocols. No labelling was observed under these conditions.

Table 3-1: Summary details of primary and secondary antibodies

Antigen	Host	Species reactivity	Manufacturer	Dilution used	Secondary Antibody used
TrkA	Rabbit	Rat	Abcam (#ab8871)	1:500	DαRb-AF555 or DαRb-AF488 (both at 10 µg/ml)
P55	Rabbit	Rat, mouse, human	Santa Cruz Biotechnology (#sc-7895)	1:100	DαRb-AF555 or DαRb-AF488 (both at 10 µg/ml)
Gp130	Rabbit	Rat, mouse, human	Santa Cruz Biotechnology (#sc-656)	1:200	DαRb-TRITC (1:200)
TRPV1	Goat	Rat	Neuromics (#GT15129)	1:1k	DαG-FITC (1:200)
TRPV1	Guinea Pig	Rat	Neuromics (#GP14100)	1:4k	DαG-P-DyLight 549 (1:200)
TRPM8	Rabbit	Rat, mouse, human	Alamone Labs (#ACC-049)	1:500	DαRb-AF555 or DαRb-AF488 (both at 10 µg/ml)

3.2.3. Immunohistochemistry

Indirect dual immunofluorescence was performed on naïve adult rat TG and DRG as described in Chapter 2. Briefly, slides were blocked for 1 h in 10% donkey serum (0.01 M PBS/0.2% Triton X/0.1% Azide) then incubated with primary antibodies overnight at room temperature. Slides were then incubated with secondary antibodies and left for 3 h at room temperature (for TrkA staining, secondary antibodies were left on for 5 h). The slides were stained with DAPI (100 ng/ml, in 0.01 M PBS) for 1 h at room temperature in order to stain nuclei, coverslipped with the use of FluorSave mounting media (Calbiochem), dried overnight and sealed.

3.2.4. Image acquisition and analysis

As described in Chapter 2, Images were acquired with the use of a Nikon Eclipse 80i epifluorescence microscope. Counting and measuring were carried out including only those neuronal profiles with visible nuclei DAPI staining. High-expressing

TRPV1+ profiles were readily discernible by eye although a fluorescence intensity measurement was used to confirm visual identification. Profile area values were binned to create neuron size frequency profiles. Expression and co-expression data are expressed as mean ± SEM. Statistical differences in proportions of cells expressing markers or cells within size ranges between TG and DRG were assessed on raw data using a 2-sample T-test. Significance was set at p=<0.05. * p=<0.05; ** p=<0.01; *** p=<0.001.

3.3. Results

3.3.1. TrkA – Expression, co-expression and cell size distribution

Indirect dual immunofluorescence was used to define the proportion of neurons expressing the high affinity receptor for NGF, TrkA, within the TG and DRG and to observe the degree of co-localisation with the neurochemical markers NF200, CGRP and IB4. The total proportion of neuronal profiles which were TrkA+ in the TG compared to the DRG was, 24.2±0.82% (n=6) vs. 27.87±1.94% (n=6) respectively (Figure 3-1, Table 3-2 A). There was no significant difference between these values. Within the TG, TrkA was co-localised as follows: NF200+/TrkA+, 16.52±1.25% (n=3); CGRP+/TrkA+, 60.63±3.76% (n=5); IB4+/TrkA+, 11.32±1.59% (n=3). Corresponding values within the DRG were: NF200+/TrkA+, 22.80±6.53% (n=3); CGRP+/TrkA+, 78.54±2.5% (n=5); IB4+/TrkA+, 11.22±1.09% (n=3) (Figure 3-1 J-O, Table 3-2 B-D). Although overall levels of TrkA expression were not significantly different between TG and DRG, our data appear to show that TrkA was differentially distributed across neurochemical populations with significantly lower CGRP/TrkA co-localisation (p=<0.01) along with a trend towards lower NF200/TrkA co-localisation in TG compared to DRG (Figure 3-1, Table 3-2).

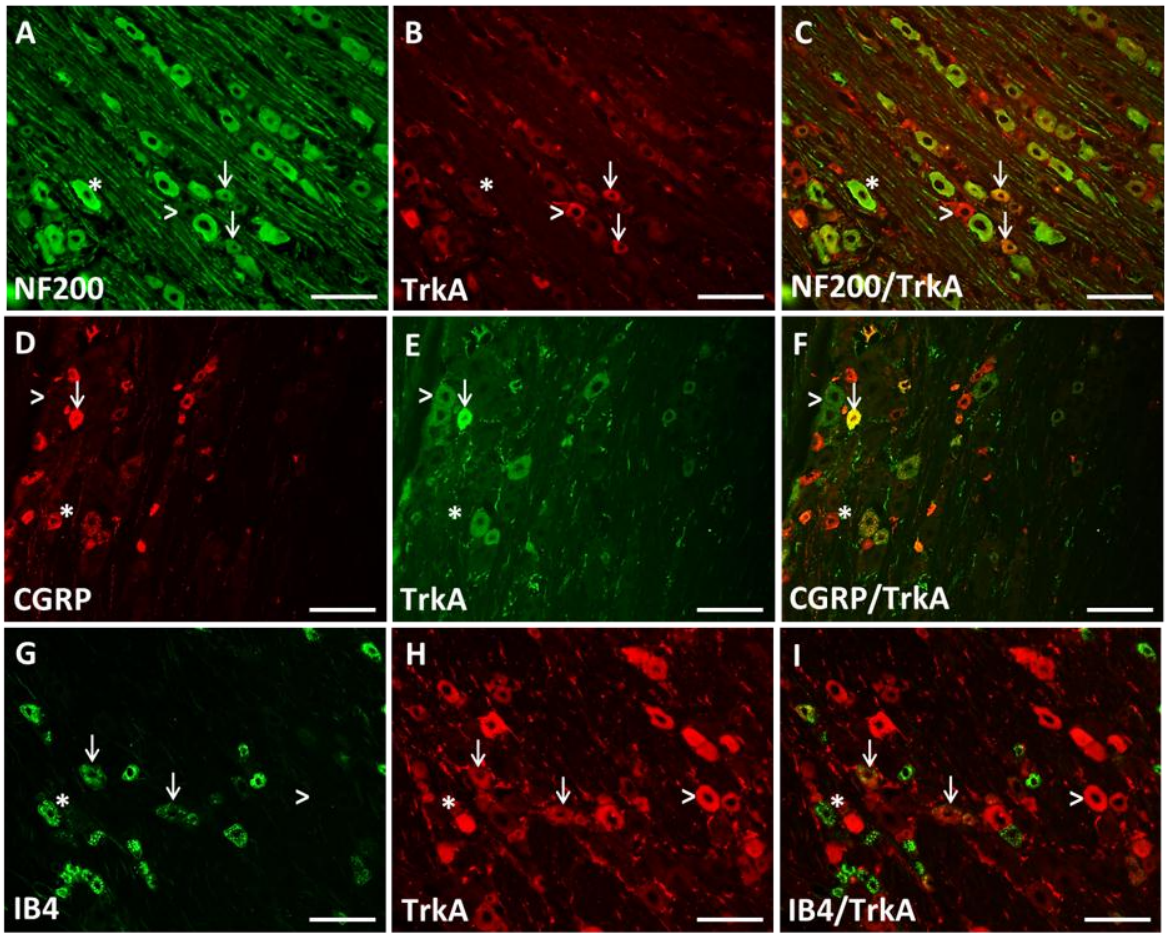

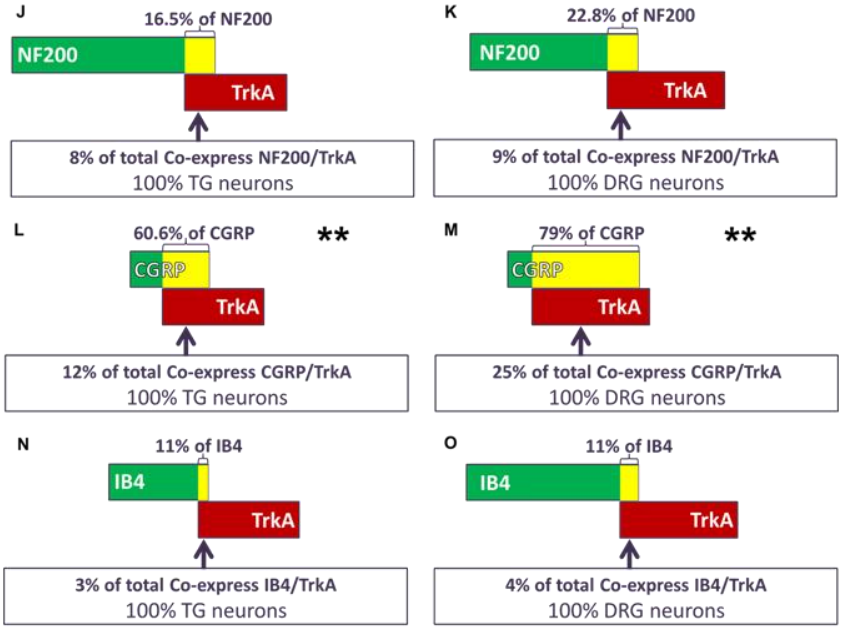

Figure 3-1: Photomicrographs showing expression and co-expression in TG of TrkA with standard phenotypic markers NF200 (**A-C**), CGRP (**D-F**) and IB4 (**G-I**). Bars illustrate levels of expression and co-expression as a proportion of each phenotypic marker and as a percentage of entire TG or DRG. NF200 (**J** (TG) **K** (DRG)) CGRP (**L** (TG) **M** (DRG)) IB4 (**N** (TG) **O** (DRG)). A significantly lower proportion of CGRP+ cells (p=<0.01) co-localised with TrkA in TG compared to DRG. Panels A-I (*) shows marker of interest only; (arrowheads) TrkA only; (arrows) co-expression. Scale bar 100 µm.

In TG, the overall cell size distribution for TrkA+ profiles ranged from 100 – 2,000 µm² (median value 530 µm²; 1,884 profiles) with a peak at 400 µm² (Figure 3-2 A). In DRG, cell size range was 200 – 3,300 µm² (median value 641 µm²; 1,014 profiles) with a peak at 400 µm² (Figure 3-2 B). There was a significant difference between mean values for overall cell size distributions of TrkA+ profiles in TG compared to DRG (p=<0.001 t-test) (Figure 3-2 A-B, Table 3-3). Cells were further analysed as per distribution within small, medium and large size ranges (see section 2.3.2). TrkA+ profiles were distributed within cell size groups in TG and DRG as follows: small 44.41% vs. 38.02%, medium 44.88% vs. 37.56%, large 10.71% vs. 24.42% respectively (Figure 3-2 C). These data show that there was a significantly higher proportion of TrkA+ profiles in the medium cell size group in TG (p=<0.05 t-test) and a significantly lower proportion of TrkA+ profiles in the large cell size group in TG compared to DRG (p=<0.01 t-test) (Figure 3-2 C, Table 3-3).

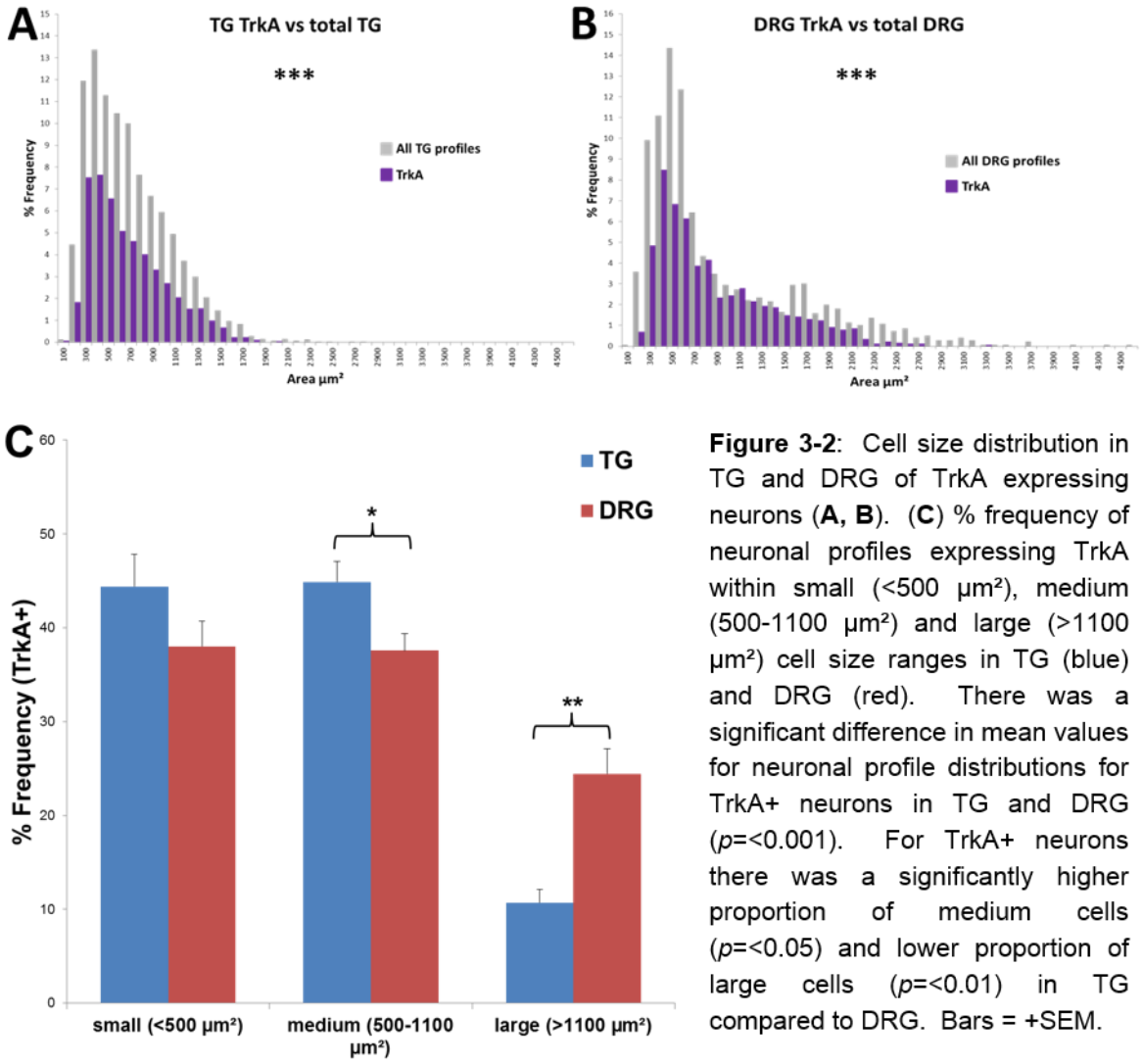

Figure 3-2: Cell size distribution in TG and DRG of TrkA expressing neurons (**A, B**). (**C**) % frequency of neuronal profiles expressing TrkA within small (<500 µm²), medium (500-1100 µm²) and large (>1100 µm²) cell size ranges in TG (blue) and DRG (red). There was a significant difference in mean values for neuronal profile distributions for TrkA+ neurons in TG and DRG (p=<0.001). For TrkA+ neurons there was a significantly higher proportion of medium cells (p=<0.05) and lower proportion of large cells (p=<0.01) in TG compared to DRG. Bars = +SEM.

3.3.2. P55 – Expression, co-expression and cell size distribution

Indirect dual immunofluorescence was used to define the proportion of neurons expressing the receptor for TNFα, p55, within the TG and DRG to observe the degree of co-localisation with NF200, CGRP and IB4. The total proportion of neuronal profiles which were p55+ in the TG compared to the DRG was 33.01±4.21% (n=4) vs. 38.05±2.85% (n=3) respectively (Figure 3-3, Table 3-2 A). There was no significant difference between these values. Within the TG, p55 was co-localised as follows: NF200+/p55+, 26.53±2.15% (n=3); CGRP+/p55+,

38.45±3.11% (n=3); IB4+/p55+, 60.82±1.52% (n=3). Corresponding values within the DRG were: NF200+/p55+, 29.76±7.02% (n=3); CGRP+/p55+, 32.56±1.42% (n=3); IB4+/p55+, 88.83±1.41% (n=3) (Figure 3-3 J-O, Table 3-2 B-D). Although there was no significant difference in overall expression levels between TG and DRG these data show differential distribution of p55 across neurochemical populations with significantly lower IB4/p55 co-localisation (p=<0.01 t-test) within the TG along with trends towards higher levels of CGRP/p55 co-localisation and lower levels of NF200/p55 co-localisation in TG compared to DRG (Figure 3-3, Table 3-2).

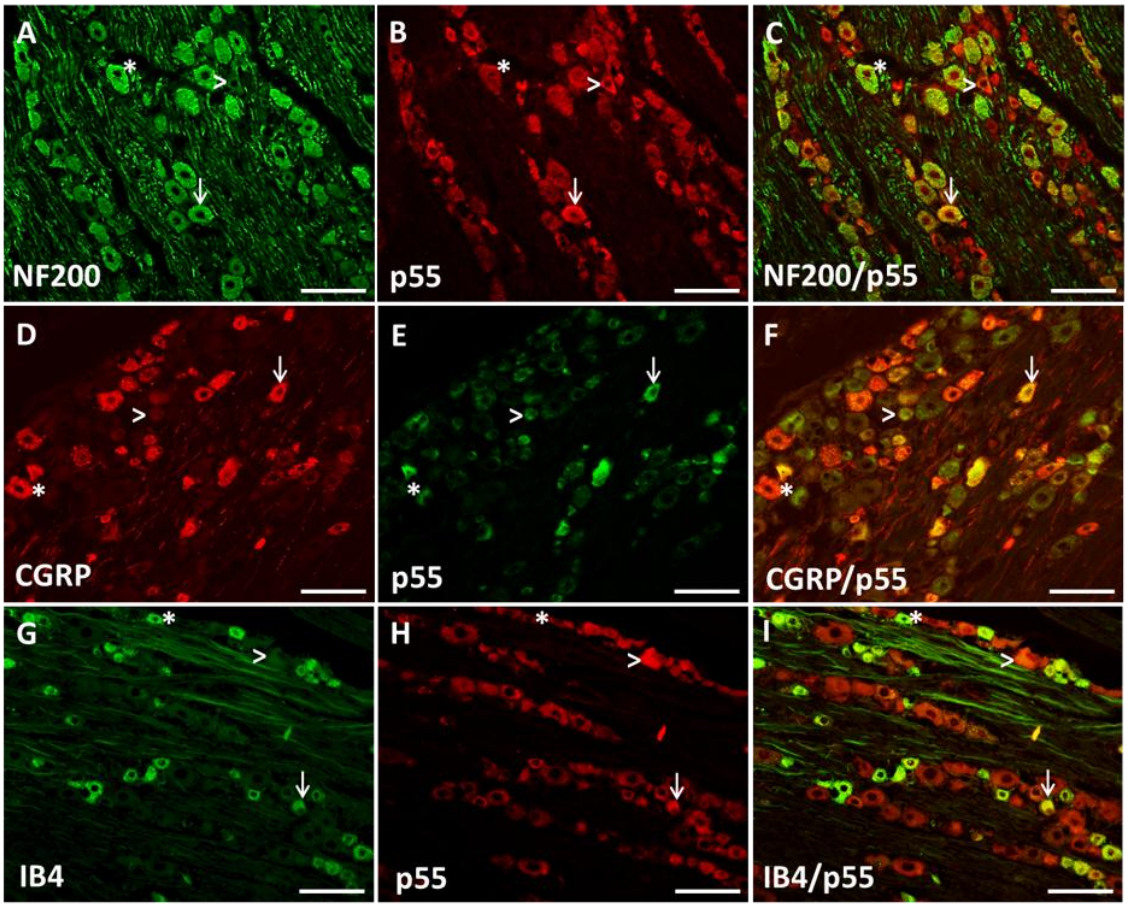

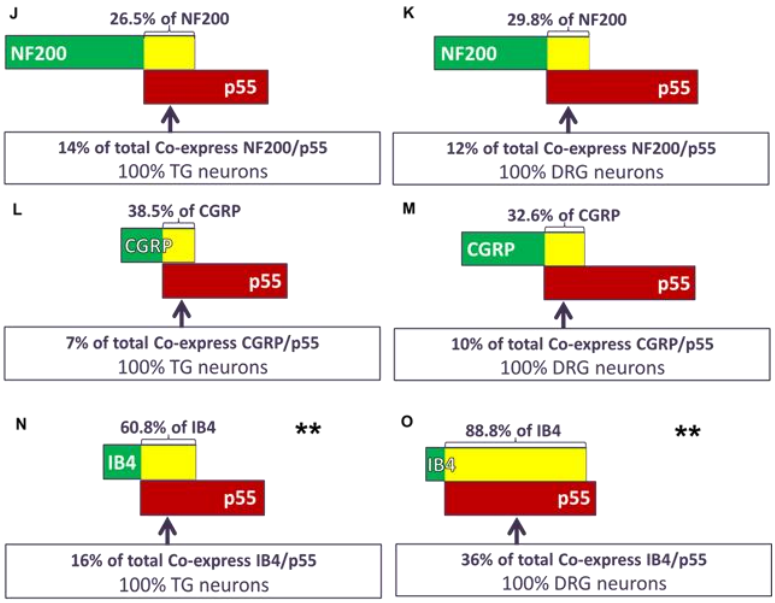

Figure 3-3: Photomicrographs showing expression and co-expression in TG of p55 with standard phenotypic markers NF200 (**A-C**), CGRP (**D-F**) and IB4 (**G-I**). Bars illustrate levels of expression and co-expression as a proportion of each phenotypic marker and as a percentage of entire TG or DRG. NF200 (**J** (TG) **K** (DRG)) CGRP (**L** (TG) **M** (DRG)) IB4 (**N** (TG) **O** (DRG)). A significantly lower proportion of IB4+ cells (p=<0.01) co-localised with p55 in TG compared to DRG. Panels **A-I** (*) shows marker of interest only; (arrowheads) p55 only; (arrows) co-expression. Scale bar 100 µm.

In TG, the overall cell size distribution for p55+ profiles ranged from 200 – 2,200 µm² (median value 530 µm²; 816 profiles) with a peak at 400 µm² (Figure 3-4 A). In DRG, cell size range was 200 – 2,600 µm² (median value 636 µm²; 773 profiles) with a peak at 600 µm² (Figure 3-4 B). There was a significant difference between mean values for overall cell size distributions of p55+ profiles in TG compared to DRG (*p*=<0.001 t-test) (Figure 3-4 A-B, Table 3-3). P55+ profiles were distributed within cell size groups in TG and DRG as follows: small 46.84% vs. 28.57%, medium 43.14% vs. 51.24%, large 10.02% vs. 20.2% respectively (Figure 3-4 C). These data show that p55 was preferentially and significantly distributed within the small cell size group in TG compared to DRG (*p*=<0.05 t-test) (Figure 3-4 C, Table 3-3).

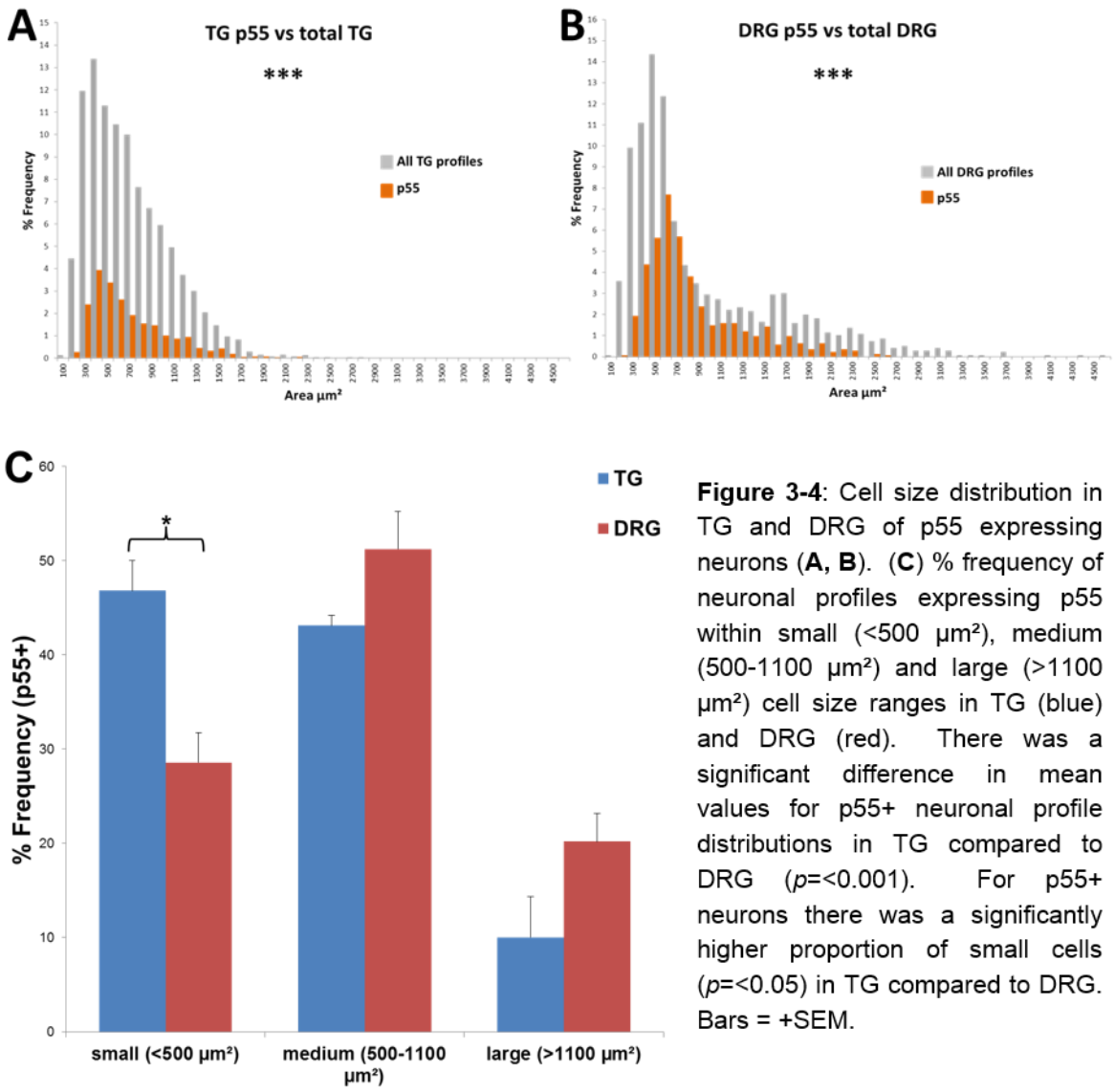

Figure 3-4: Cell size distribution in TG and DRG of p55 expressing neurons (**A, B**). (**C**) % frequency of neuronal profiles expressing p55 within small (<500 µm²), medium (500-1100 µm²) and large (>1100 µm²) cell size ranges in TG (blue) and DRG (red). There was a significant difference in mean values for p55+ neuronal profile distributions in TG compared to DRG (p=<0.001). For p55+ neurons there was a significantly higher proportion of small cells (p=<0.05) in TG compared to DRG. Bars = +SEM.

3.3.3. Gp130 – Expression, co-expression and cell size distribution

Indirect dual immunofluorescence was used to define the proportion of neurons expressing the IL-6 family receptor, gp130, within the TG and DRG and to observe the degree of co-localisation with standard neurochemical markers. The proportion of neuronal profiles which were gp130+ in the TG and DRG was 99.29±0.42% vs. 100% respectively (n=3). These data were not significantly different between TG

compared to DRG. Examination of co-expression of gp130 with NF200 revealed virtual complete co-localisation in both TG and DRG (Figure 3-5).

Gp130 was found to be ubiquitously expressed throughout both the TG and DRG. Therefore, cell size distribution for gp130 matches our results for the entire TG and DRG presented in Chapter 2, section 2.3.2.

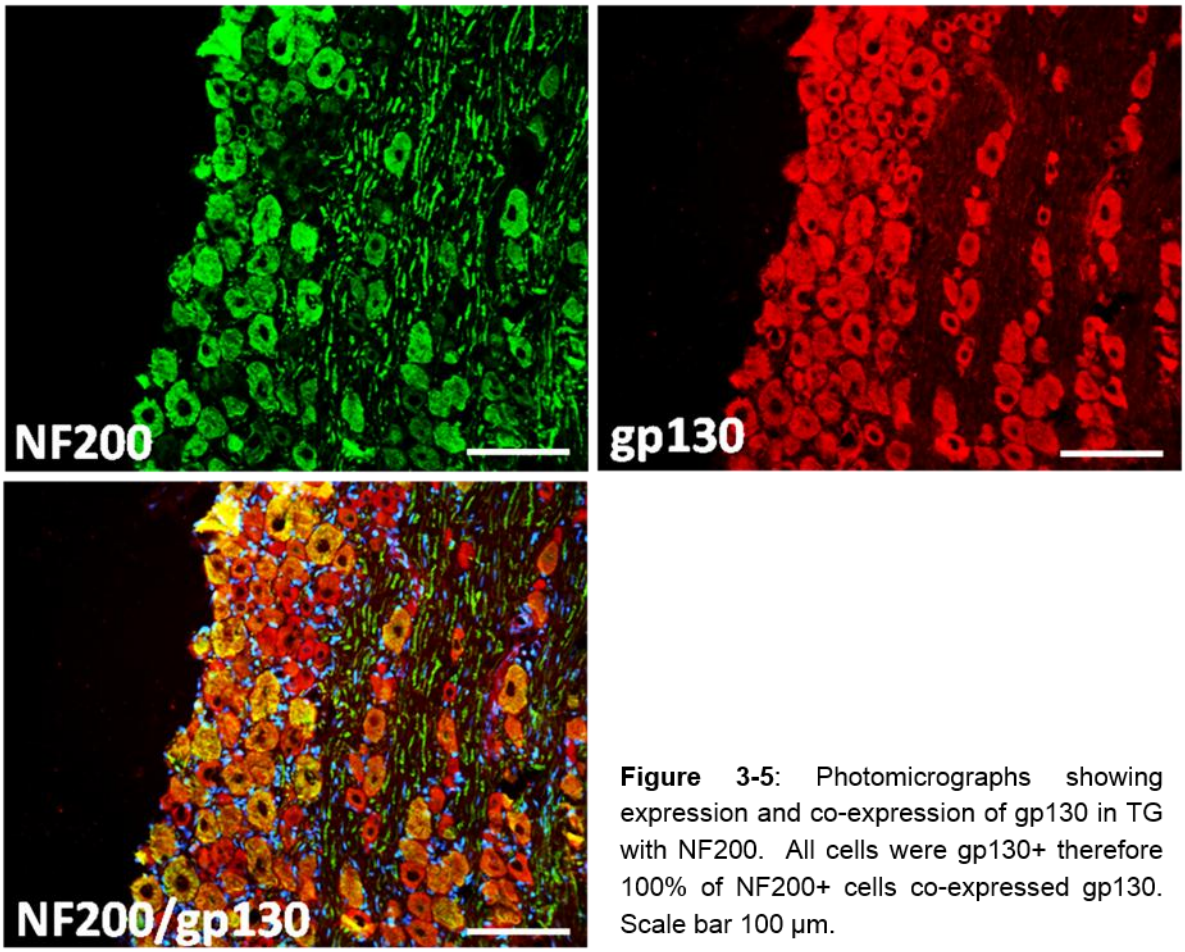

Figure 3-5: Photomicrographs showing expression and co-expression of gp130 in TG with NF200. All cells were gp130+ therefore 100% of NF200+ cells co-expressed gp130. Scale bar 100 µm.

3.3.4. TRPV1 – Expression, co-expression and cell size distribution

Indirect dual immunofluorescence was used to define the proportion of neurons expressing the transducer protein TRPV1, within the TG and DRG and to observe the degree of co-localisation with NF200, CGRP and IB4 (Figure 3-6). Previous work

(Michael and Doufexi, 2000) has identified small sub-populations of DRG and TG neurons expressing high levels of TRPV1. Furthermore, these neurons do not express the markers normally associated with nociceptors and appear to express a unique repertoire of neurotrophic factor receptors (Michael and Doufexi, 2000, Kiasalari *et al.*, 2010). When examining expression levels for TRPV1 across the entire TG or DRG we have therefore distinguished a separate population of high-expressing TRPV1 neuronal profiles (HE-TRPV1+) from normal expressing TRPV1 neurons (TRPV1+). As described earlier, distinction between levels of expression for HE-TRPV1+ and normal TRPV1+ neurons was made by visual examination and by using a threshold measurement of fluorescence intensity.

The proportion of profiles which were HE-TRPV1+ in the TG compared to the DRG was, 0.25±0.03% (n=5) vs. 0.89±0.14% (n=5) respectively (Table 3-2 A). The proportion of profiles which were TRPV1+ in the TG compared to the DRG was, 26.73±1.3% (n=5) vs. 33.12±1.8% (n=5) respectively (Table 3-2 A). Within the TG, TRPV1 was co-localised as follows: NF200+/TRPV1+, 3.13±0.33% (n=3); CGRP+/TRPV1+, 68.5±4.0% (n=3); IB4+/TRPV1+, 61.67±5.3% (n=3). Corresponding values within the DRG were: NF200+/TRPV1+, 5.23±0.28% (n=3); CGRP+/TRPV1+, 48.93±5.6% (n=3); IB4+/TRPV1+, 52.9±6.6% (n=3) (Figure 3-6 J-O, Table 3-2 B-D). Overall levels of both HE-TRPV1 and TRPV1 were significantly lower in TG compared to DRG (p=<0.05, p=<0.05 respectively). Similarly, there was significantly less co-localisation of NF200/TRPV1 in TG compared to DRG (p=<0.05). Moreover, there were trends towards higher levels of CGRP/TRPV1 and IB4/TRPV1 co-localisation in TG compared to DRG (Figure 3-6, Table 3-2).

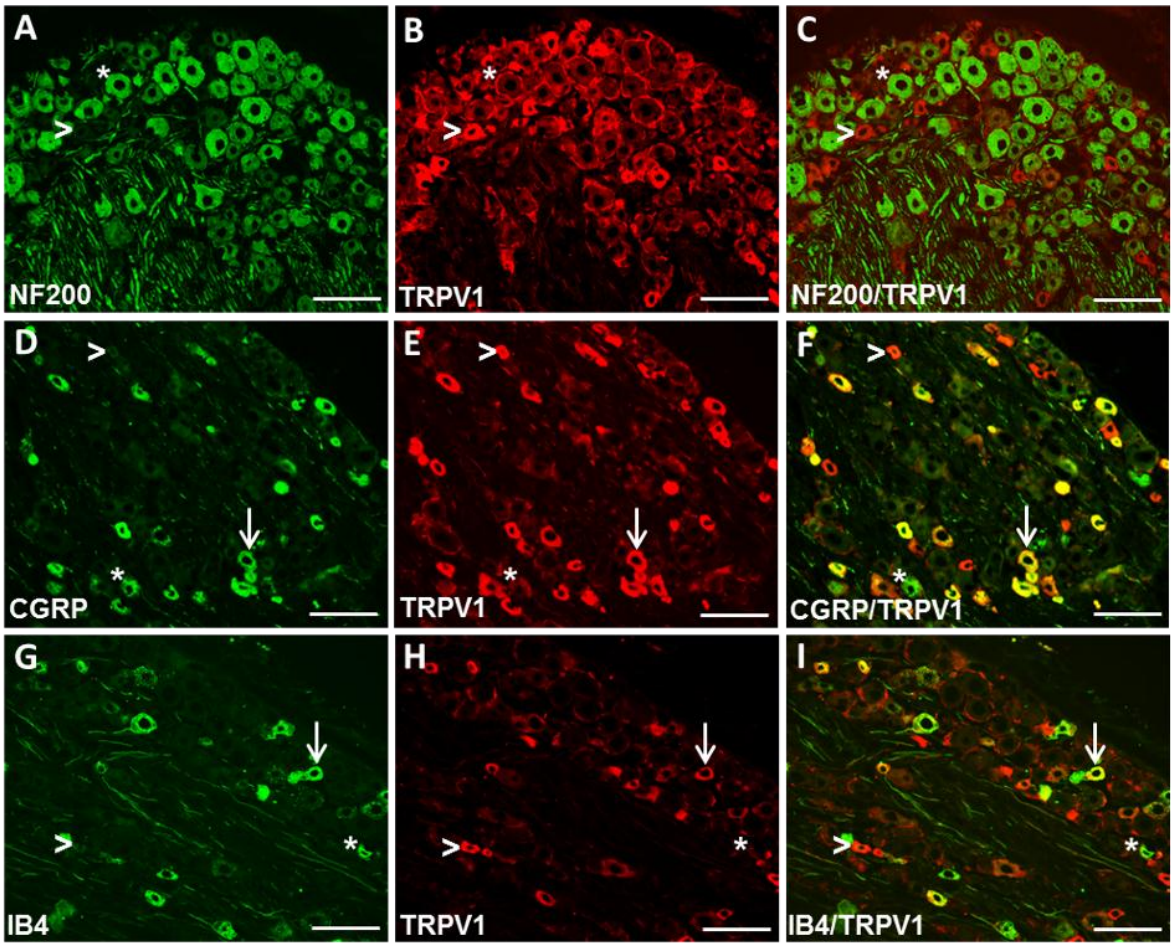

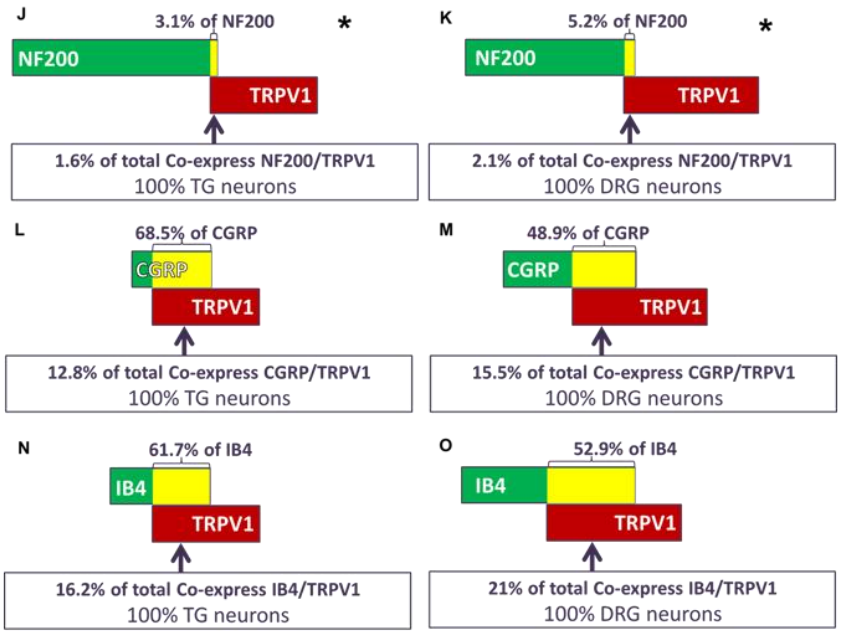

Figure 3-6: Photomicrographs showing expression and co-expression in TG of TRPV1 with standard phenotypic markers NF200 (**A-C**), CGRP (**D-F**) and IB4 (**G-I**). Bars illustrate levels of expression and co-expression as a proportion of each phenotypic marker and as a percentage of entire TG or DRG. NF200 (**J** (TG) **K** (DRG)) CGRP (**L** (TG) **M** (DRG)) IB4 (**N** (TG) **O** (DRG)). A significantly lower proportion of NF200+ cells (p=<0.05) co-localised with TRPV1 in TG compared to DRG. Panels A-I (*) shows marker of interest only; (arrowheads) TRPV1 only; (arrows) co-expression. Scale bar 100µm.

In TG, the overall cell size distribution for TRPV1+ profiles ranged from 200 – 1,800 µm² (median value 440 µm²; 1851 profiles) with a peak at 400 µm² (Figure 3-7 A). In DRG, cell size range was 200 – 1,900 µm² (median value 595 µm²; 1463 profiles) with a peak at 700 µm² (Figure 3-7 B). There was a significant difference between mean values for overall cell size distributions of TRPV1+ profiles in TG compared to DRG (p=<0.001 t-test) (Figure 3-7 A-B, Table 3-3). TRPV1+ profiles were distributed within cell size groups in TG and DRG as follows: small 59.81% vs. 33.04%, medium 37.19% vs. 64.98%, large 2.1% vs. 1.98% respectively (Figure 3-7 C). These data show that TRPV1 was significantly enriched in the small cell size group in TG (p=<0.01 t-test) whilst being significantly lower in the medium cell size group in TG compared to DRG (p=<0.01 t-test) (Figure 3-7 C, Table 3-3).

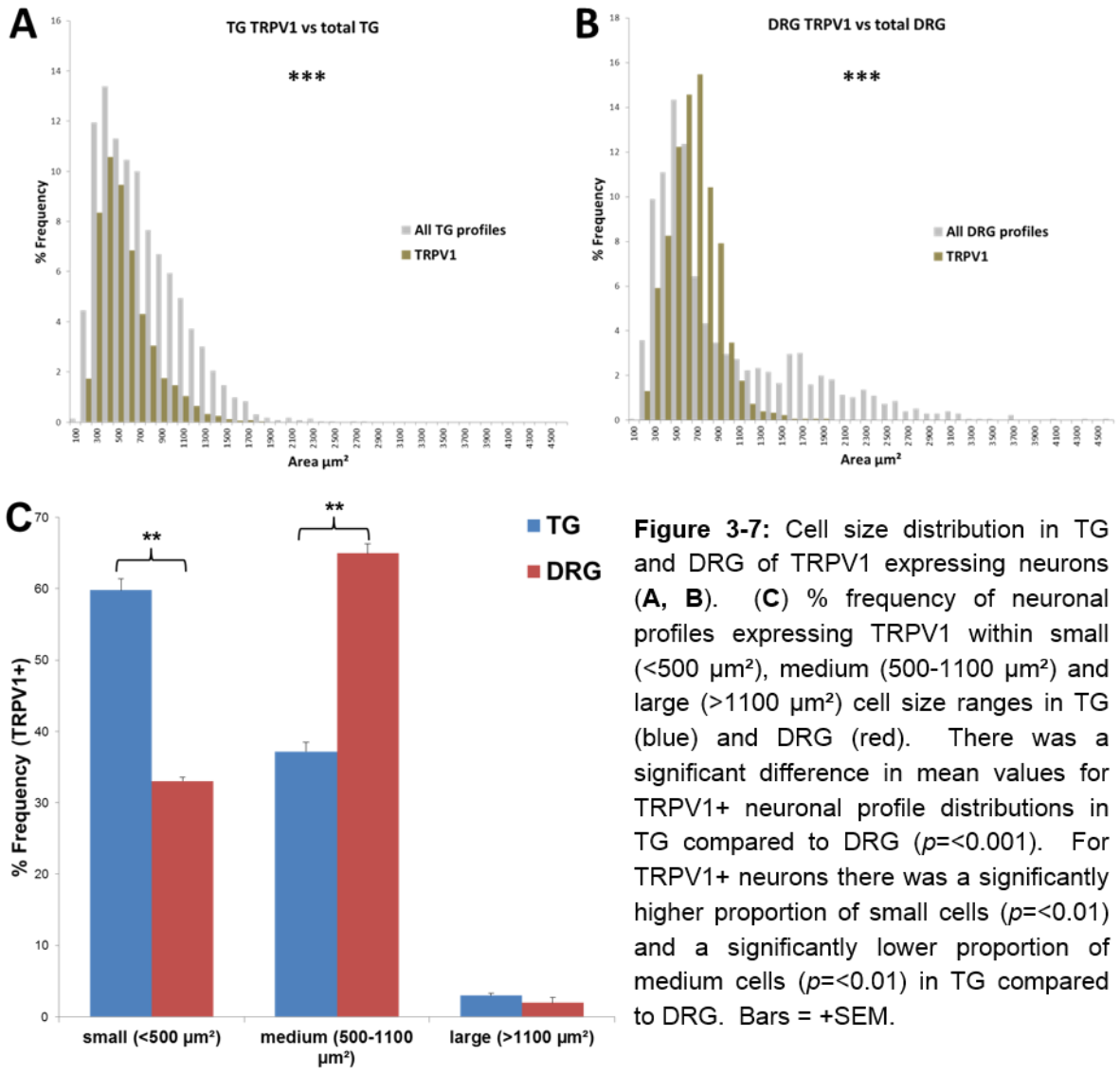

Figure 3-7: Cell size distribution in TG and DRG of TRPV1 expressing neurons (**A, B**). (**C**) % frequency of neuronal profiles expressing TRPV1 within small (<500 µm²), medium (500-1100 µm²) and large (>1100 µm²) cell size ranges in TG (blue) and DRG (red). There was a significant difference in mean values for TRPV1+ neuronal profile distributions in TG compared to DRG (p=<0.001). For TRPV1+ neurons there was a significantly higher proportion of small cells (p=<0.01) and a significantly lower proportion of medium cells (p=<0.01) in TG compared to DRG. Bars = +SEM.

3.3.5. TRPM8 – Expression, co-expression and cell size distribution

Indirect dual immunofluorescence was used to define the proportion of neurons expressing the transducer protein TRPM8 within the TG and DRG and to observe the degree of co-localisation with NF200, CGRP and IB4 (Figure 3-8). The proportion of total profiles which were TRPM8+ in the TG compared to the DRG was, 10.89±1.3% (n=3) vs. 6.24±0.3% (n=3) respectively (Table 3-2 A). There was no significant difference between these values. Expression of TRPM8 was found to be completely

exclusive of all standard neurochemical markers (NF200, CGRP or IB4) in both TG and DRG (Figure 3-8, Table 3-2).

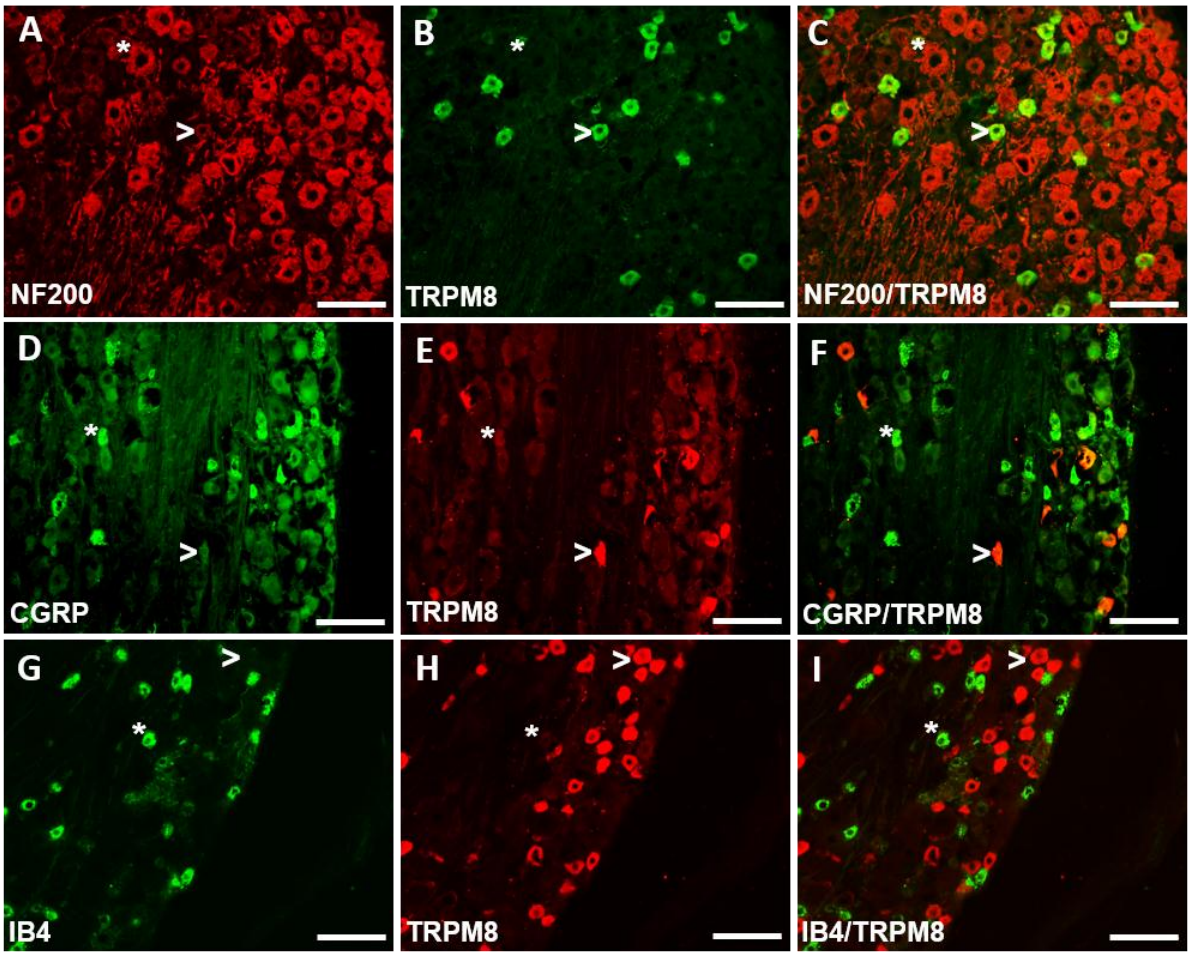

Figure 3-8: Photomicrographs showing expression and co-expression in TG of TRPM8 with standard phenotypic markers NF200 (**A-C**), CGRP (**D-F**) and IB4 (**G-I**). In both TG and DRG, TRPM8 expression was completely exclusive of all standard neurochemical markers (NF200, CGRP or IB4). Panels A-I (*) shows marker of interest only; (arrowheads) TRPM8 only. Scale bar 100µm.

In TG, the overall cell size distribution for TRPM8+ profiles ranged from 100 – 800 µm² (median value 327 µm²; 752 profiles) with a peak at 400 µm² (Figure 3-9 A). In DRG, cell size range was 100 – 900 µm² (median value 224 µm²; 333 profiles) with a peak at 200 µm² (Figure 3-9 B). There was a significant difference between mean values for overall cell size distributions of TRPM8+ profiles in TG compared to DRG

(*p*=<0.001 t-test) (Figure 3-9 A-B, Table 3-3). TRPM8+ profiles were distributed within cell size groups in TG and DRG as follows: small 90.06% vs. 91.05%, medium 9.94% vs. 8.95% respectively (Figure 3-9 C). No neuronal profiles in either TG or DRG were found within the large cell size group (Figure 3-9 A-C, Table 3-3). The significant difference in mean values for overall cell size distribution indicates that although the majority of cells in both TG and DRG are within the small cell size group, the cells from each ganglion are differentially distributed within this size range.

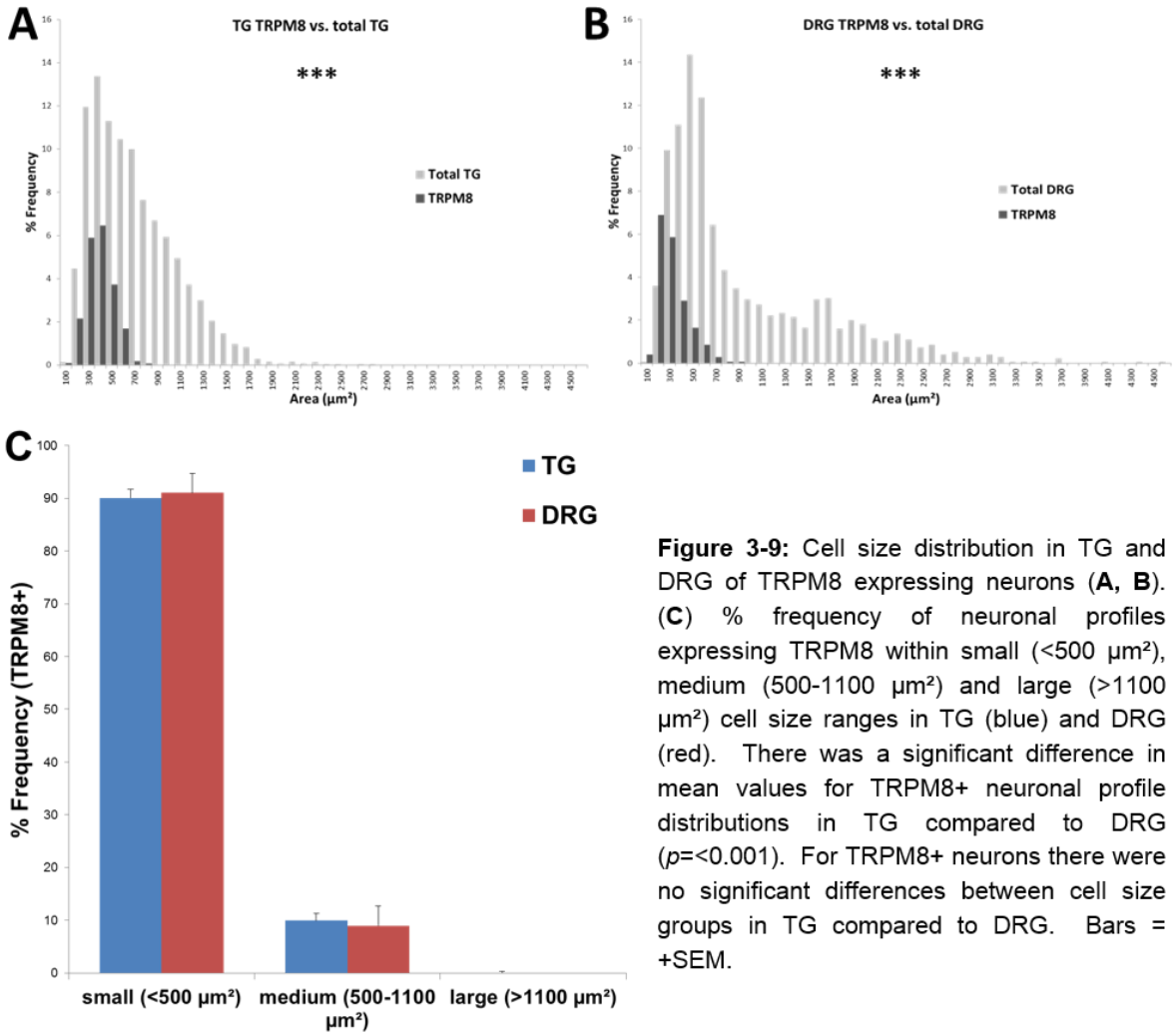

Figure 3-9: Cell size distribution in TG and DRG of TRPM8 expressing neurons (**A, B**). (**C**) % frequency of neuronal profiles expressing TRPM8 within small (<500 µm²), medium (500-1100 µm²) and large (>1100 µm²) cell size ranges in TG (blue) and DRG (red). There was a significant difference in mean values for TRPM8+ neuronal profile distributions in TG compared to DRG (*p*=<0.001). For TRPM8+ neurons there were no significant differences between cell size groups in TG compared to DRG. Bars = +SEM.

Table 3-2: **A**) Proportion of neuronal profiles in entire TG and DRG expressing TrkA, p55, HE-TRPV1, TRPV1 and TRPM8. **B,C,D**) Proportion of neuronal profiles co-expressing neurochemical phenotypic markers (NF200 (B), CGRP (C), IB4 (D)) and TrkA, p55 and TRPV1.

A	% expression in entire TG and DRG (positive neuronal profiles/total counted)				
	TrkA	P55	HE-TRPV1	TRPV1	TRPM8
TG	**24.2±0.8%** (4,800/20,048) (n=6)	**33.01±4.2%** (5,915/17,937) (n=4)	**0.25±0.03%** (61/23,478) (n=5)	**26.73±1.3%** (6,367/23,478) (n=5)	**10.89±1.3%** (807/6,915) (n=3)
DRG	**27.87±1.9%** (2,943/9,968) (n=6)	**38.05±2.9%** (1,883/4,914) (n-3)	**0.89±0.14%** (138/15,049) (n=5)	**33.12±1.8%** (5,152/15,049) (n=5)	**6.24±0.3%** (350/5,437) (n=3)
	n/s	n/s	**(*p*=<0.05)**	**(*p*=<0.05)**	n/s (*p*=0.076)

B	% NF200 expressing other		
	TrkA	P55	TRPV1
TG	**16.52±1.3%** (419/2,458) (n=3)	**26.53±2.2%** (915/3,390) (n=3)	**3.13±0.33%** (78/2,442) (n=3)
DRG	**22.80±6.5%** (173/600) (n=3)	**29.8±7.0%** (201/627) (n=3)	**5.23±0.28%** (55/1,061) (n=3)
	n/s	n/s	**(*p*=<0.05)**

C	% CGRP expressing other		
	TrkA	P55	TRPV1
TG	**60.63±3.8%** (1,021/1,708) (n=5)	**38.45±3.1%** (539/1,360) (n=3)	**68.5±4.0%** (709/1,047) (n=3)
DRG	**78.54±2.5%** (1,090/1,481) (n=5)	**32.56±1.4%** (158/484) (n=3)	**48.93±5.6%** (289/582) (n=3)
	(*p*=<0.01)	n/s	n/s (*p*=0.066)

D	% IB4 expressing other		
	TrkA	P55	TRPV1
TG	**11.32±1.6%** (121/1,067) (n=3)	**60.82±1.5%** (612/1,006) (n=3)	**61.67±5.3%** (775/1,273) (n=3)
DRG	**11.22±1.1%** (118/1,052) (n=3)	**88.83±1.4%** (599/676) (n=3)	**52.9±6.6%** (755/1,430) (n=3)
	n/s	**(*p*=<0.01)**	n/s

Table 3-3: Summary of cell size distribution data for neuronal profiles expressing TrkA, p55, TRPV1 and TRPM8 in TG and DRG.

	Neuronal Profile range (μm^2)	Median value (μm^2)	*P=*	Modal Peak value(s) (μm^2)	% small <500 μm^2	*P=*	% medium 500-1100μm^2	*p=*	% large >1100 μm^2	*P=*	No. profiles measured
TrkA											
TG	100-2000	530.27	<0.001	400	44.41	n/s	44.88	<0.05	10.71	<0.01	1884
DRG	200-3300	641.33		400	38.02		37.56		24.42		1014
P55											
TG	200-2200	529.64	<0.001	400	46.84	<0.05	43.14	n/s	10.02	n/s	816
DRG	200-2600	635.92		600	28.57		51.24		20.2		773
TRPV1											
TG	200-1800	439.59	<0.001	400	59.81	<0.01	37.19	<0.01	2.10	n/s	1851
DRG	200-1900	595.44		700	33.04		64.98		1.98		1463
TRPM8											
TG	100-800	326.6	<0.001	400	90.06	n/s	9.94	n/s	Nil	n/s	752
DRG	100-900	223.84		200	91.05		8.95		Nil		333

Table 3-4: Summary of expression and cell size data in TG and DRG from previous research studies on TrkA, p55, gp130, TRPV1 and TRPM8.

Region	Rat (R) Mouse (M)	Protein (P) or mRNA	% Neuronal expression over entire ganglia	% Expression within neuronal sub-population	% Co-Expression (x/y = % of x which co-express y)	% Co-Expression within sub-populations (x/y = % of x which co-express y)	Cell size	Reference
TrkA								
DRG	R	P	40-45%				<706 µm²	(Averill *et al.*, 1995, McMahon, 1996, Kobayashi *et al.*, 2005)
DRG	R	P			90% CGRP/TrkA			(Averill et al., 1995)
DRG	R	P			25% NF200/TrkA			(McMahon and Priestley, 2005)
DRG	R	P			6-12% IB4/TrkA			(Averill et al., 1995, McMahon, 1996)
DRG	R	mRNA	45%					(Wetmore and Olson, 1995)
TG	R	P	40%	70% gingivomucosa			Most small-medium	(Gaspersic *et al.*, 2007)
TG	R	mRNA	45%					(Wetmore and Olson, 1995)
TG	R	P	68%				<530 µm²	(Jacobs and Miller, 1999)
TG	M	P		10% incisor pulp	43% TrkA/CGRP	Nil CGRP/TrkA (incisor pulp)	Medium-large	(Mosconi *et al.*, 2001)
TG	M	mRNA	53%				<1300 µm²	(Krol *et al.*, 2001)
TG	R	P		78% molar pulp 38% non-pulpal neurons		100% CGRP/TrkA (molar pulp)	Molar pulp - Peak between 1257-1590 µm²	(Yang *et al.*, 2006)
TG	R	P		72% molar pulp 55% surrounding maxillary region			>500 µm² (pulp) <500 µm² (neighbouring cells)	(Pan *et al.*, 2000)
TG	R	P		70% masseter			All cell sizes	(Svensson *et al.*, 2010)
P55								
DRG	R	P	13%					(Sakuma *et al.*, 2007)
DRG	R	P	15%				Small (C fibres)	(Xu *et al.*, 2006)
TG	R	P			>90% TRPV1/p55			(Khan *et al.*, 2008)
TG	R	P	None					(Zhang *et al.*, 2011)
TG	R	P			Majority CGRP/p55			(Bowen *et al.*, 2005)
TG	R	P		29% masseter				(Hakim *et al.*, 2009)
Gp130								
DRG	R	P	100%					(Gardiner *et al.*, 2002)
TG	R	mRNA	>90%					(Mizuno *et al.*, 1997)

Table 3-4: continued.

Region	Rat (R) Mouse (M)	Protein (P) or mRNA	% Neuronal expression over entire ganglia	% Expression within neuronal sub-population	% Co-Expression (x/y = % of x which co-express y)	% Co-Expression within sub-populations (x/y = % of x which co-express y)	Cell size	Reference
TRPV1								
DRG	R	P	50%					(Guo *et al.*, 1999, Kobayashi et al., 2005, Kiasalari *et al.*, 2010)
DRG	R	P			65% CGRP/TRPV1 75% IB4/TRPV1 3% NF200/TRPV1			(Guo et al., 1999, Priestley *et al.*, 2002, McMahon and Priestley, 2005)
TG	R	P	50%				Most <175 µm²	(Simonetti *et al.*, 2006)
TG	R	P	48%		44% TRPV1/CGRP		Most <800 µm²	(Bae *et al.*, 2004)
TG	R	P	46%				Most <706 µm²	(Tanimoto *et al.*, 2005, Kiasalari et al., 2010)
TG	R	P	44%					(Kobayashi et al., 2005)
TG	R	P	27%				Most <314 µm²	(Nagamine *et al.*, 2006)
TG	R	P	26%	17% molar pulp 26% periodontal tissues				(Gibbs *et al.*, 2011)
TG	R	P	24%				Most <800 µm²	(Pei *et al.*, 2007)
TG	R	P	20%	8% molar pulp 26% facial skin	53% CGRP/TRPV1	20% CGRP/TRPV1 (molar pulp) 63% CGRP/TRPV1 (facial skin)	Mean 427 µm²	(Ichikawa and Sugimoto, 2001)
TG	R	P	16%		68% CGRP/TRPV1 28% IB4/TRPV1		Mean 400 µm²	(Price and Flores, 2007)
TG	R	P		21-23% molar pulp 21-26% gingiva				(Stenholm *et al.*, 2002)
TG	R	P		35% masseter region				(Saloman *et al.*, 2013)
TG	R	P		37% cornea				(Murata and Masuko, 2006)
TG	R	P				21% TRPV1/CGRP (dura mater)		(Shimizu *et al.*, 2007)

Table 3-4: continued.

Region	Rat (R) Mouse (M)	Protein (P) or mRNA	% Neuronal expression over entire ganglia	% Expression within neuronal sub-population	% Co-Expression (x/y = % of x which co-express y)	% Co-Expression within sub-populations (x/y = % of x which co-express y)	Cell size	Reference
TRPM8								
DRG	R	mRNA	23%		8% TRPM8/TRPV1 21% TRPM8/TrkA			(Kobayashi et al., 2005)
DRG	R	mRNA	5-10%				Mean 254 µm²	(Peier *et al.*, 2002)
DRG	R	P	6%					(Su *et al.*, 2011)
DRG	R	P			81% TRPM8/NF200 22% TRPM8/CGRP 5% TRPM8/IB4 17% TRPM8/TRPV1			(Hayashi *et al.*, 2009)
DRG	M	P	13%		14% TRPM8/NF200 20% TRPM8/CGRP 24% TRPM8/TRPV1		Most <380 µm²	(Takashima *et al.*, 2007)
DRG	M	P	7-9%					(Harrington *et al.*, 2011)
DRG	M	P	8%		12% TRPM8/TRPV1			(Dhaka *et al.*, 2008)
TG	R	mRNA	35%					(Kobayashi et al., 2005)
TG	R	P	12%		76% TRPM8/NF200 3% TRPM8/CGRP 5% TRPM8/TRPV1		Mean 380 µm²	(Abe *et al.*, 2005)
TG	M	P	13%		26% TRPM8/NF200 32% TRPM8/CGRP 39% TRPM8/TRPV1		Most <380 µm²	(Takashima et al., 2007)
TG	M	P	10%		19% TRPM8/TRPV1			(Dhaka et al., 2008)

3.3.6. Summary of results

- There are significantly lower levels of CGRP/TrkA co-localisation in TG, along with a trend towards lower levels of NF200/TrkA co-localisation in TG compared to DRG (Figure 3-1, Table 3-2). There are significantly more TrkA+ cells within the medium cell size range and significantly fewer within the large cell size range in TG, along with a trend towards a higher number of TrkA+ cells within the small cell size range in TG compared to DRG (Figure 3-2, Table 3-3).

- There are significantly lower levels of IB4/p55 co-localisation in TG, along with trends towards less NF200/p55 co-localisation and more CGRP/p55 co-localisation in TG compared to DRG (Figure 3-3, Table 3-2). There are significantly more p55+ cells within the small cell size range, along with trends towards a lower number of p55+ cells within both medium and large cell size ranges in TG compared to DRG (Figure 3-4, Table 3-3).

- Gp130 was found to be constitutively expressed in all cells in both TG and DRG, thus gp130+ cells are present throughout all cell size ranges (Figure 3-5).

- Overall there are significantly lower levels of both HE-TRPV1 and TRPV1 expression in TG compared to DRG. Furthermore, there are significantly lower levels of NF200/TRPV1 co-localisation, along with trends towards higher levels of CGRP/TRPV1 and IB4/TRPV1 co-localisation in TG compared to DRG (Figure 3-6, Table 3-2). There are significantly more TRPV1+ cells within the small cell size range and significantly less within the medium cell size range in TG compared to DRG (Figure 3-7, Table 3-3).

- Overall, there was a trend towards higher levels of TRPM8 expression in TG compared to DRG. No co-localisation of TRPM8 was found with NF200, CGRP or IB4 in either TG or DRG (Figure 3-8, Table 3-2). There was no difference between proportions of TRPM8+ cells within cell size groups in TG compared to DRG (Figure 3-9, Table 3-3).

3.4. Discussion

Approximately 95% of chronic orofacial pain arises from diseases of the teeth or periodontal region (Scully, 2008). In addition, around 7% of the UK population suffer from chronic orofacial pain of a non-dental origin (Zakrzewska, 2007). Furthermore, the aetiology of syndromes with significant non-dental contributions such as burning mouth syndrome (BMS), a relatively common condition, atypical facial pain and trigeminal neuralgia are poorly understood (Scully, 2008). It is likely that many of these syndromes may have precipitating factors that involve activation of TG neurons by injury-induced inflammatory mediators. In order to understand the interaction of such mediators within the TG system, we have determined expression patterns and cell size distributions for several markers conferring a nociceptive phenotype and compared our results with those in the DRG.

Previous clinical and animal studies have concluded that the some of the most potent inflammatory mediators present during chronic inflammatory states are NGF, TNFα and IL-6 (Pezet and McMahon, 2006, Andratsch *et al.*, 2009, Miller *et al.*, 2009). We have therefore made a detailed study on expression levels of receptor components for these inflammatory mediators in TG and DRG, namely TrkA, p55 and gp130. In addition we have investigated expression of two thermal transducer proteins, TRPV1 and TRPM8, both of which have been linked to inflammatory pain (Patapoutian *et al.*, 2009, Babes *et al.*, 2011).

A summary of expression and cell size data from previous research studies investigating the markers of interest to this study, can be found in Table 3-4, in addition to a more detailed analysis below.

3.4.1. Expression of cytokine receptors and transducers: a direct comparison between TG and DRG

In the somatosensory system TrkA is traditionally thought to be a marker of nociceptive function, being almost exclusively co-expressed by CGRP+ neurons within DRG (Priestley, 2009). TrkA expression in the TG was found to correspond with levels in the DRG by Gaspersic *et al*. (2007), who showed that approximately 40% of neurons within the rat TG expressed TrkA. Their results also showed that 90% of TrkA-expressing neurons were small to medium in size, suggesting that most TG TrkA-expressing neurons were nociceptors. Of interest were their findings that 70% of TG neurons innervating the gingivomucosa were TrkA-expressing. Thus this unique orofacial region appears to be predominately innervated by nociceptors and would therefore be highly susceptible to NGF released within the inflammatory soup. Furthermore, a study investigating expression of rat TrkA mRNA in TG and DRG found levels to be the same in both ganglia at 45% (Wetmore and Olson, 1995).

There is evidence however, that the accepted levels of TrkA expression in the DRG may not directly transpose to the TG. One study observed TrkA expression of around 68%, all within small sized neurons (<530 μm^2) in rat TG (Jacobs and Miller, 1999). Mosconi *et al*. (2001) found that the relationship between TrkA expression and nociceptive phenotype appeared to be less clear-cut within the TG. Their results on mice TG, showed that most cells expressing TrkA were medium to large in size. Furthermore, only 43% TrkA+ cells co-expressed CGRP, whereas in the DRG TrkA is expressed almost exclusively in CGRP+ cells which are mostly small to medium in size (<706 μm^2) (Averill *et al.*, 1995). Another study using mice observed 53% of TG neuronal cells expressed TrkA mRNA, although cell size was more in line with TrkA+

cells of the DRG, as these were found to be predominantly small to medium in size (<1300 μm²) (Krol *et al.*, 2001).

Further contradictory results arise when investigating subpopulations of TG neurons. Mosconi *et al*. (2001) found only 10% of neurons innervating incisor pulp in mice were TrkA+ and of particular interest, they demonstrated no co-expression within these neurons of TrkA and CGRP. In contrast, Yang *et al.* (2006) showed 78% of neurons innervating rat molar pulp expressed TrkA with only 38% TrkA-expressing neurons in non-pulpal afferents, suggesting a larger proportion of nociceptors innervating tooth pulp than the surrounding tissues. Moreover, when investigating co-expression of TrkA and CGRP, they found that all CGRP+ cells also expressed TrkA. Interestingly, the majority of TrkA+ cells within the molar pulp were in the medium to large cell size range, peaking at around 1257-1590 μm² (Yang *et al.*, 2006). These findings concur with an earlier study by Pan *et al.* (2000) who observed TrkA expression in 72% of rat molar pulp neurons and 55% in surrounding maxillary neurons. Here again, pulpal neuronal cells were found to be considerably larger than their neighbouring cells, with the majority of pulp cells shown to be medium to large (>500 μm²) and the majority of neighbouring cells small (<500 μm²). Finally, 70% of rat TG masseter neurons were TrkA+ and expression was uniformly distributed among all cell size ranges (Svensson *et al.*, 2010). These data show that there is significant discrepancy between the DRG and TG in relation to the potential for TG cells to respond to NGF, an important inflammatory mediator.

Over the entire ganglia, we have observed TrkA expression to be slightly lower in TG compared to DRG (24% and 28% respectively). Interestingly, we have shown significantly less co-expression of TrkA within the CGRP+ population in TG (61%) compared to DRG (79%). Expression of TrkA within the IB4+ population was similar

in both ganglia at 11%. Whereas we observed a trend towards less co-expression of TrkA in the NF200+ population in TG compared to DRG (17% and 23% respectively) (Figure 3-1, Table 3-2).

When interpreting our data, the results from a previous study by Yang *et al.* (2006) on rat molar pulp are of particular interest. In their study, although all CGRP+ cells also expressed TrkA, only 35% of TrkA+ cells co-expressed CGRP. Furthermore, 65% of pulpal neuronal cells co-expressed TrkA and GFRα-1, the receptor for glial cell line-derived neurotrophic factor (GDNF). In the DRG, TrkA and CGRP are almost exclusively co-expressed and make up the peptidergic population of nociceptors, whereas, GFRα-1, is almost exclusively expressed on the IB4+ population of non-peptidergic nociceptors (McMahon and Priestley, 2005). Therefore, within the tooth pulp, this unusual co-expression of TrkA and GFRα-1, and reduced neuropeptide expression, may indicate a population of neurons with a unique functional phenotype. Our data would concur with this, in that we have shown a significantly smaller population of CGRP+ neurons over the entire TG (see Chapter 2) and in addition, only 48% of TrkA+ cells were CGRP+. Conversely, 39% of CGRP+ cells did not express TrkA, the activation of which is known to regulate neuropeptide expression (Pezet and McMahon, 2006). This could imply regulation of neuropeptide expression by a neurotrophin other than NGF, possibly GDNF via its receptor GFRα-1.

Our study shows that a significant portion of TG neurons express the TNFα receptor, p55. TNFα has been shown to activate sensory neurons directly (Schäfers *et al.*, 2003) and sensitise them via post-translational modification of transducer proteins such as TRPV1 (Nicol *et al.*, 1997). TNFα interacts with cells through two structurally related receptors, p55 and p75. Interestingly, activation of the p55 component has

been shown to play a key role in the development of hyperalgesia and allodynia (Sommer *et al.*, 1998, Moalem and Tracey, 2006, Schäfers *et al.*, 2008). Within the somatosensory system, p55 mRNA has been found to be constitutively expressed in the rat DRG (Li *et al.*, 2004). Protein levels however, have been observed as 13% and 15% in rat DRG (Xu *et al.*, 2006, Sakuma *et al.*, 2007). There is a paucity of previous evidence for p55 expression within rat TG. Bowen *et al.* (2005) showed p55 in the majority of CGRP+ neurons, and Hakim *et al.* (2009) found that 29% of masseter nociceptors expressed p55. Interestingly, another study was unable to locate p55 expression on any TG neurons and only observed expression in non-neuronal cells (Zhang *et al.*, 2011). Our study has for the first time determined p55 expression levels within neurochemically defined subpopulations of the TG. Over the entire TG and DRG, we have observed p55 expression in a similar proportion of neurons in both ganglia (33% and 38% respectively). In addition co-expression of p55 within the NF200+ populations were similar in both ganglia (27% TG vs. 30% DRG). We observed a slight trend towards higher CGRP/p55 co-expression with levels of 39% and 33% in TG compared to DRG respectively. Moreover, we can report significantly less co-expression of p55 within the IB4+ population of non-peptidergic nociceptors in TG compared to DRG (61% and 89% respectively), suggesting that in the TG, a smaller proportion of these nociceptors could respond either directly or indirectly to TNFα.

IL-6 is one of the most potent inflammatory mediators (Andratsch *et al.*, 2009) and is upregulated in various pathological conditions such as temporomandibular joint disorder (Wang *et al.*, 2009b). Following activation of its receptor subunits, IL-6 has been found to be a critical mediator of increased pain and hyperalgesia experienced following injury (Wang *et al.*, 2009c). Indeed, increased levels of IL-6 and NGF are suggested to contribute to the development of mechanical allodynia following

trigeminal nerve injury (Anderson and Rao, 2001). Expression of gp130 has been found to be almost ubiquitously expressed across all neurochemical sub-populations of the rat DRG (Gardiner *et al.*, 2002). Only one previous study has examined gp130 within rat TG and their findings showed that the majority of neurons expressed gp130 mRNA (Mizuno *et al.*, 1997). As far as we are aware, ours is the first study examining gp130 protein expression within the rat TG. We can report that our findings are in agreement with Gardiner *et al*. (2002), as we observed almost complete expression of gp130 across both TG (99%) and DRG (100%) (Figure 3-5). Thus, within the TG and DRG, all neuronal cells, including non-nociceptors, have the potential to respond to and be influenced by, the potent inflammatory cytokine, IL-6. Indeed, since gp130 has been shown to be essential for the long-term potentiation of hypersensitivity (Quarta *et al.*, 2011), these findings could have important implications in understanding the mechanisms underlying chronic pain conditions.

The thermal transducer protein TRPV1, is a common target for post-translational modification by potent inflammatory mediators such as NGF and TNFα (Nicol *et al.*, 1997, Bonnington and McNaughton, 2003b). In the DRG, previous data has shown that TRPV1 is expressed in around 50% of neurons, with the majority within the peptidergic and non-peptidergic populations of nociceptors (Guo *et al.*, 1999, McMahon and Priestley, 2005). As mentioned previously, one research group has identified a small sub-population of sensory neurons expressing high levels of TRPV1 (HE-TRPV1) and which display an unusual repertoire of receptor co-expression (Michael and Doufexi, 2000). Their results for HE-TRPV1 expression in TG and DRG (L4/5) were <1% and around 2% respectively. Our results for HE-TRPV1 expression are similar to this previous study, in that we observed significantly less expression within the TG compared to DRG (0.3% and 0.9% respectively) (Table 3-2).

In contrast to the generally agreed levels of TRPV1 expression and co-expression within the DRG, a number of reports show a wide variation in the proportions of neurons expressing TRPV1 in the TG. For instance, levels of TRPV1 expression in rat TG have been observed as: 50%, mostly in cells <175 μm² (Simonetti *et al.*, 2006); 48%, mostly in small to medium cells <800 μm² (Bae *et al.*, 2004); 46%, mostly in small cells <706 μm² (Tanimoto *et al.*, 2005, Kiasalari *et al.*, 2010); 44% (Kobayashi *et al.*, 2005); 27%, mostly in small cells <314 μm² (Nagamine *et al.*, 2006); 26% (Gibbs *et al.*, 2011); 24%, mostly in small to medium cells <800 μm² (Pei *et al.*, 2007); 20%, in cells with a mean area of 427 μm² (Ichikawa and Sugimoto, 2001); 16%, in cells with a mean area of around 400 μm² (Price and Flores, 2007); and the proportion of rat TG neurons responding to capsaicin as: 24% (although this study only tested Aδ and C fibre neurons) (Lam *et al.*, 2009).

TRPV1 expression has also been described with reference to the innervation targets of the neurons. Thus TRPV1 expression in sub-populations of rat TG have been reported as: 21-23% (Stenholm *et al.*, 2002), 17% (Gibbs *et al.*, 2011) and 8% in molar pulp (Ichikawa and Sugimoto, 2001); 26% in periodontal tissues (Gibbs *et al.*, 2011); 26% in facial skin (Ichikawa and Sugimoto, 2001); 21-26% in gingiva (Stenholm *et al.*, 2002); 35% in masseter afferents (Saloman *et al.*, 2013); 37% in cornea (Murata and Masuko, 2006); and that the proportion of rat TG neurons innervating molar pulp which respond to capsaicin as: 65% ranging across all cell sizes (Chaudhary *et al.*, 2001) and 82% in cells <1,260 μm² (Kim *et al.*, 2010). Furthermore, co-expression of TRPV1 with neurochemical markers in rat TG have also varied widely across the accepted levels within the DRG. For instance 68% of CGRP+ but only 28% of IB4+ cells co-expressed TRPV1 (Price and Flores, 2007); 53% of CGRP+ cells were TRPV1+ (Ichikawa and Sugimoto, 2001); and 44% of TRPV1+ cells were CGRP+ (Bae *et al.*, 2004). Whereas in CGRP+ subpopulations

of rat TG, 63% of cutaneous neurons and 20% of molar pulp neurons co-expressed TRPV1 (Ichikawa and Sugimoto, 2001); and 21% of TRPV1+ neurons innervating the dura mater were CGRP+ (Shimizu *et al.*, 2007).

Our data has shown there to be less expression of TRPV1 over the entire TG compared to DRG (27% vs. 33% respectively). In our direct comparison of the co-expression of TRPV1 with other neurochemical phenotypes, we note some significant differences between TG and DRG. For instance, we found less co-expression of NF200/TRPV1 in TG compared to DRG (3% vs. 5%), and marked trends towards higher levels of co-expression in both the CGRP+ and IB4+ populations in TG compared to DRG (69% vs. 49% and 62% vs. 53% respectively) (Figure 3-6, Table 3-2). These results would suggest that in the TG, although there was slightly less TRPV1 expression over the entire ganglia, a relatively larger proportion of peptidergic and non-peptidergic nociceptors appear to express the thermotransducer TRPV1 in the TG and therefore could presumably be sensitised via signalling mechanisms from inflammatory mediators such as NGF and TNFα.

There has been growing interest in the thermal transducer protein TRPM8 since it was first reported around a decade ago (McKemy *et al.*, 2002) and it is now known to be activated by both non-noxious cool and noxious cold temperatures (Knowlton and McKemy, 2011). The proportion of neurons expressing TRPM8 within the rat DRG have previously been reported as: 23% (mRNA) (Kobayashi *et al.*, 2005); 5-10% (mRNA) in cells with a mean area of 254 μm² (Peier *et al.*, 2002) and 6% (Su *et al.*, 2011); and in mouse DRG: 13%, the majority in cells <380 μm² (Takashima *et al.*, 2007); 7-9% (Harrington *et al.*, 2011) and 8% (Dhaka *et al.*, 2008).

The proportion of TRPM8+ neurons co-expressing other markers has been reported as follows, in rat DRG: 81% TRPM8/NF200+, 22% TRPM8/CGRP+, 5% TRPM8/IB4+, 17% TRPM8/TRPV1+ (Hayashi *et al.*, 2009) and 8% TRPM8/TRPV1+, 8% TRPM8/TRPA1+, 21% TRPM8/TrkA (mRNA) (Kobayashi *et al.*, 2005); and in mouse DRG: 14% TRPM8/NF200+, 20% TRPM8/CGRP+, 24% TRPM8/TRPV1+ (Takashima *et al.*, 2007) and 12% TRPM8/TRPV1+ (Dhaka *et al.*, 2008)

Similarly, within the TG, the proportion of neurons expressing TRPM8 show wide variation with levels in rat TG being reported as: 35% (mRNA) (Kobayashi *et al.*, 2005) and 12%, in cells with a mean area of 380 μm² (Abe *et al.*, 2005); and in mouse TG: 13%, the majority in cells <380 μm² (Takashima *et al.*, 2007); 10% (Dhaka *et al.*, 2008), and in a study using menthol-evoked responses as a marker of TRPM8 expression in mouse TG, they found that 94% of low-threshold cold sensitive neurons and 62% of high-threshold cold sensitive neurons responded to menthol (Madrid *et al.*, 2009). The proportion of TRPM8+ neurons co-expressing other markers has been reported as follows in rat TG: 76% TRPM8/NF200+, 3% TRPM8/CGRP+, 5% TRPM8/TRPV1+ (Abe *et al.*, 2005); and in mouse TG: 26% TRPM8/NF200+, 32% TRPM8/CGRP+, 39% TRPM8/TRPV1+ (Takashima *et al.*, 2007) and 19% TRPM8/TRPV1+ (Dhaka *et al.*, 2008).

Although these studies are varied, the majority show that TRPM8 is expressed within a relatively small population of TG and DRG neuronal cells. However, the main discrepancies between studies appear to be in establishing co-expression patterns of TRPM8 with other markers. For instance, as detailed above, previous research has reported no co-expression of TRPM8 within the NF200, CGRP or IB4 populations of sensory neurons (Peier *et al.*, 2002, Dhaka *et al.*, 2008). Others have reported TRPM8 expression to be in small sub-populations of NF200 or CGRP expressing

neurons (Takashima *et al.*, 2007), whilst a few studies have shown TRPM8 to be almost exclusively expressed with NF200 (Abe *et al.*, 2005, Hayashi *et al.*, 2009). What is clear from the above is that a definitive assessment of TRPM8 expression levels is lacking in the rat TG.

Our data show a trend towards higher levels of TRPM8 expression within the TG compared to DRG (11% and 6% respectively). We can also report that we found no co-expression of TRPM8 within any of the neurochemical populations being examined in both TG and DRG. Our results, along with some of the previous research, seem to suggest that TRPM8+ neurons make up a distinct population of sensory neurons. In TG and DRG therefore, TRPM8 appears to be expressed completely exclusively of all other common neurochemical markers. It is not currently known what the functional correlate of this is likely to be.

3.4.2. Cell size distributions of nociceptive markers: a direct comparison between TG and DRG

Cell size distribution profiles for all markers (TrkA, p55, gp130, TRPV1 and TRPM8) across both ganglia were significantly different. All markers appeared to be preferentially expressed on neuronal profiles towards the smaller size range in TG compared to DRG.

Our results showed that the majority of TrkA+ cells within the TG and DRG were within the small and medium cell size groups, but there were significantly fewer TrkA+ cells in the large cell size group in TG compared to DRG (Figure 3-2, Table 3-3). Of particular interest was the significantly larger proportion of TrkA+ TG neurons within the medium cell size group, suggesting that within the TG, there is a larger number of TrkA+ Aδ fibre nociceptors. This would concur with two previous studies

in rat TG where the majority of TrkA+ neurons were within the medium cell size group (Pan *et al.*, 2000, Yang *et al.*, 2006).

Our study has for the first time established a neuronal profile distribution and the proportions of p55+ neurons within each cell size group. We found a significantly larger proportion of p55+ cells within the small cell size group in TG compared to DRG. In addition, there were trends towards less p55 expression in both the medium and large cell size groups within the TG compared to DRG (Figure 3-4, Table 3-3). This would suggest that within the TG, a larger proportion of C fibre nociceptors were able to respond to TNFα than in the DRG.

We have for the first time examined gp130 protein expression within the TG. We showed ubiquitous expression of gp130 and can therefore report that this protein is expressed across all cell size ranges in both TG and DRG. Therefore, all neurons including non-nociceptors have the potential to respond to its ligand, IL-6 and other gp130 cytokines.

Our results showed that the majority of TRPV1+ neurons in the TG were within the small cell size group, whereas in the DRG, TRPV1+ neurons were mostly in the medium cell size group. Furthermore, there was an almost complete lack of TRPV1 expression within the large cell size range in both TG and DRG which is in line with previous research and gives credence to TRPV1 being a purported nociceptive marker (McMahon and Priestley, 2005) (Figure 3-7, Table 3-3). Our results would also suggest that within the TG, TRPV1+ neurons were more likely to be C fibre than Aδ fibre nociceptors.

We also report that >90% of TRPM8+ neurons were within the small cell size group in both TG and DRG. This would be in agreement with previous studies in rat showing mean cell size of TRPM8 cells to be <400 μm² (Peier *et al.*, 2002, Abe *et al.*, 2005) and suggests that TRPM8 is expressed exclusively on C fibre nociceptive neurons.

3.4.3. Conclusion

In conclusion, whilst we reported earlier that there is a significantly larger proportion of neurons that express NF200 in the TG, there is a similar level of co-expression of receptors for NGF and TNFα, and the transducer proteins TRPV1 and TRPM8, with these NF200+ neurons in the TG compared with the DRG. However, we can report for the first time, that gp130 protein is expressed throughout the TG and therefore, all NF200+ neurons could potentially respond to IL-6 and assume a nociceptive phenotype. In addition, within the TG, the almost exclusive co-expression of TrkA and CGRP seen within the DRG, does not seem to occur. Indeed only half TrkA+ neurons showed CGRP expression and around 40% of CGRP+ neurons did not co-express TrkA in the TG. This would strongly suggest that within the TG, alternative mechanisms and neurotrophins are potentially regulating both neuropeptide expression and neuronal phenotype.

Taken together, our findings suggest significant differences in proportions of neurochemically defined sub-populations of neurons in TG compared to DRG in a manner that reflects both the unique regions of target innervation found within the TG and the requirement for a rapidly conducting surveillance system to monitor potential pathological insults to the orofacial region. We provide definitive data relating to expression levels of receptor components for the potent inflammatory mediators

NGF, TNFα and IL-6 and for transducer proteins TRPV1 and TRPM8. In addition, we report profile distributions for all markers and offer quantitative data for expression of these markers within cell size groups in both TG and DRG. Notably, we provide evidence that significant proportions of neurons with both nociceptive and non-nociceptive neurochemical phenotypes have the potential to respond directly to these potent inflammatory mediators. Finally, our data supports the notion that the accepted patterns of gene expression defining nociceptors and non-nociceptors within the DRG, may not strictly apply within the TG.

4. Cytokine receptor function and activation within neurochemically defined neuronal populations of the trigeminal ganglion

4.1. Introduction

IL-6 is a pleiotropic cytokine that has wide ranging biological actions on a variety of target cells, mainly related to the regulation of inflammatory and immune responses (see Verri *et al.*, 2006a). IL-6 has also been recognised as one of the most potent pro-inflammatory mediators present within the inflammatory milieu (Andratsch *et al.*, 2009). Indeed, IL-6 is now thought to play a more prominent role in the cytokine cascade than first appreciated, as it has been shown to upregulate the production of other pro-inflammatory cytokines (see Austin and Moalem-Taylor, 2010). Studies are increasingly showing that IL-6 is a key mediator in the development and progression of some chronic inflammatory conditions such as rheumatoid arthritis (Gadient and Patterson, 1999). Furthermore, accumulating evidence points to IL-6 having a crucial role in the development of hypernociception, mechanical hyperalgesia and mechanical allodynia (Arruda *et al.*, 1998, Anderson and Rao, 2001, Verri *et al.*, 2006a, Manjavachi *et al.*, 2010).

The importance of IL-6 in nociception has been further demonstrated since elevated levels of IL-6 have been found in patients with chronic pain conditions such as complex regional pain syndrome (Heijmans-Antonissen *et al.*, 2006) and temporomandibular disorder (Wang *et al.*, 2009b) with pain intensity being positively correlated with rising levels of IL-6 (Wang *et al.*, 2009c). In addition, IL-6 is thought to contribute to the pathogenesis of migraine headaches by increasing the excitability of dural afferent neurons (Yan *et al.*, 2012). Interestingly, it has been shown that IL-

6-evoked signalling contributes towards abnormal pain behaviour following nerve injury to the sciatic nerve, but not following injury to the trigeminal nerve, suggesting that different mechanisms may contribute towards the development of cephalic (i.e. relating to the head) and extra-cephalic neuropathic pain (Latremoliere *et al.*, 2008).

IL-6, released from immune cells, fibroblasts, keratinocytes and endothelial cells, signals via a membrane complex consisting of one transmembrane α-receptor subunit, IL-6Rα, that binds IL-6 directly, and two transmembrane signal transducing components, gp130 (see Heinrich *et al.*, 1998) known as the 'classic' signalling pathway (Chalaris *et al.*, 2011). IL-6 can also regulate cells via 'trans-signalling', whereby IL-6 binds to a soluble form of its receptor component (sIL-6Rα) forming a complex which then binds to membrane-bound gp130 signal transducing components (Rincon, 2012). The soluble IL-6Rα is generated by alternative splicing which accounts for around 10% of sIL-6Rα, however, the majority of sIL-6Rα is produced by ectodomain shedding via the cleaving action of a disintegrin and metalloproteinase, ADAM17 (Chalaris *et al.*, 2011). Thus, trans-signalling allows IL-6 to influence cells without the need for them to express IL-6Rα. Indeed, gp130 has been shown to be ubiquitously expressed within the DRG (Gardiner *et al.*, 2002), and as a consequence, all somatosensory neurons could be directly regulated via IL-6 signalling mechanisms. Interestingly, both IL-6 and sIL-6Rα have been shown to be upregulated during inflammatory conditions (Jones *et al.*, 2010). In addition, it has been suggested that IL-6 classic signalling responses tend to be more regenerative or anti-inflammatory, whereas IL-6 trans-signalling responses are pro-inflammatory and contribute towards the maintenance of inflammatory states (Chalaris *et al.*, 2011, Scheller *et al.*, 2011(a), Scheller *et al.*, 2011(b), Rose-John, 2012).

Binding of IL-6 to IL-6Rα and association with gp130 triggers activation of the Janus kinase (JAK) and signal transducer and activator of transcription (STAT) signalling cascade, specifically, JAK1, JAK2 and Tyk2 which in turn leads to phosphorylation and activation of STAT3 and STAT1. IL-6 is a potent activator of STAT3, and STAT1 to a lesser extent. In addition, STAT3 activation is often used as a measure of IL-6 signalling (Zhang *et al.*, 1995, Burton *et al.*, 2011). Activated STATs form homo- or hetero-dimers which translocate to the nucleus and regulate transcription of target genes involved in inflammatory and immunological responses such as acute phase proteins (see Akira, 1997, Heinrich *et al.*, 1998). In addition to the JAK/STAT pathway, IL-6 can initiate two further cell signalling pathways, namely the MAPK (mitogen-activated protein kinase) ERK1/2 pathway and the PI3K/Akt pathway. These two additional pathways rely on IL-6-evoked phosphorylation of the scaffolding adaptor protein Gab1 (see Heinrich *et al.*, 2003). Furthermore, ERK1/2 is an important mediator for the development of hypersensitivity and central sensitisation following peripheral inflammation (Lai *et al.*, 2011).

We have previously demonstrated for the first time, the ubiquitous expression of gp130 protein in rat TG (see previous chapter). The question to investigate further is whether functional activation of these receptor signalling components occur on TG neurons. We have therefore assessed signalling activation in TG neurons by analysing STAT3 phosphorylation following exposure to IL-6 with or without the presence of its soluble receptor IL-6Rα. We have used both immunocytochemical analysis of STAT3 phosphorylation and Western blot analysis to further quantify the increase in pSTAT3 following exposure of neurons to IL-6. Finally, we have determined the neurochemical phenotype of activated neurons in order to better understand possible response mechanisms of TG neurons to the potent inflammatory mediator, IL-6.

4.2. Methods

4.2.1. Animals

Experiments were conducted on adult naive male and female Sprague Dawley rats ranging from 220-350 g body weight (Charles River, Margate, UK). All procedures were conducted in accordance with the UK 1986 Animals (Scientific Procedures) Act. Animals were housed in a temperature controlled room on a 12:12 h light/dark cycle, food and water was available *ad libitum*. Following Schedule 1 killing, animals were transcardially perfused with ice-cold Hanks balanced salt solution (HBSS) (Fisher #VX14175053). TG and DRG were swiftly removed and placed on ice in HBSS. TG were cut into smaller pieces using spring scissors and ganglia were transferred into 15 ml Falcon tubes containing 1.5 ml HBSS on ice.

4.2.2. Cell Culture

LabTek chamber slides (Fisher #TKT-210-916Y) were poly-D-lysine/laminin coated (Sigma #P6407/#L2020) as follows: 100 µl of laminin stock (1 mg laminin in 5 ml HBSS (without Ca^{2+}/Mg^{2+}, Invitrogen, #14175-053)) was added to 1.1 ml poly-D-lysine solution (100 µl aliquot of poly-D-lysine stock (5 mg poly-D-lysine in 2.5 ml sterile H_2O) in 10 ml HBSS). Wells were washed X2 in sterile H_2O (Sigma (#W3500)). 125 µl of the prepared poly-D-lysine/laminin solution was added to each well and the LabTek chamber slides were stored at 4°C for at least 1 h before use. Prior to the plating of cells, wells were washed X2 in sterile H_2O.

TG and DRG neurons were cultured using a protocol adapted from Malin *et al.* (2007) as follows. Pre-warmed papain solution (1.5 ml HBSS, 3 µl saturated

$NaHCO_3$ (Sigma #S5761), 1 mg L-Cysteine (Sigma #C7352), 60 U papain (Fisher #76218)) was added to tissue in Falcon tubes containing 1.5 ml HBSS and incubated at 37°C for 20 min. The tissue was agitated at 10 min. The suspension was centrifuged at 2000 rpm for 1 min to pellet tissue followed by careful aspiration of supernatant. The pellet was re-suspended in pre-warmed collagenase/dispase solution (3 ml HBSS, 12 mg Collagenase Type II (Sigma #C1764), 14 mg Dispase Type II (Sigma #D4693)) and incubated at 37°C for 20 min. The tissue was agitated at 10 min. The equivalent volume of pre-warmed Trypsin inhibitor (1 mg/ml (Sigma #T6522)) was added and the suspension was centrifuged at 2000 rpm for 4 min. Supernatant was carefully aspirated and the pellet was re-suspended in 0.5 ml pre-warmed L15 growth medium (Leibovitz's L-15 medium with L-Glutamine (Fisher #VX11415049), 2% HEPES (1 M) (Invitrogen #15630-056), 1% penicillin/streptomycin (Invitrogen #15140-122)). The tissue was triturated with a silicon-coated (Repelcote, VWR #632474U) flame-polished Pasteur pipette approximately 10 times until the solution appeared cloudy. The cell suspension was gently layered over a 12.5% - 28% percoll gradient (Sigma #P4937) and centrifuged at 3,000 rpm for 10 min. The upper 4.5 ml of supernatant including interface with debris was carefully aspirated and 4 ml of pre-warmed L15 growth medium added. The cells were centrifuged at 3,000 rpm for 6 min. The pellet was resuspended in 500 µl pre-warmed F12 culture medium (Ham's F12 nutrient mixture with L-Glutamine (Fisher #VX21765029), 1% penicillin/streptomycin). The cells were then plated on 8-well LabTek chamber slides pre-coated with poly-D-lysine/laminin. The cells were incubated at 37°C 5% CO_2 for 1-2 h after which time the wells were flooded with pre-warmed F12 culture medium and incubated at 37°C 5% CO_2 for a further 18 h.

4.2.3. Cell Viability Assays

4.2.3.1. Trypan Blue

The cells were cultured as previously described and 0.4% Trypan blue (Sigma #T8154) was added to the culture medium to a final concentration of 0.2% w/v. Cells were then incubated at 37°C for 10 min. The culture medium was aspirated then cells were washed in PBS and viewed on an inverted microscope to determine cell viability.

4.2.3.2. Terminal deoxynucleotidyl transferase-dUTP nick end labelling (TUNEL) assay

A Click-iT Tunel AF-488 imaging assay was carried out to determine cell viability (Invitrogen #C1-245). Briefly, cells were fixed by adding 4% ice cold formaldehyde (4% w/v in double-distilled H_2O, Sigma (#F15587)) and left on ice for 15 min. The cells were permeabilised by adding cold methanol and left at room temperature (RT) for 3 min followed by washing X2 with PBS. For the positive control, cells were washed with double-distilled H_2O and 100 µl of DNase I solution (1 µl DNase 1/10 µl DNase I buffer/89 µl deionised H_2O) was added to the appropriate wells. The cells were incubated for 30 min at RT followed by a further wash with double-distilled H_2O. All cells were then treated with 100 µl terminal deoxynucleotidyl transferase (TdT) reaction buffer and incubated for 10 min at RT. The buffer was then aspirated and cells were treated with 100 µl of TdT reaction cocktail (2 µl EdUTP nucleotide mixture/4 µl TdT recombinant/94 µl TdT reaction buffer) and incubated for 60 min at 37 °C. Cells were then washed X2 with 3% donkey serum in PBS for 2 min each wash. Following this, 100 µl of Click-IT reaction cocktail (2.5 µl Click-IT reaction

buffer additive/97.5 µl Click-IT reaction buffer containing Alexa Fluor 488) was added and the cells were left for 30 min at RT protected from light. The cells were washed once with 3% donkey serum for 5 min. For the antibody staining, cells were first blocked with 10% donkey serum for 20 min at RT followed by X2 washes in PBS. Primary antibody (rabbit-anti-β-Tubulin III, 1:2K, Sigma #T2200) was added and the cells were left for 45 min at RT followed by X2 washes in PBS. Secondary antibody (DαRb-Alexa Fluor 555, 10 µg/ml, Abcam, #ab150074) was added and the cells were left for 30 min at RT followed by X2 washes in PBS. DAPI (100 ng/ml, in 0.01 M PBS) was added, left on for 15 min at RT followed by X1 wash in PBS. The chambers were removed from the slides and coverslips were added using Fluorsave mounting medium. The slides were left to dry overnight at RT and sealed with nail varnish. The cells were visualised using an epifluorescence microscope.

4.2.3.3. Neurite outgrowth assay

The cells were plated on poly-D-lysine/laminin coated 8-well LabTek chamber slides. The cells were incubated at 37°C 5% CO_2 for 1-2 h after which time wells were flooded with pre-warmed F12 culture medium and incubated at 37°C 5% CO_2 for a further 18 h. Cells were then flooded with fresh pre-warmed F12 culture medium and incubated at 37°C 5% CO_2 for a further 24 h. The cells were then fixed and stained as described below and visualised using a Nikon Eclipse 80i epifluorescence microscope.

4.2.4. Immunocytochemistry

4.2.4.1. Neurochemical populations within TG and DRG cell cultures

In order to determine the proportion of viable cells within each neurochemical population, immunocytochemistry was carried out as follows. Cells were cultured as previously described, the F12 culture medium was aspirated and cells were fixed in 4% ice cold formaldehyde. Cells were left on ice for 15 min. The formaldehyde was aspirated and cells permeabilised by adding cold methanol for 3 min at RT. The methanol was aspirated and cells were washed X2 in PBS. Cells were blocked with 10% donkey serum (as per Chapter 1) for 20 min at RT followed by X2 washes in PBS. Primary antibodies were added for 45 min at RT as follows: rabbit-anti-β-Tubulin III (1:2K, Sigma #T2200) with either mouse-anti-NF200 (1:8K, Sigma #N0142), sheep-anti-CGRP (1:600, Enzo Life Sciences #CA1137), or IB4-FITC (5 µg/ml, Sigma #L2895). The cells were washed X2 in PBS and secondary antibodies were added for 30 min at RT (DαRb-AF-488, DαRb-AF-555, DαM-AF-555, DαS-AF-555, all at 10 µg/ml). Cells were then washed X2 in PBS. DAPI (100 ng/ml, in 0.01 M PBS) was added for 15 min at RT followed by X1 wash in PBS. Cover slips were then added using Fluorsave mounting medium and left to dry overnight at RT. The slides were sealed with nail varnish.

4.2.4.2. Optimisation of STAT3 activation in TG

In order to determine the optimum treatment time for signalling activation, cells were cultured on four 8-well LabTek chamber slides and treated with IL-6 (20 ng/ml, R&D Systems #206-IL-010) ±IL-6Rα (30 ng/ml, R&D Systems #227-SR-025) for 1 min, 5 min, 10 min or 15 min. Using the immunocytochemistry protocol described above,

cells were stained with antibodies for mouse-anti-β-Tubulin III (1:2K, Sigma #T8578) and rabbit-anti-pSTAT3^{Tyr705} (1:100, New England Biolabs #9145S). Further experiments were carried out to quantify STAT3 phosphorylation following treatment with IL-6±IL-6Rα in TG cells.

4.2.4.3. Triple staining using Fab fragment

In order to determine STAT3 activation within neurochemical populations the immunocytochemistry protocol was adapted to perform a triple stain using a Fab fragment as follows. Briefly, following fixation, blocking and washing, primary antibodies for rabbit-anti-pSTAT3 and mouse-anti-NF200 were added for 45 min at RT. The cells were washed X2 in PBS and goat-anti-mouse Fab fragment (20 µg/ml, (monovalent Fab fragment goat anti-mouse IgG (H+L)) Stratech Scientific #115-007-003) was added for 45 min at RT. The cells were washed X2 in PBS and blocked in 10% donkey serum for 20 min at RT. Cells were then washed X2 in PBS and primary antibody for mouse-β-Tubulin III added for 45 min at RT. Following further washes, secondary antibodies were added (DαRb-AF-555 (10 µg/ml), DαG-AF-647 (10 µg/ml), DαM-FITC (1:200) and the protocol was followed as previously described.

4.2.5. Western blotting

The cells were cultured and treated as previously described except that two animals were used per 8-well LabTek slide in order to increase final protein levels. Culture medium was aspirated and cells flooded with ice cold PBS and kept on ice. In order to lyse cells, PBS was aspirated and 25 µl of ice cold RIPA lysis buffer (RIPA buffer (Sigma #R0278) 5% Protease Inhibitor Cocktail (Sigma #P8340) 1% Phosphatase Inhibitor Cocktail 2 (Sigma #P5726)) was added to each well and left on ice for 10

min. The wells were scraped and cell lysate was added to micro-centrifuge tubes. Cell lysate was centrifuged at 3,500 rpm at 4°C for 30 min to pellet cell debris. The supernatant was carefully removed without disturbing the pellet and added to fresh micro-centrifuge tubes. In order to keep our protein of interest at its optimal level for electrophoresis, we were reluctant to use any to carry out protein estimation assays. Therefore, in order to decrease variability in protein levels, equal volumes of vortexed supernatant was carefully added to fresh micro-centrifuge tubes before adding the appropriate volume of 6X Laemmli SDS-Sample buffer (Bioquote Ltd #10570021-1) to each tube. Variability in protein levels were also reduced by using the constitutively expressed protein β-Tubulin III as a loading control. Samples were vortexed then boiled for 5 min, vortexed again then cooled on ice. Prior to loading, samples were centrifuged for 30 s to spin down any condensate. Proteins were separated by SDS-PAGE using 12% Precise Protein Gels (Fisher #PN25202) and Tris-HEPES-SDS running buffer (Fisher #PN28368). The protein samples and ladders (BLUeye Pre-Stained protein ladder (Geneflow #S6-0024) plus Biotinylated protein ladder (New England Biolabs #7727S)) were loaded onto the gel and run at 120V for <45 min. The proteins were blotted onto PVDF membrane (Fisher #FDR-520-027U), pre-soaked in methanol (15 s), distilled water (2 min) and transfer buffer (>5 min), and run at 100V for 35 min. The membrane was cut horizontally between the protein of interest band at 79-86 kDa and the loading control band at 50 kDa and placed in separate 50 ml Falcon tubes with protein side facing inwards. Membranes were then blocked in blocking serum (5% w/v bovine serum albumin (Sigma (#A2153)) in TBS-Tween20 (Sigma (T9039)) (0.1% w/v)) for 1 h at RT on a roller. Primary antibodies were added as follows: rabbit-anti-pSTAT3^{Tyr705} (1:250 in blocking serum) or mouse-anti-β-Tubulin III (2 µg/ml in 50:50 blocking serum:TBS-Tween20 (0.1% w/v)). The membranes were incubated overnight on a roller at 4°C.

Membranes were then washed 3X 5 min in TBS-Tween20 (0.1% w/v) on a roller at RT. Secondary antibody was added (1:2500, GαRb IgG or GαM IgG both Abcam #ab97080 #97040) and the membranes were incubated for 2 h on a roller at RT. The membranes were washed 3X 5 min in TBS-Tween20 (0.1% w/v) on a roller at RT followed by one wash in TBS (Sigma (#T6664)) only (0.1% w/v). The membranes were developed using ECL-Plus (Fisher #GZRPN2132) and visualised with an EC3 Imaging System using VisionWorks L.S. software (both UVP Bioimaging Systems). Specificity of the pSTAT3 antibody was determined using a pSTAT3^{Tyr705} blocking peptide (New England Biolabs #1195S).

4.2.6. Data Imaging and Analysis

As described in Chapter 2, images for immunocytochemistry were acquired with the use of a Nikon Eclipse 80i epifluorescence microscope. Western blots were imaged using an EC3 Imaging System and optical density readings for pSTAT3 were normalised against those for β-tubulin III (loading control) in each well to eliminate any variability in total protein loading. Data are expressed as mean ± SEM. Normal distribution was determined using the Anderson-Darling test. Statistical differences were assessed on raw data using a 2-sample T-test. Significance was set at p=<0.05. * p=<0.05; ** p=<0.01; *** p=<0.001.

4.3. Results

4.3.1. Cell Viability

A confounding issue surrounding all *in vitro* assays of primary cells is the possibility of injury-induced cell death or preferential survival of neuronal sub-populations over others. Therefore, in order to determine the ability of cells to survive axotomy and culturing protocols we carried out several viability assays. Dye exclusion tests such as Trypan blue, are used to determine the number of viable cells present and works on the principle that viable cells are able to actively extrude the dye whereas dying or dead cells cannot extrude the dye and appear blue (Figure 4-1 A). In the Trypan blue assay, 4.3±1.3% of cells were shown to be unable to extrude the dye.

The TUNEL assay carried out incorporates fluorescent markers to fragmented DNA. Figure 4-1C illustrates the TUNEL positive control where all cells are nick-end labelled with fluorescent marker. Healthy cells with intact DNA can be seen in Figure 4-1D. In the TUNEL assay, 1.7±0.4% of cells were shown to have DNA fragmentation.

In a further assay, cell viability was assessed by determining the ability of neurons to mount a regenerative response. Hence neurons were cultured for an additional 24 h period in order to allow time for neurite outgrowth in healthy cells (Figure 4-1 B). Following the additional 24 h culture period, 96.8±2.1% of cells appeared to display neurite outgrowth.

Data from all three cell viability assays showed cell death to range from 1.7% - 4.3%.

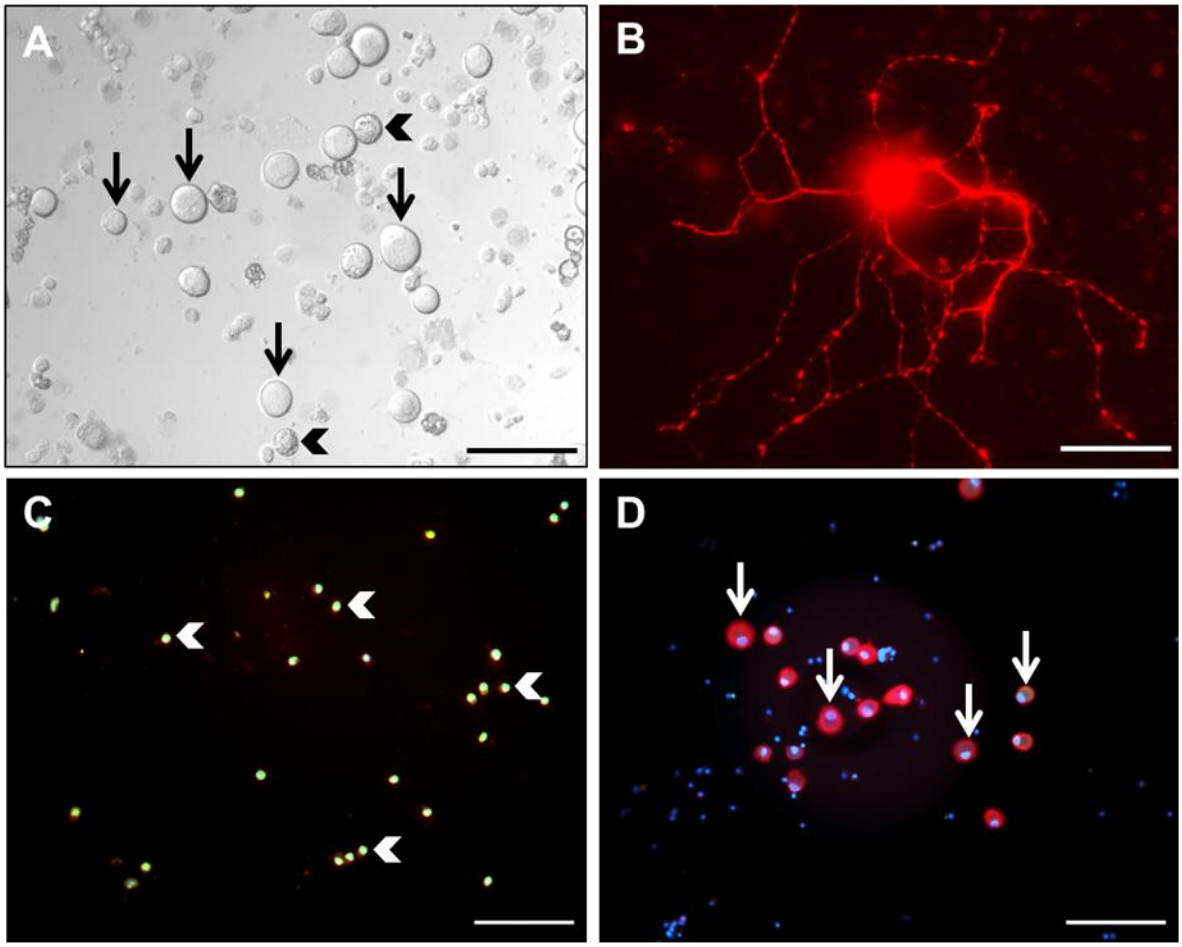

Figure 4-1: Cell viability assays – **A**) Trypan Blue assay demonstrating viable TG neuronal cells able to extrude the dye (arrows) and non-viable cells unable to extrude the dye (arrowheads). Viable cells across all cell size ranges were present. 4.3% of the total cells were found to be non-viable. **B**) Cells were cultured for an additional 24 h to allow time for neurite outgrowth in viable cells. After 48 h culture 96.8% of β-Tubulin III positive cells displayed neurite outgrowth. **C**) TUNEL assay positive control demonstrating nick-end labelling with fluorescent markers to fragmented DNA in all cells undergoing apoptosis (green, arrowheads). **D**) TUNEL assay showing viable TG neuronal cells across all cell size ranges (arrows). 1.7% of cells were shown to be non-viable. (**A-D**) Data from all three viability assays showed cell death to range from 1.7% - 4.3%. Scale bar 100 µm.

4.3.2. Viability of neurochemical populations in culture

In order to draw conclusions from our *in vitro* studies, it is important to demonstrate that similar proportions of cells are present within each neurochemical population *in vitro* compared to that found *in vivo* and that no preferential cell death is observed. We therefore carried out immunocytochemistry on TG and DRG cell cultures using

antibodies for NF200, CGRP and IB4. An antibody for β-tubulin III was used to identify all neuronal cells within the culture, being a neuron-specific β-tubulin isotype (Guo *et al.*, 2011). The proportions of cultured TG neurons expressing NF200, CGRP and IB4 was similar to that observed *in vivo*. DRG cell cultures also showed the same proportions of neurochemically identified cells as seen *in vivo*. Furthermore, the proportional discrepancies between neurochemical phenotypes observed *in vivo* between TG and DRG was also mirrored *in vitro*. Therefore, *in vitro* a significantly higher proportion of TG neurons expressed NF200 compared to DRG (63.9±0.8% vs. 39.23±0.5%, p=<0.001). Our findings also confirmed significantly lower proportions of both CGRP and IB4 populations of neuronal cells in TG than in DRG (34.4±0.6% vs. 50.96±1.0% (p=<0.01) and 37.55±0.9% vs. 45.49±0.4% (p=<0.05) respectively) (Figure 4-2). Overall our results demonstrate that no significant preferential cell death was occurring during the cell culture process in either TG or DRG cell populations.

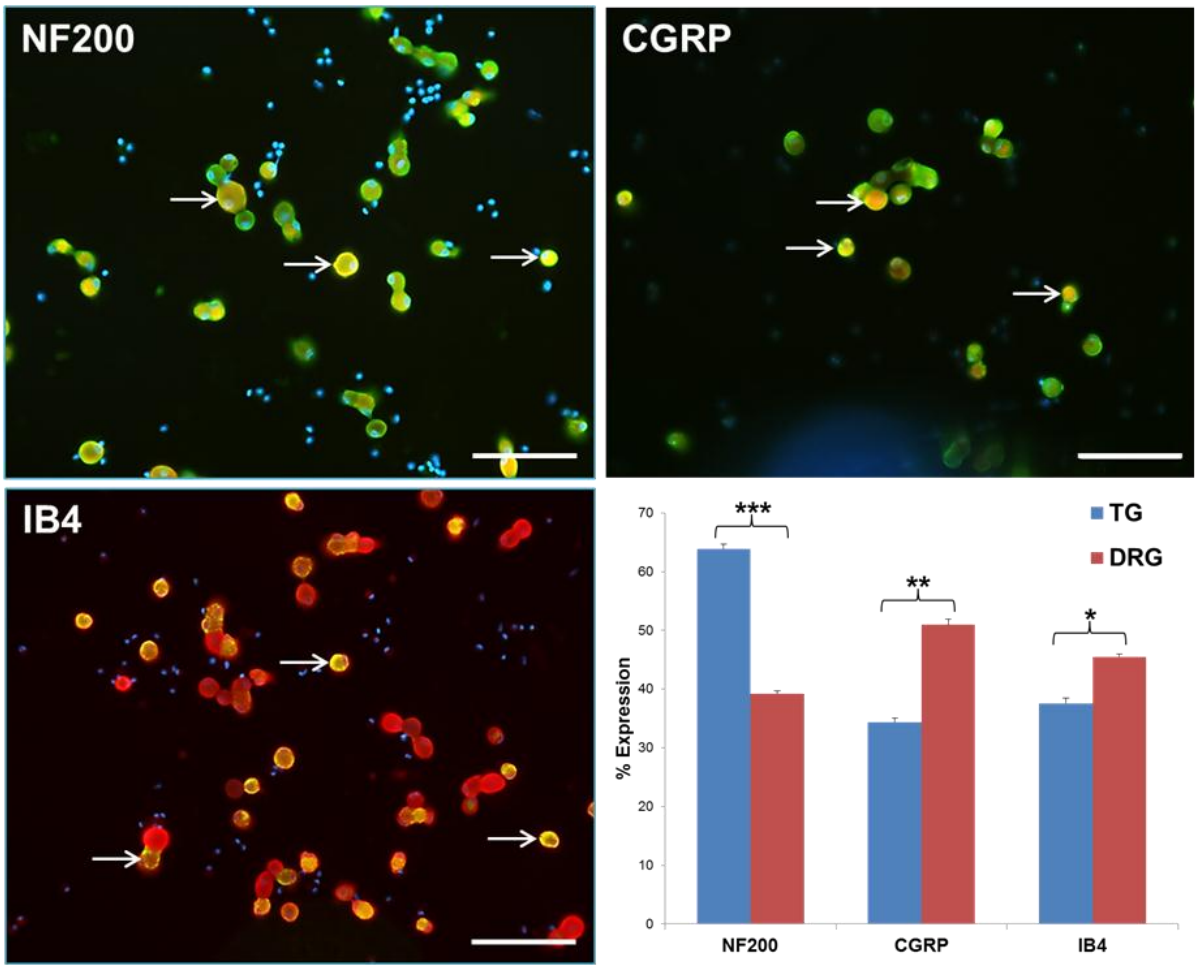

Figure 4-2: Viability of neurochemical phenotypic populations. Photomicrographs show TG neuronal cell cultures stained for neurochemical markers NF200, CGRP and IB4. Arrows show cells which are NF200+, CGRP+ and IB4+ 18 h after plating. Bar chart illustrates proportions of cultured neuronal cells within each neurochemical population in TG (blue) and DRG (red). The proportions of neurochemical populations *in vitro* were shown to be similar to those from our *in vivo* data presented in Chapter 2. Furthermore, our *in vitro* data also demonstrated the same discrepancy in proportions as shown *in vivo*, with a larger population of NF200+ cells and smaller populations of both CGRP+ and IB4+ cells in TG compared to DRG. Our results confirm that no significant preferential cell death was occurring during culture. Scale bar 100 µm. Bars = +SEM.

4.3.3. Activation of STAT3 following IL-6 exposure

Downstream signalling activation in TG neurons was assessed by analysing STAT3 phosphorylation following exposure to IL-6 with or without IL-6Rα. Preliminary experiments showed that optimal STAT3 phosphorylation was observed in TG neuronal cells following exposure to IL-6±IL-6Rα for 10 min. This is in line with

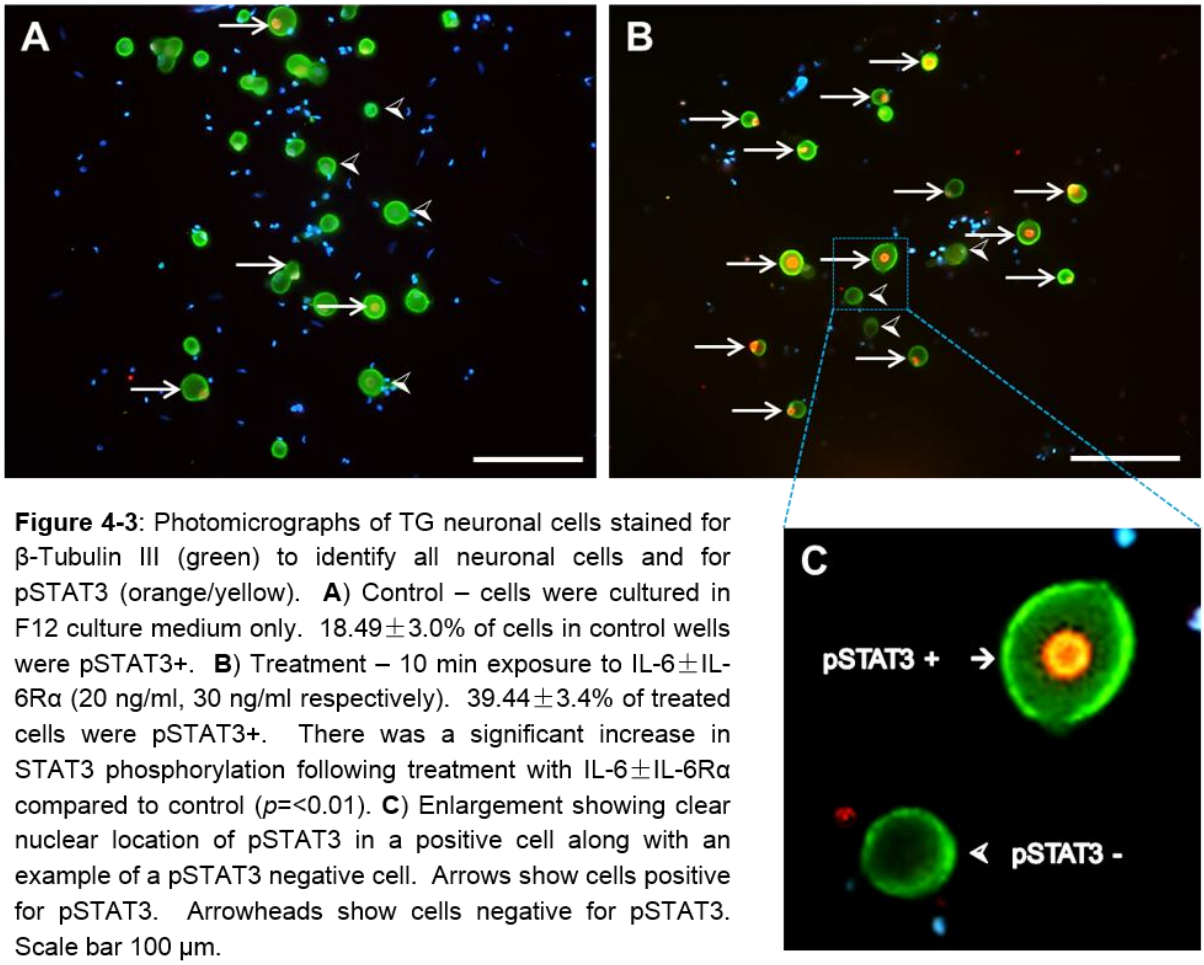

Figure 4-3: Photomicrographs of TG neuronal cells stained for β-Tubulin III (green) to identify all neuronal cells and for pSTAT3 (orange/yellow). **A**) Control – cells were cultured in F12 culture medium only. 18.49±3.0% of cells in control wells were pSTAT3+. **B**) Treatment – 10 min exposure to IL-6±IL-6Rα (20 ng/ml, 30 ng/ml respectively). 39.44±3.4% of treated cells were pSTAT3+. There was a significant increase in STAT3 phosphorylation following treatment with IL-6±IL-6Rα compared to control (p=<0.01). **C**) Enlargement showing clear nuclear location of pSTAT3 in a positive cell along with an example of a pSTAT3 negative cell. Arrows show cells positive for pSTAT3. Arrowheads show cells negative for pSTAT3. Scale bar 100 µm.

previous studies that have shown optimal pSTAT3 levels at ≤10 min (Zhang *et al.*, 1995) and that tyrosine^{705} phosphorylation of STAT3 occurred within 5 min (Schuringa *et al.*, 2000) following IL-6 exposure. Following treatment, cells were rapidly fixed and immunocytochemistry was carried out and neuronal cells were identified by staining with β-tubulin III. In order to quantify neuronal response to IL-6±IL-6Rα, total neuronal cells were counted and the proportion of neurons showing nuclear translocation of pSTAT3 (pSTAT3+) was assessed. Ten minutes following exposure to IL-6±IL-6Rα (20 ng/ml, 30 ng/ml respectively) 39.44±3.4% of neurons were pSTAT3+. This was significantly different to control treatment (18.49±3.0%) (p=<0.01, n=3). No significant difference was found in the proportions of pSTAT3+ cells between treatments with IL-6 only (38.27±4.4%) or IL-6 plus IL-6Rα

(40.6±3.2%). Figure 4-3 illustrates enhanced STAT3 phosphorylation in TG neuronal cells following 10 min exposure to IL-6±IL-6Rα.

4.3.4. Quantification of STAT3 phosphorylation following exposure to IL-6

We have further quantified the increase in STAT3 phosphorylation observed in our earlier experiments by using Western blot analysis. TG neuronal cells were cultured as previously described and cells were exposed to IL-6 only or IL-6+IL-6Rα for 10 min. Activation of STAT3 was assessed using a pSTAT3^{Tyr705} antibody and was analysed by Western blot from whole-cell lysates. To help eliminate any variability in total protein levels loaded onto gels, the data for pSTAT3 was normalised against levels of β-Tubulin III which was used as a loading control. The Western blot image in Figure 4-4A displays bands at the appropriate molecular weights for pSTAT3α (86 kDa), pSTAT3-β (79 kDa) and β-tubulin III (50 kDa) and clearly exemplifies an increase in pSTAT3 following exposure of TG neuronal cells to IL-6 only and IL-6+IL-6Rα. Following data analysis, our results confirmed our earlier findings that there was no significant difference in the levels of STAT3 activation between treatments with IL-6 only or IL-6+IL-6Rα. Furthermore, our results confirmed a significant increase in pSTAT3 following treatment with IL-6±IL-6Rα ($p=<0.01$) when compared to control. To further quantify our results, the following fold increases were observed in levels of pSTAT3 when compared to control: IL-6 only, 2.6-fold increase; IL-6+IL-6Rα, 3-fold increase; combined treatments (IL-6±IL-6Rα), 2.7-fold increase (Figure 4-4 B).

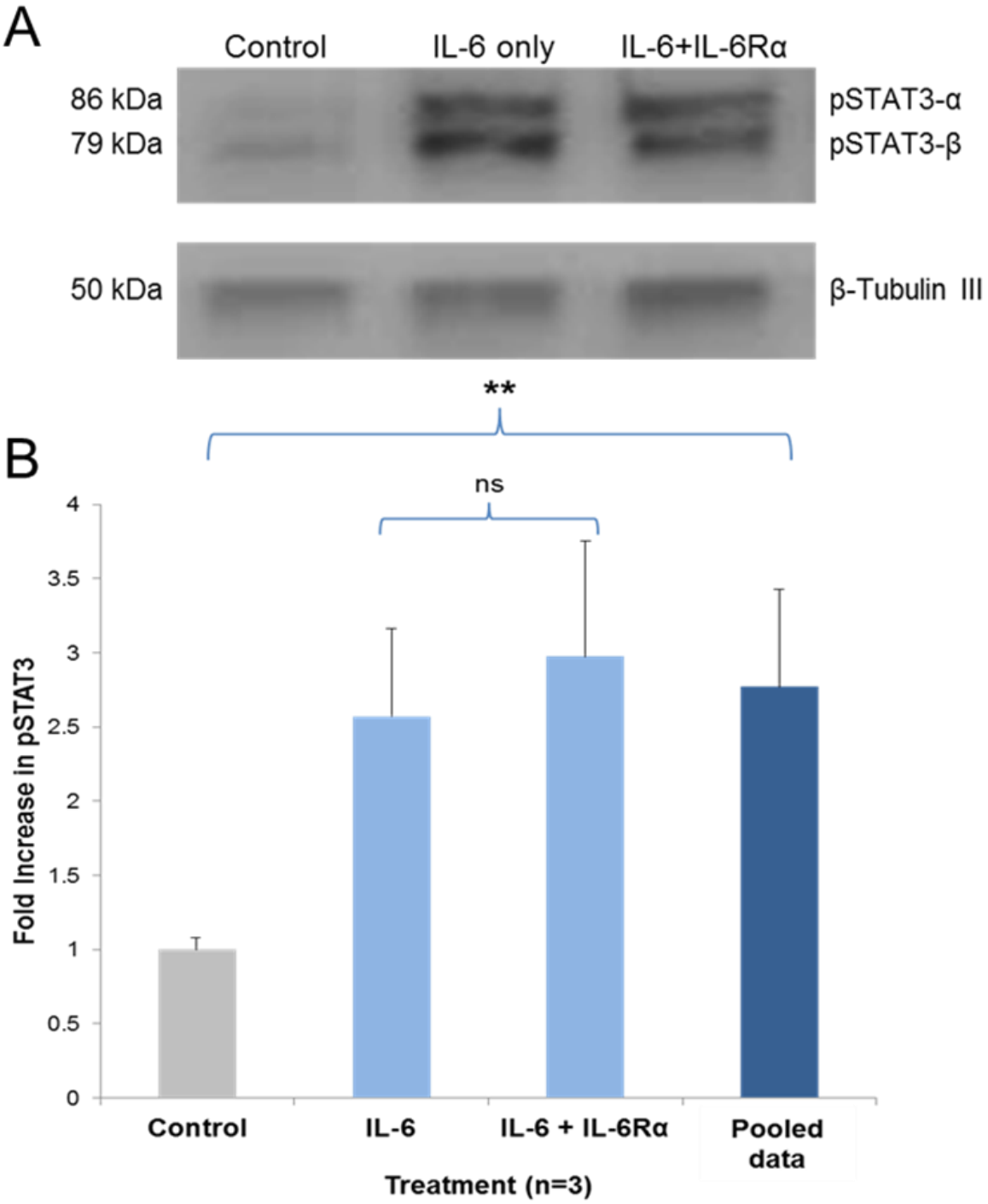

Figure 4-4: Exposure to IL-6±IL-6Rα leads to a significant increase in pSTAT3 in TG neuronal cells. **A**) Activation of STAT3 was analysed by Western blot from whole-cell lysates. Cells were treated with IL-6 only (10 min, 20 ng/ml) or IL-6 plus IL-6Rα (10 min 20 ng/ml and 30 ng/ml respectively). β-Tubulin III was used as a loading control. **B**) Western blot analysis confirmed data from immunocytochemistry. No significant difference was found between treatments. There was a significant increase in pSTAT3 in cells exposed to IL-6±IL-6Rα (p=<0.01). Treatment with IL-6 resulted in a 2.6-fold increase in pSTAT3 and treatment with IL-6+IL-6Rα resulted in a 3-fold increase in pSTAT3 when compared with control.

4.3.5. IL-6 preferentially activates STAT3 within the NF200 population of TG neuronal cells

In order to determine the phenotype of activated neurons, co-staining of TG cultures with NF200 was performed following exposure to IL-6 only or IL-6+IL-6Rα (Figure 4-5). Preliminary experiments showed that as a percentage of total neurons, the proportion of cells which were pSTAT3+ was as follows: control, 28.14±6.4%; IL-6 only, 60.37±4.8%; IL-6+IL-6Rα, 61.21±6.4%. These results confirmed our earlier findings in that there was no significant difference between treatment groups with IL-6 only, and IL-6+IL-6Rα and our data for these treatments were pooled. Again, confirming our earlier experiments, there was a significant increase in STAT3 phosphorylation following treatment with IL-6±IL-6Rα when compared to control (p=<0.01) (Figure 4-6 A). We further analysed our data to determine phenotypic populations of TG neurons which were pSTAT3+. Our data indicate that the majority of the increase in STAT3 phosphorylation occurs within the NF200+ population of neuronal cells. Figure 4-6A illustrates that total STAT3 phosphorylation increased by 26% within the NF200+ population but only 7% within the combined CGRP+ and IB4+ populations. Furthermore, as illustrated in figure 4-6 B-D, the preferential increase in pSTAT3 within the NF200+ population was significant when compared to untreated/control cells as follows: NF200+/pSTAT3+ co-expression increased from 16% in control cells to 38% in IL-6±IL-6Rα treated cells (*p*=<0.01); the proportion of total NF200+ cells which were pSTAT3+ increased from 31% in control cells to 63% in IL-6±IL-6Rα treated cells (*p*=<0.01); the proportion of total pSTAT3+ cells which were NF200+ increased from 42% in control cells to 62% in IL-6±IL-6Rα treated cells (*p*=<0.01).

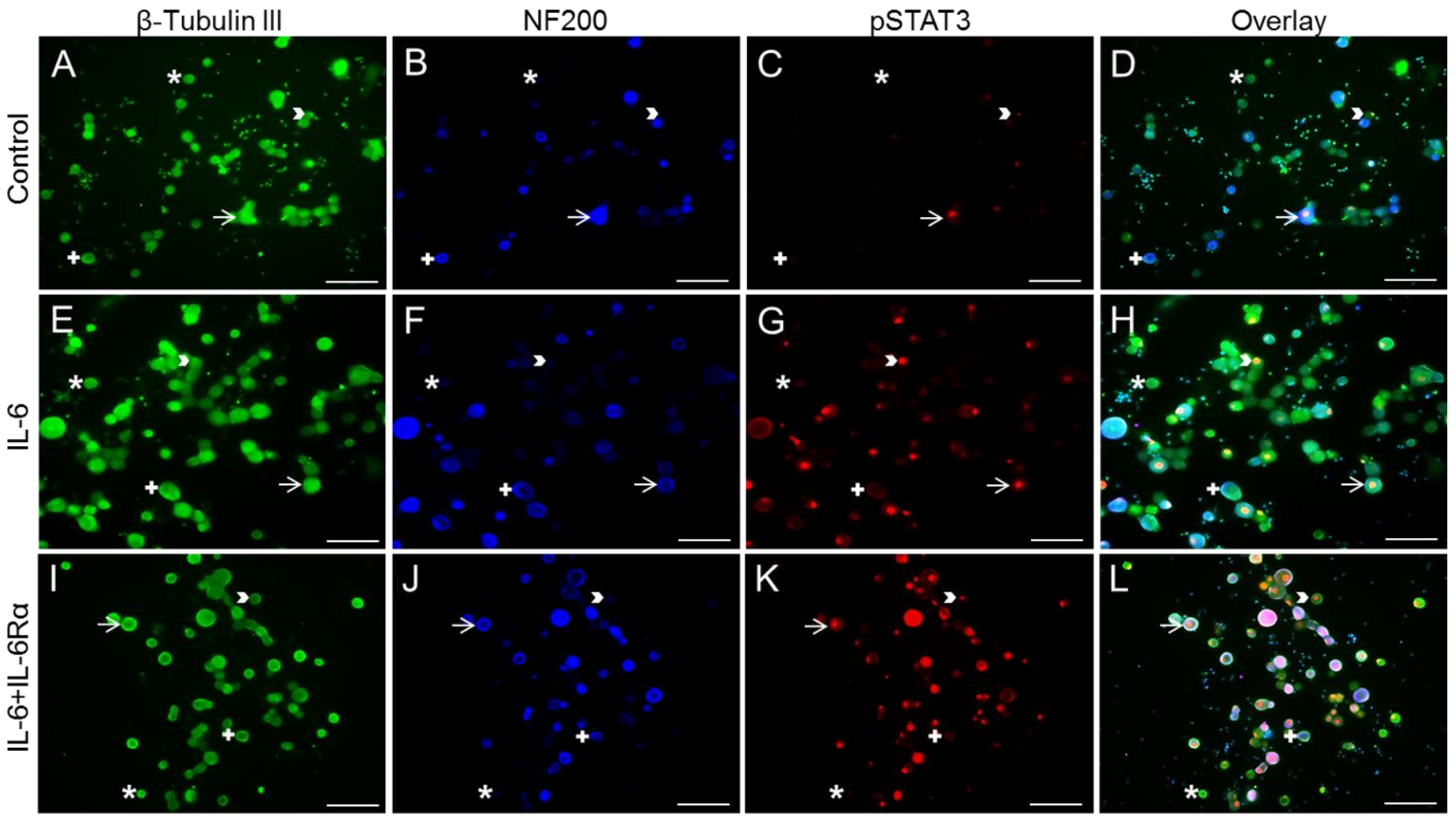

Figure 4-5: Photomicrographs of TG neuronal cells stained for β-Tubulin III to identify neuronal cells (**A, E, I**), NF200 (**B, F, J**) and pSTAT3 (**C, G, K**), with co-expression of all three markers shown in **D**, **H** and **L**. (**A-D**) Control/untreated cells. (**E-H**) Cells treated with IL-6 only (10 min at 20 ng/ml). (**I-L**) Cells treated with IL-6 plus IL-6Rα (10 min at 20 ng/ml and 30 ng/ml respectively). There was no significant difference between treatments with IL-6 only and IL-6+IL-6Rα. There was a significant increase in STAT3 phosphorylation in cells treated with IL-6±IL-6Rα when compared to control (p=<0.01). (Arrows) NF200+/pSTAT3+ cells. (Arrow-heads) NF200-/pSTAT3+ cells. (+) NF200+/pSTAT3- cells. (*) NF200-/pSTAT3- cells. Scale bar 100 µm.

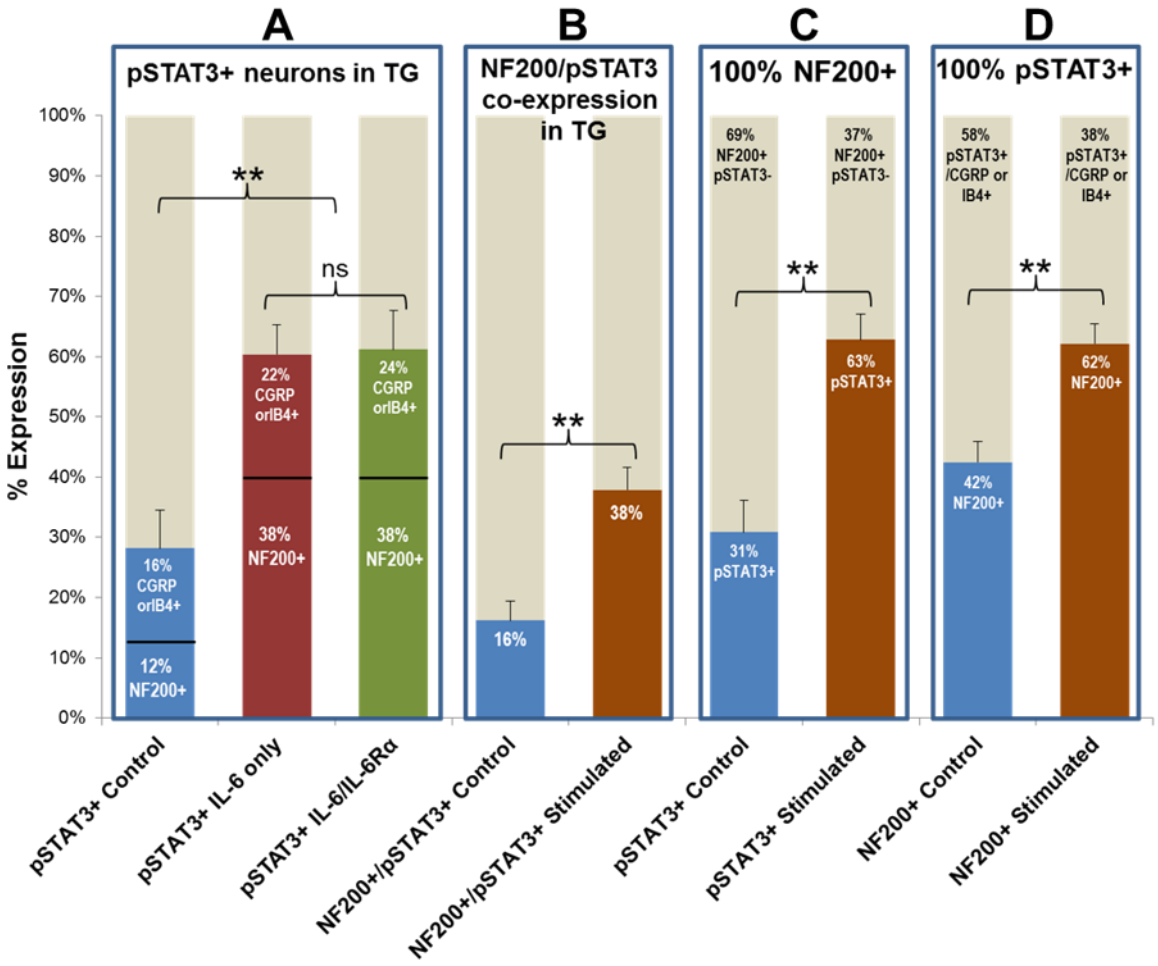

Figure 4-6: Exposure of TG neuronal cells to IL-6±IL-6Rα results in preferential STAT3 phosphorylation in NF200+ cells. (**A**) pSTAT3+ cells as a proportion of total TG cells. There was no significant difference in levels of STAT3 phosphorylation between treatments with IL-6 only and IL-6+IL-6Rα. There was a significant increase in STAT3 phosphorylation in cells exposed to IL-6±IL-6Rα when compared to control (p=<0.01). (**B-D**) Data represented as a proportion of cells within populations: (**B**) as a % of total TG cells co-expressing NF200/pSTAT3, (**C**) as a % of total NF200+ cells, and (**D**) as a % of total pSTAT3+ cells. All populations show significant increases in STAT3 phosphorylation in NF200+ cells following treatment with IL-6±IL-6Rα (p=<0.01). (**A**) STAT3 phosphorylation was shown to occur preferentially in NF200+ cells with an increase of 26% within the NF200+ population but only 7% within the combined CGRP+ and IB4+ populations. Grey bars represent the remaining cells within each population negative for markers of interest.

4.4. Discussion

Our previous data has shown that the gp130 signal transducing receptor component is ubiquitously expressed in rat TG neurons. IL-6 is a potent activator of STAT3 (Zhang *et al.*, 1995), therefore, in order to test the functional competency of the receptor component gp130, we investigated the upregulation of pSTAT3 in cultured TG neurons following exposure to IL-6. We first established the viability of TG and DRG neuronal cell cultures and determined that similar proportions of neurons within each neurochemical population were surviving *in vitro* as were found in our *in vivo* experiments. We observed a similar discrepancy in proportions of neurochemical populations between TG and DRG *in vitro* that we found *in vivo*, in that there was a significantly larger population of NF200+ neurons, and significantly smaller populations of CGRP+ and IB4+ neurons in TG compared to DRG (Figure 4-2). We are confident therefore, that all neuronal sub-populations are represented in our cultures in similar proportions that appear in situ.

Our results showed a significant increase in pSTAT3 in TG cells following 10 min exposure to IL-6±IL-6Rα, with 39.4% of cells being pSTAT3+ compared to 18.5% in control cells (Figure 4-3). Somewhat surprisingly, we found no significant difference in the levels of pSTAT3 between cells treated with IL-6 only and IL-6+IL6Rα (38.3% and 40.6% respectively). To further quantify this increase in STAT3 phosphorylation, we carried out Western blot analysis on TG neuronal cells following identical treatment protocols as per our immunocytochemistry experiments. Here again, we found that pre-treatment with IL-6±IL-6Rα led to a significant 2.7-fold increase in STAT3 phosphorylation. Our Western blot analysis also confirmed our previous

findings of no significant difference in levels of pSTAT3 between treatments with IL-6 alone or IL-6+IL-6Rα (Figure 4-4 B).

As described earlier, IL-6 can signal via the classic signalling pathway, which requires expression on the target cell of its cognate receptor, IL-6Rα, in addition to the signal transducing component gp130. However, cells which only express gp130 but do not express IL-6Rα, are still able to be influenced by IL-6 via the trans-signalling mechanism, using a soluble IL-6Rα which has been made available, mainly by the cleaving action of ADAM17 (see Gardiner *et al.*, 2002, Chalaris *et al.*, 2011). The membrane expression of IL-6Rα, is thought to be predominantly restricted to leukocytes and hepatocytes (see Rincon, 2012). Therefore, for neuronal cells to be able to respond to IL-6, one could assume that it was a necessity for the soluble form of the IL-6Rα to be present within the surrounding media. Indeed, in the *in vivo* state, this may be the case, as sIL-6Rα could be shed from surrounding non-neuronal cells. However, within the *in vitro* state, this would not occur to such an extent, of course, depending upon the homogeneity of the cultured cells. Nonetheless, we are not the first to report such findings, indeed, Vardanyan *et al*. (2010), when investigating IL-6-evoked CGRP release from rat DRG, recorded no difference in response when co-administering IL-6+IL-6Rα than with IL-6 alone. There is evidence to suggest that the classic signalling and trans-signalling pathways, activate alternative downstream signalling cascades (Chalaris *et al.*, 2011, Scheller *et al.*, 2011(a), Scheller *et al.*, 2011(b)). Therefore, in order to record a difference in treatments with or without exogenous IL-6Rα, we may need to investigate an additional outcome to STAT3 phosphorylation, such as the activation of ERK1/2. We can only conclude therefore, that under our present culture conditions and within the confines of our experimental protocol, the presence of additional exogenous IL-6Rα was not required for TG neuronal cells to respond to IL-6.

In order to determine the phenotype of neurons expressing pSTAT3 we carried out co-staining of TG cultures for phenotypic markers. We observed that the majority of the increase in STAT3 phosphorylation was occurring within the NF200+ population of neuronal cells. For instance, under control (untreated) conditions, STAT3 phosphorylation was split almost equally between the population of NF200+ cells (12%), and the remaining neuronal cells (16%), which were assumed to be the combined populations of pSTAT3+ CGRP expressing and IB4 binding cells. However, following exposure to IL-6±IL-6Rα, there was a significant increase in pSTAT3 observed only within the NF200+ population, which increased from 12% to 38%, equivalent to a 3.2-fold increase. The increase in pSTAT3 in the remaining population of neuronal cells was only a small amount, from 16% to 23%, representing a 1.4-fold increase (Figure 4-6A-D).

Since we have demonstrated that gp130 appears to be ubiquitously expressed throughout TG neuronal cells, our results showing that STAT3 was preferentially activated in NF200+ cells following IL-6 exposure, is a notable finding and requires examination. As far as we are aware, only one other study has investigated IL-6-evoked STAT phosphorylation within neurochemical populations of TG neuronal cells, albeit, in a mouse model. Although this study used pSTAT1 as an outcome measure rather than pSTAT3, they also found that the activation of STAT1 was preferentially within the NF200+ population of neuronal cells (Kobierski *et al.*, 2000). There is the possibility that although gp130 is ubiquitously expressed, its levels of expression may not be uniformly distributed across all populations of neuronal cells. Higher levels of expression may occur within the myelinated population of cells, allowing for greater levels of signalling and enhanced STAT3 activation within this population. Although STAT3 phosphorylation may also have been occurring to a lesser extent within the NF200-negative population of cells, in some of these cells,

activation may have been at such a low level to have been below the threshold set within our experimental protocol for marking cells as pSTAT3+. Alternatively, IL-6 may be activating other signalling cascades within the NF200-negative population, which we have not monitored and this would require a different outcome measure, such as phosphorylation of ERK1/2 or PI3K to be quantified. However, if NF200+ neurons have higher levels of expression of gp130 and enhanced levels of STAT3 activation, then IL-6 could be preferentially acting on what would traditionally be classified as non-nociceptors which may have important implications during inflammatory conditions, such as altering the phenotype and function of these cells. Indeed, this would have an even greater impact within the trigeminal nervous system due to the significantly larger population of NF200+ neurons which we have observed within the TG.

There is growing evidence to support the importance of IL-6 in the development of chronic pain conditions and its involvement in the pathogenesis of temporomandibular disorder and migraine headaches (Heijmans-Antonissen *et al.*, 2006, Wang *et al.*, 2009a, Wang *et al.*, 2009c, Yan *et al.*, 2012). In addition, IL-6 is now thought to have a crucial role in the development of mechanical hyperalgesia and mechanical allodynia (Arruda *et al.*, 1998, Anderson and Rao, 2001, Verri *et al.*, 2006a, Manjavachi *et al.*, 2010). In combination with the fact that myelinated neurons are generally thought to be either low- or high-threshold mechanoreceptors (see McMahon and Priestley, 2005), along with our previous results of a much larger population of NF200+ neurons within the TG, these additional findings may go towards explaining the high prevalence of mechanical hyperalgesia and allodynia observed in some orofacial pain conditions, in particular, temporomandibular joint disorders and following intradental injury and inflammation (Anderson and Rao, 2001,

Sessle, 2005, Takeda *et al.*, 2005(a), Takeda *et al.*, 2006, Morgan and Gebhart, 2008, Takeda *et al.*, 2008(a), Takeda *et al.*, 2008(b), Takeda *et al.*, 2008(c)).

5. Cytokine receptor-mediated sensitisation of thermo-transducer function in trigeminal neurons

5.1. Introduction

The binding of IL-6 to its cognate receptor, IL-6Rα, and association with its signal transducing receptor component gp130, triggers activation of the JAK/STAT signalling cascade (Zhang *et al.*, 1995, Burton *et al.*, 2011). We have shown previously that IL-6 application to TG neurons in culture results in STAT3 phosphorylation and translocation of this signal transducer to the nucleus. This implies a potential functional outcome of exposure to IL-6 in TG neurons (see Chapter 4). However, IL-6 is capable of triggering two additional signalling pathways namely, the Gab1/MAPK/ERK1/2 pathway and the Gab1/PI3K/Akt pathway (see Heinrich *et al.*, 2003). Given the number of signalling pathways, it is important to determine whether a functional response occurs within TG neurons following exposure to IL-6 and by which pathway. Therefore, by using different outcome measures to STAT3 phosphorylation, we could investigate functional responses via alternative signalling pathways.

One outcome we have used is CGRP release as a functional measure of TG neuron activation and subsequent sensitisation by IL-6. Previous studies have demonstrated that activation of neurons by TRPV1 ligands leads to neuronal activation and the release of CGRP (Flores *et al.*, 2001, Fehrenbacher *et al.*, 2009, Meng *et al.*, 2009, Loyd *et al.*, 2012). CGRP is a vasoactive neuropeptide, the actions of which increase neurotransmitter release leading to hyperalgesia and central sensitisation. Furthermore, CGRP can be released antidromically in the periphery where it has

been strongly linked with neurogenic inflammation and chronic pain conditions such as migraine and temporomandibular joint disorder (Sixt *et al.*, 2009, Eftekhari *et al.*, 2010, Benarroch, 2011, Cady *et al.*, 2011, Ceruti *et al.*, 2011). CGRP release therefore, is a useful indicator of functional activation of primary sensory neurons.

Furthermore, it is also widely known that post-translational modifications of thermo-transducer channels can significantly alter neuronal response properties. For instance, phosphorylation of TRPV1 at serine or threonine amino acid residues, results in transducer sensitisation that leads to exaggerated responses to subsequent noxious stimuli (Numazaki *et al.*, 2002, Zhang and McNaughton, 2006, Jeske *et al.*, 2008, Studer and McNaughton, 2010). Many inflammatory mediators such as, NGF, bradykinin, prostaglandins, brain-derived neurotrophic factor (BDNF), GDNF and TNFα are known to be responsible for triggering the phosphorylation and sensitisation of TRPV1 (Shu and Mendell, 1999, 2001, Bonnington and McNaughton, 2003a, Price *et al.*, 2005, Huang *et al.*, 2006b, Zhu and Oxford, 2007, Khan *et al.*, 2008, Schmutzler *et al.*, 2009). One consequence of TRPV1 sensitisation by inflammatory mediators has been the demonstration of an increased release of CGRP following exposure of neurons to the TRPV1 agonist capsaicin. Hence, TNFα, BDNF and GDNF have all been shown to increase levels of capsaicin-evoked CGRP release (Price *et al.*, 2005, Khan *et al.*, 2008, Schmutzler *et al.*, 2009).

Only a minority of studies have investigated the functional outcome of IL-6-receptor activation in sensory neurons, either in terms of direct neuronal activation or sensitisation to subsequent stimuli. Using behavioural outcome measures, IL-6 has been shown to decrease paw withdrawal latencies to heat stimulation in mice, and to decrease withdrawal latencies to both mechanical and heat stimulation in rats (Andratsch *et al.*, 2009, Vardanyan *et al.*, 2010). Furthermore, *in vitro* studies have

demonstrated that IL-6 increases thermal hyperalgesia, decreases thermal threshold and increases CAPS-evoked inward currents and augments CGRP release (Oprée and Kress, 2000, Obreja *et al.*, 2002, Obreja *et al.*, 2005, Andratsch *et al.*, 2009, Vardanyan *et al.*, 2010). All these studies have addressed activation and sensitisation of sensory neurons in the somatosensory system. To our knowledge, no studies to date have investigated the effect of IL-6 on TRPV1 sensitisation within the rat TG.

The cellular mechanisms underlying TRPV1 sensitisation by inflammatory mediators remain unclear. However, protein kinase C (PKC) and more particularly, PKCδ, are believed to have key roles in the potentiation of TRPV1 activity and in regulating the IL-6 signalling pathway (Jain *et al.*, 1999, Schuringa *et al.*, 2001, Vellani *et al.*, 2001, Novotny-Diermayr *et al.*, 2002, Bhave *et al.*, 2003, Obreja *et al.*, 2005, Honan and McNaughton, 2007, Andratsch *et al.*, 2009, Studer and McNaughton, 2010, Wallerstedt *et al.*, 2010). We have investigated therefore, the effect of IL-6 signalling and possible TRPV1 sensitisation on rat TG neurons. We have used two independent and distinct measures of neuronal excitation and sensitisation. First, we have examined the effect of IL-6 on CAPS-evoked CGRP release by analysing cell supernatant using an *in vitro* enzyme immunoassay. In addition, we have investigated potential signalling pathways involved in IL-6 mediated effects by using the specific PKCδ inhibitor, Rottlerin. Second, we have performed *in vitro* electrophysiological experiments to monitor the functional outcome of capsaicin activation of TG neurons and the modification of responses in the presence of IL-6. Through specific membrane capacitance measurement, these studies have additionally allowed estimation of neuronal cell size and potential functional modality to be made.

5.2. Methods

5.2.1. CGRP release Enzyme Immunoassay

TG cells were cultured as previously described except that four animals were used per 8-well LabTek slide to ensure optimum protein levels. The protein kinase inhibitor Rottlerin, which preferentially inhibits the PKCδ isoenzyme (Gschwendt *et al.*, 1994), was used to investigate a possible role for PKCδ in the sensitisation of TRPV1 following IL-6-evoked downstream activation of PKCδ. TG cells were cultured overnight and culture medium was aspirated and replaced with fresh pre-warmed F12. Different treatments were performed in each of the 8 wells as follows: (1) F12 only; (2) CAPS only; (3) IL-6 only; (4) IL-6+IL-6Rα; (5) CAPS+IL-6; (6) CAPS+IL-6+IL-6Rα; (7) CAPS+IL-6+Rottlerin; (8) CAPS+IL-6+IL-6Rα+Rottlerin (Figure 5-1 C). The timeline for the treatment of cells was as follows and as illustrated in Figure 5-1A. Rottlerin (6 µM, Fisher #32849-0100) was added and cells incubated at 37°C for 30 min. Following this IL-6 (20 ng/ml) ±IL-6Rα (30 ng/ml) was added and cells were incubated at 37°C for 20 min. Capsaicin (CAPS) (30 µM, Sigma #M2028) was then added and cells were incubated for a further 20 min at 37°C. The supernatant was collected and CGRP levels determined by carrying out an enzyme immunoassay (EIA) (CGRP (rat) enzyme immunoassay kit (SPI-bio), Bioquote Ltd #589001). Briefly, samples, standards and controls, all in duplicate, were added to a 96-well plate pre-coated with mouse-anti-CGRP monoclonal antibody. Following this anti-CGRP acetylcholinesterase conjugate was added to each well and the plate was incubated overnight at +4°C. Following several washes, Ellman's Reagent (5,5'-dithiobis-(2-nitrobenzoic acid), 2% w/v in deionized H_2O and 2% v/v wash buffer) was added to all wells and incubated on an orbital shaker for 30

– 60 min protected from light. The plates were read at 405 nm in a Versa Max plate reader using SoftMax Pro software (Molecular Devices). Serial dilutions of a known concentration of CGRP were run in duplicate and used to produce a standard curve for each experiment. Polynomial regression analysis was applied to each standard curve and used to determine unknown concentrations of CGRP from samples. Control experiments were also carried out using TNFα (10 ng/ml, 50 ng/ml, 100 ng/ml, R&D #510-RT) with and without TNFα neutralizing antibody (60 µg/ml, R&D #AF-510-NA) (Figure 5-1 B, C).

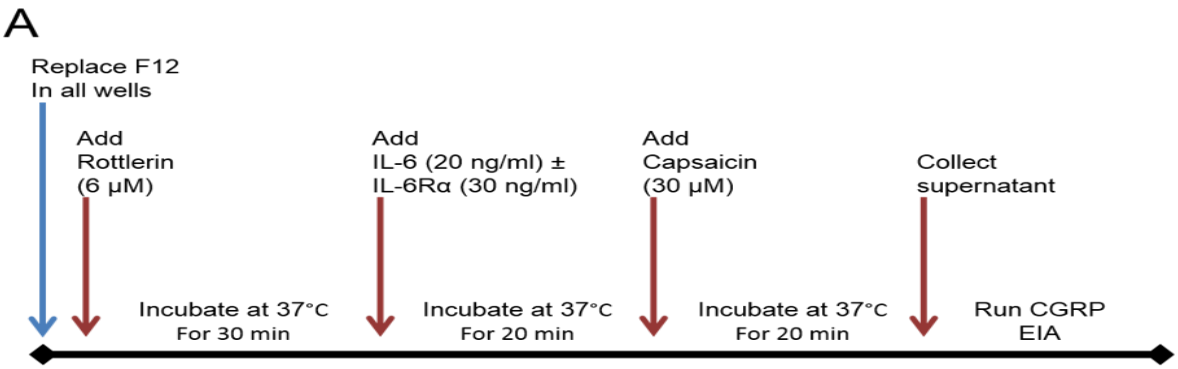

C

8-well LabTek slide				
	Control F12	IL-6	IL-6 + CAPS	IL-6 + CAPS + Rottlerin
	Control CAPS	IL-6 + IL-6Rα	IL-6 + IL-6Rα + CAPS	IL-6 + IL-6Rα + CAPS + Rottlerin

8-well LabTek slide				
	Control F12	TNFα	TNFα + CAPS	TNFα + CAPS + Neutralising Ab
	Control CAPS	TNFα	TNFα + CAPS	TNFα + CAPS + Neutralising Ab

Figure 5-1: (**A-B**) Timelines for treatment of cells prior to CAPS-evoked CGRP-release EIA. TG cells were cultured overnight and treated as follows: (**A**) TNFα with or without TNFα neutralising antibody; (**B**) IL-6 with or without IL-6Rα, in the presence or absence of Rottlerin. (**C**) Example LabTek slides illustrating treatment layout for each experiment.

5.2.2. Electrophysiology

TG neuronal cells were cultured as previously described except that cells were plated onto Melinex (Agar Scientific #L4103). The Melinex sheeting was pre-treated as follows. The Melinex was cut to size, washed X2 in 70% ethanol and rinsed with L15 medium. The Melinex was then pre-coated with poly-D-lysine/laminin and rinsed with sterile water before plating cells. All electrophysiological recordings were carried out at room temperature with an Axopatch 200B amplifier (Axon CNS). The output was digitized with a Digidata 1440A converter (Axon CNS) and was sampled every 5 ms. Data was visualised using Axoscope software. Patch pipettes were pulled on a Narishige 2-stage puller from borosilicate glass capillaries (1.5 mm O.D. X 0.86 mm I.D., Harvard Apparatus #30-0058) and fire polished using a Microforge MF-90. Following overnight incubation, cells were placed into the recording chamber and were continuously superfused (1 ml/min) with physiological solution containing (in mM): 140 NaCl, 5 KCl, 2 $CaCl_2$, 1 $MgCl_2$, 10 D-glucose and 10 HEPES (pH adjusted to 7.4 with NaOH). Single cells were patch clamped in the whole-cell configuration using pipettes with a resistance of 3-5 MΩ when filled with (in mM): 140 KCl, 1 $MgCl_2$, 1 $CaCl_2$, 10 EGTA and 10 HEPES (pH adjusted to 7.3 with KOH). The cells were voltage clamped at holding membrane potential of -60 mV. Series resistance was compensated by >80%. CAPS (10 µM) was delivered via a syringe through a narrow tube located close to the cell. A pulse of solution containing CAPS (200 µl, 2 s) was applied at 1 min intervals. Under these conditions, an habituation of the response to repeated CAPS pulses (tachyphylaxis) was observed. The effect of IL-6 on response tachyphylaxis was examined by pre-treating cells with physiological solution containing IL-6 (20 ng/ml). After 5 min, repeated CAPS pulses at 1 min intervals were applied as before whilst in the presence of IL-6. Cross-sectional areas

of cells were calculated (area = $(\pi)r^2$) following conversion of membrane capacitance to cell diameters using $d = \sqrt{[100 \text{ X } C_m/\pi]}$, where *d* (in micrometers) is cell diameter and C_m (in picofarads) is membrane capacitance (Akopian *et al.*, 2008).

5.3. Results

5.3.1. Effect of cytokines on CAPS-evoked CGRP release

TNFα has previously been shown to directly enhance TRPV1 sensitivity and lead to an increase in CAPS-evoked CGRP release in rat TG (Khan *et al.*, 2008). As a measure of control and to verify the reliability of our assay, we have confirmed these data by carrying out an initial EIA using TNFα at various concentrations (10 ng/ml, 50 ng/ml, 100 ng/ml) with and without TNFα neutralizing antibody (60 µg/ml). Optimal results were achieved using TNFα at 50 ng/ml. Baseline and evoked CGRP concentrations were as follows: basal, 78 pg/ml; CAPS, 140 pg/ml (180% of basal); TNFα, 118 pg/ml (151% of basal); TNFα+CAPS, 330 pg/ml (424% of basal); TNFα+CAPS + neutralising antibody, 218 pg/ml (280% of basal) (Figure 5-2 A-B). Our results demonstrate that exposure of TG neuronal cells to TNFα (50 ng/ml) increased levels of CAPS-evoked CGRP release by 236% over CAPS-only evoked values (n=1). This effect was reduced by the inclusion of a TNFα neutralising antibody (Figure 5-2 A-B).

Further experiments were carried out to determine the effect of IL-6 upon CAPS-evoked CGRP release. Experiments were performed in the presence and absence of the soluble receptor IL-6Rα. Experiments were also performed in the presence and absence of the specific PKCδ inhibitor, Rottlerin (Gschwendt *et al.*, 1994). Baseline and evoked CGRP concentrations were as follows: basal, 78±25 pg/ml; CAPS, 140±47 pg/ml (179±2% of basal); IL-6±IL-6Rα, 79±31 pg/ml (98±6% of basal); IL-6±IL-6Rα+CAPS, 143±48 pg/ml (182±3% of basal); IL-6±IL-6Rα+CAPS+Rottlerin, 140±36 pg/ml (186±12% of basal) (Figure 5-2 C-D). These data show that a

stimulated release of CGRP was detected in the presence of CAPS which was significant from baseline levels (p=<0.01). IL-6±IL-6Rα did not evoke a significant release of CGRP above baseline in the absence of CAPS. Furthermore, CAPS-evoked CGRP release was not significantly altered by IL-6±IL-6Rα pre-treatment or following the inclusion of Rottlerin (Figure 5-2, C, D).

These data suggest that TNFα but not IL-6 evokes a partial sensitisation of TG neurons in terms of the CAPS-mediated release of CGRP (Figure 5-2).

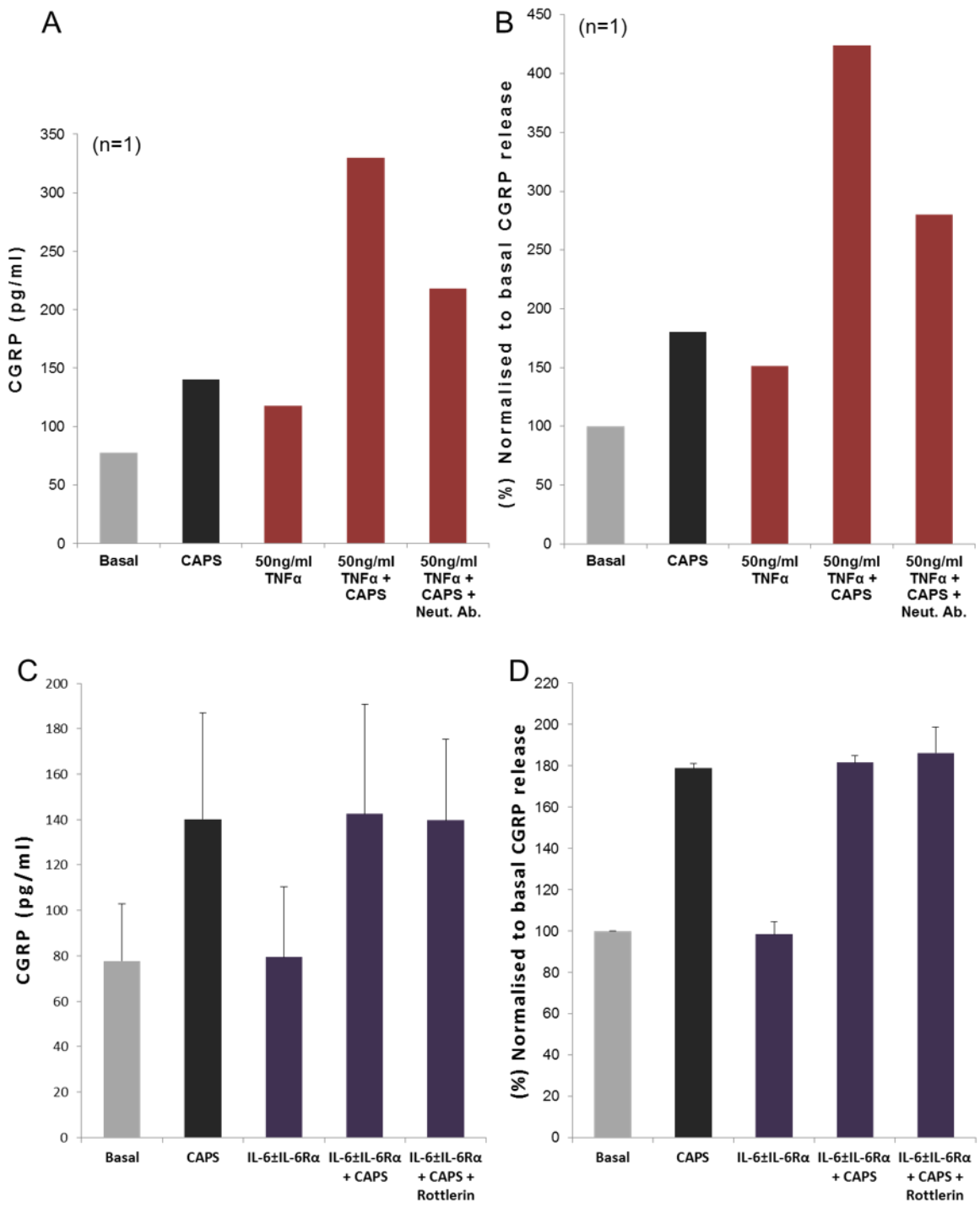

Figure 5-2: Enzyme immunoassay for CAPS-evoked CGRP release. (**A-B**) TG cells were cultured overnight and treated with TNFα (50 ng/ml) ± TNFα neutralising antibody (60 µg/ml). TNF-α enhanced CAPS-evoked CGRP release from 140 pg/ml to 330 pg/ml equivalent to an increase of 236% (n=1). (**C-D**) TG cells were cultured overnight and treated with IL-6 (20 ng/ml) ±IL-6Rα (30 ng/ml) in the presence or absence of Rottlerin (6 µM). Our results show there was no overall effect of treatment with IL-6±IL-6Rα or IL-6±IL-6Rα±Rottlerin upon CAPS-evoked CGRP release (n=3). Bars = +SEM.

5.3.2. Effect of IL-6 on CAPS-evoked electrophysiological responses

Dissociated TG cells were whole-cell clamped and held at a potential of -60 mV. Recordings were made from 31 cells from a total of 5 animals. Membrane capacitance of cells ranged from 8.5 pF to 55 pF which corresponded to cell cross-sectional areas ranging from 211 µm² to 1377 µm². CAPS (10 µM, 2 s) exposure produced an inward current in 58% (18/31) of the cells studied. The mean current amplitude following the first application of CAPS was 686±22 pA (n=18) in responding cells compared to 6.8±2.1 pA (n=13) in non-responding cells. Although the amplitude of the CAPS-evoked current varied considerably among CAPS-responsive cells (range 55 pA to 3800 pA) there was a significant difference in total current between responding and non-responding cells (p=<0.01) (Figure 5-3 A). The mean current density following the first application of CAPS was 34.5±7 pA/pF in responding cells compared to 0.33±0.1 pA/pF in non-responding cells. There was a significant difference in current density between responding and non-responding cells (p=<0.001) (Figure 5-3 B).

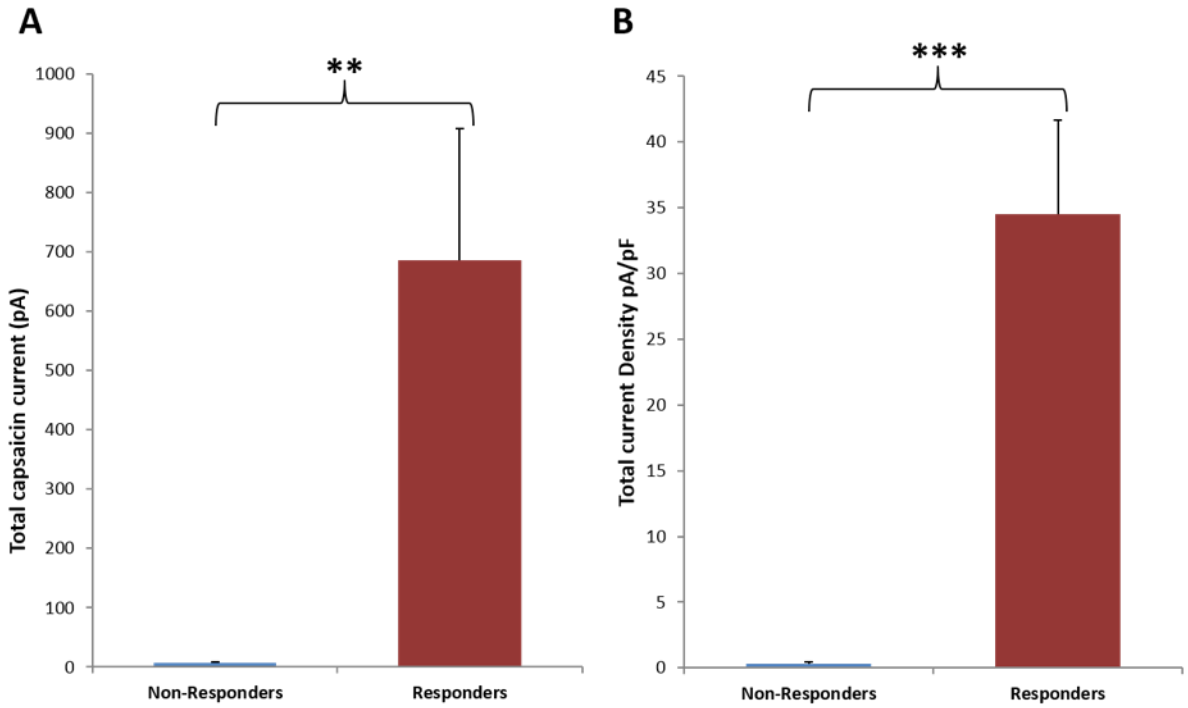

Figure 5-3: TG cells were whole-cell patch clamped at holding membrane potentials of – 60 mV. (**A**) Application of CAPS (10 µM, 2 s) resulted in a mean current amplitude of 6.8±2.1 pA in non-responding cells and 686±22 pA in responding cells. There was a significant difference in current amplitude between non-responding and responding cells (p=<0.01). (**B**) The mean current density was 0.33±0.1 pA/pF in non-responding cells and 34.5±7 pA/pF in responding cells. There was a significant difference in current density between non-responding and responding cells (p=<0.001). Bars = +SEM.

The membrane capacitance and calculated cell size areas of CAPS-responsive and non-responsive cells was further analysed. Membrane capacitance for CAPS-responsive cells ranged from 8.5 pF to 39 pF (n=18) which gave equivalent cell sizes ranging from 211 µm² to 975 µm². Membrane capacitance for CAPS non-responsive cells ranged from 10 pF to 55 pF (n=13) which gave equivalent cell sizes ranging from 250 µm² to 1377 µm² (Figure 5-4 A). There was a significant difference in mean cell size areas between CAPS-responding cells (491±54 µm²) and CAPS non-responding (757±11 µm²) (p=<0.05) (Figure 5-4 B). The proportions of cells within each cell size group (see section 2.3.2) for CAPS-responding and non-responding cells were as follows: small 59% vs. 46%, medium 41% vs. 23%, large nil vs. 31%. These data demonstrate that cells with the highest current density were within the

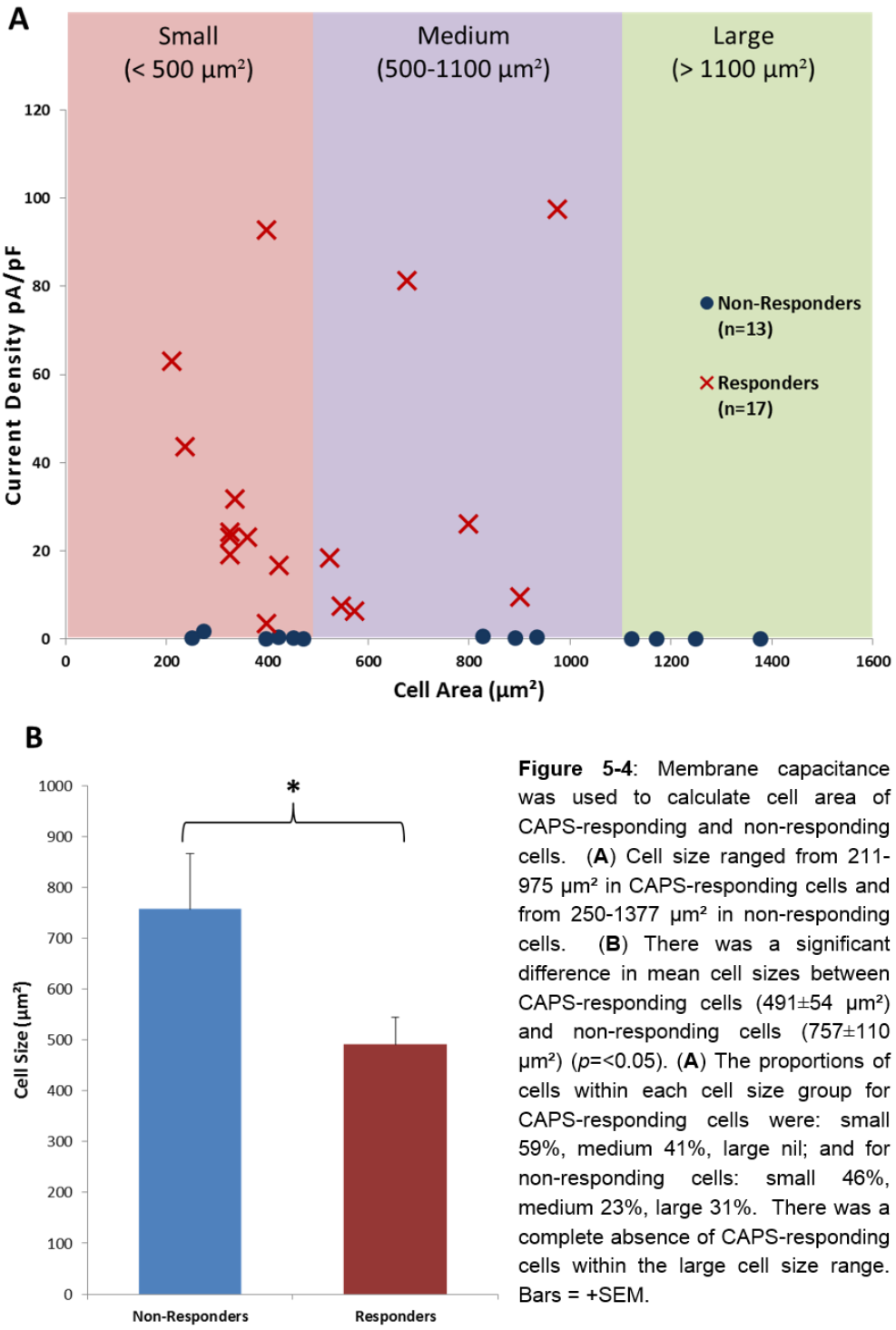

Figure 5-4: Membrane capacitance was used to calculate cell area of CAPS-responding and non-responding cells. (**A**) Cell size ranged from 211-975 µm² in CAPS-responding cells and from 250-1377 µm² in non-responding cells. (**B**) There was a significant difference in mean cell sizes between CAPS-responding cells (491±54 µm²) and non-responding cells (757±110 µm²) (p=<0.05). (**A**) The proportions of cells within each cell size group for CAPS-responding cells were: small 59%, medium 41%, large nil; and for non-responding cells: small 46%, medium 23%, large 31%. There was a complete absence of CAPS-responding cells within the large cell size range. Bars = +SEM.

small and medium cell size range (Figure 5-4 A). In addition, our data show a complete absence of CAPS responsive within the large cell size range whereas CAPS non-responsive cells were represented throughout all cell size ranges (Figure 5-4 A).

In response to repeated applications of CAPS (200 µl, 10 µM, 2 s) at 1 min intervals, tachyphylaxis was clearly demonstrated with a decrease in mean amplitude of the response from 721 pA to 8 pA over 6 successive CAPS applications. The result of repeated CAPS applications to non-responsive cells is also demonstrated for comparison (Figure 5-5 A-C).

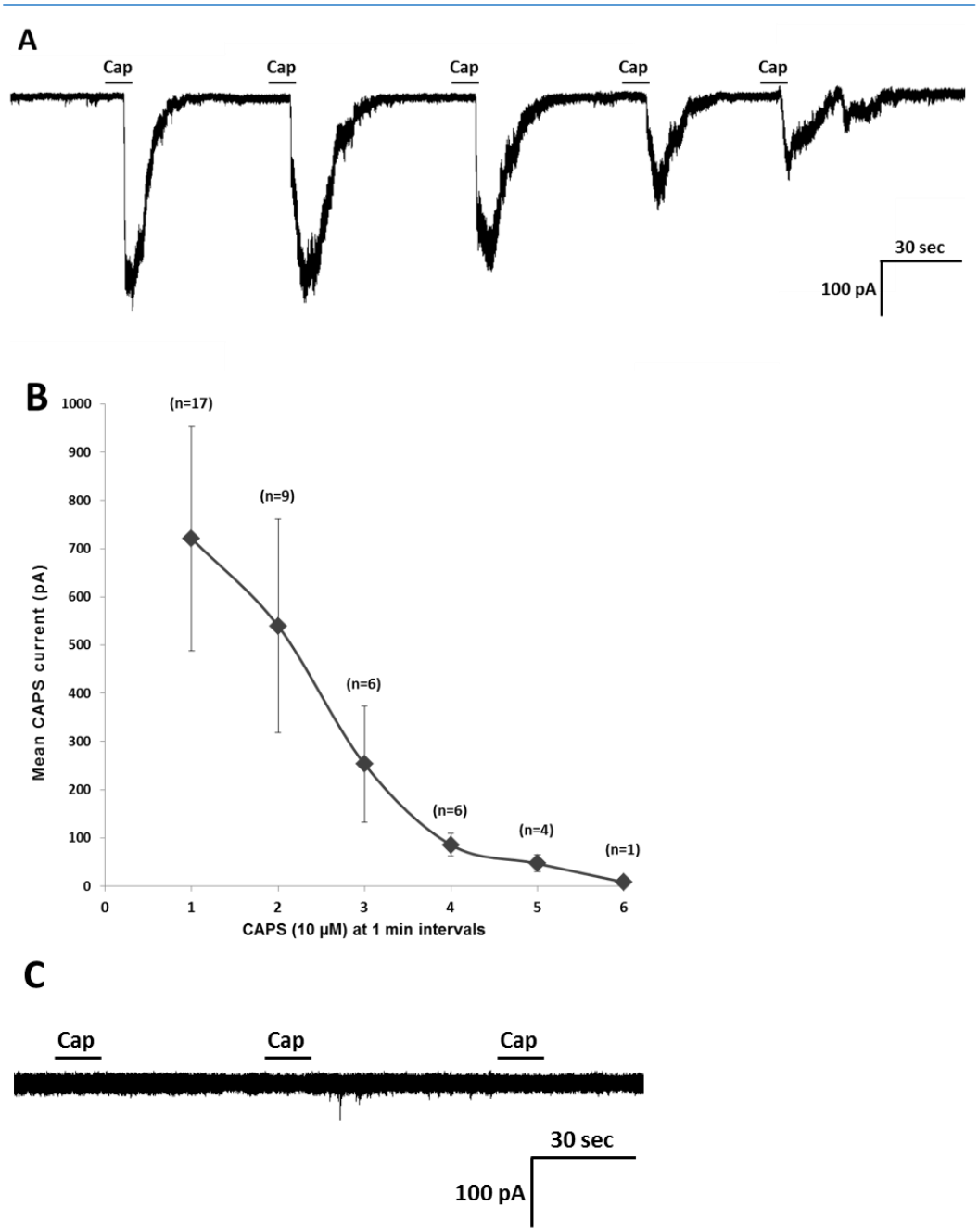

Figure 5-5: (**A**) Typical trace from a CAPS-responsive cell following repeated applications of CAPS (200 µl, 10 µM, 2 s) at 1 min intervals. (**B**) Tachyphylaxis was demonstrated by a decrease in mean CAPS current from 721 pA to 8 pA over 6 successive CAPS applications. (**C**) Typical trace from a CAPS non-responsive cell. Bars = ±SEM.

The effect of IL-6 upon CAPS-evoked tachyphylaxis was examined. An initial application of CAPS (10µM, 2 s) was given to establish that the cell was CAPS-responsive. Cells were then superfused in physiological solution containing IL-6 (20 ng/ml) for 5 min before repeated applications of CAPS at 1 min intervals. Figure 5-6A illustrates responses to successive CAPS applications in the presence or absence of IL-6. Figure 5-6B illustrates these data normalised as a percentage of the initial CAPS current for each cell examined. Our data show that superfusion with IL-6 had no significant effect upon CAPS-evoked tachyphylaxis (Figure 5-6 A-B).

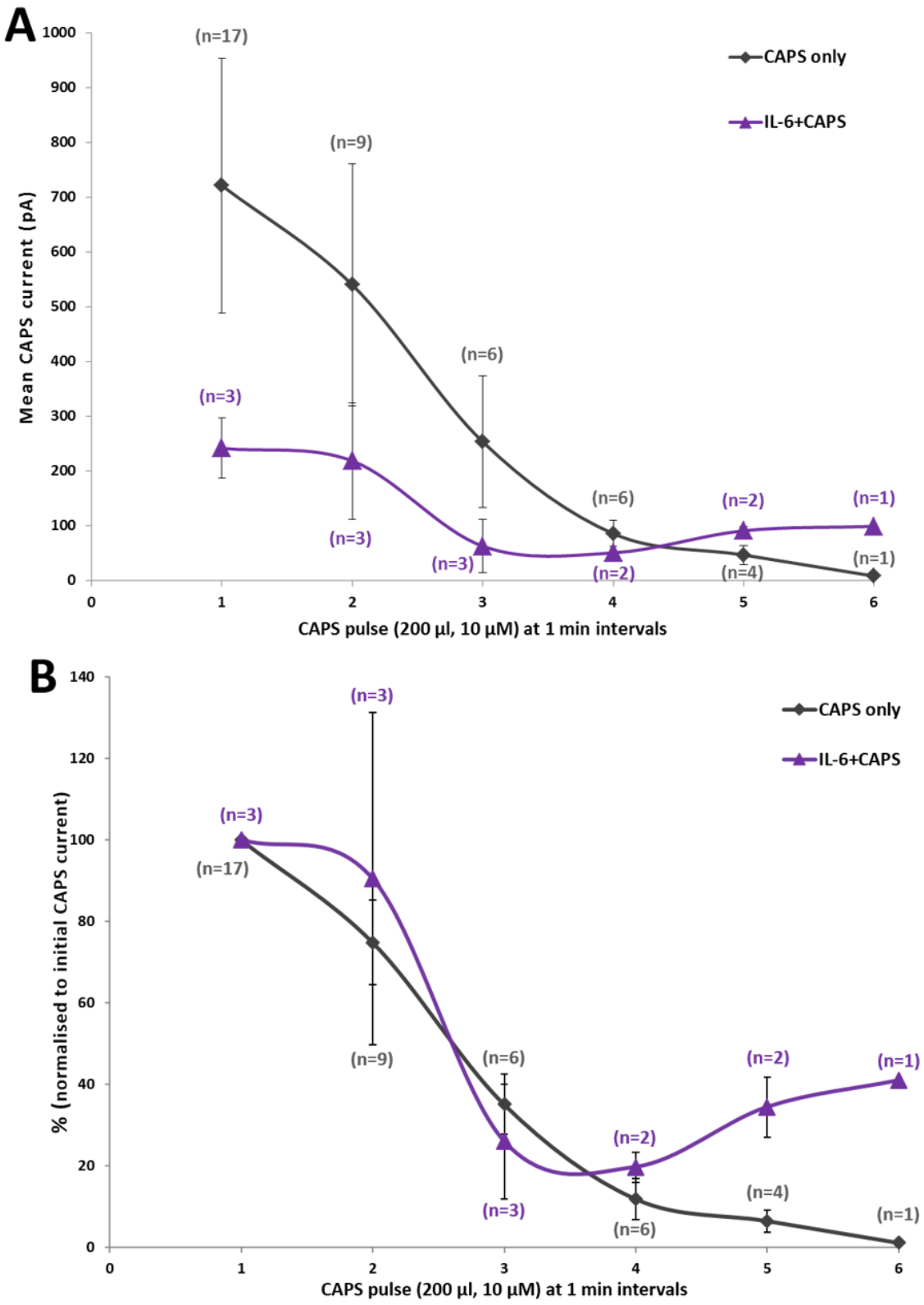

Figure 5-6: Effect of IL-6 on CAPS-induced tachyphylaxis. TG cells were superfused in physiological solution containing IL-6 (20 ng/ml) for 5 min before 6 successive applications of CAPS (200 µl, 10 µM, 2 s) at 1 min intervals. (**A**) Changes in response-amplitude for successive CAPS applications in the presence or absence of IL-6. (**B**) Data represented as % normalised to the initial CAPS current for each cell. IL-6 had no significant effect upon CAPS-evoked tachyphylaxis. Bars = ±SEM.

We further analysed CAPS-evoked current kinetics in the presence or absence of IL-6. Mean recovery time and time-to-peak of CAPS-evoked responses were further analysed. Figure 5-7(A, B) illustrates the typical responses of a cell to a single pulse of CAPS in the presence or absence of IL-6. Mean recovery times were measured from peak current to the time taken for return to baseline current levels. Mean recovery time of CAPS-evoked current was greater in IL-6 treated populations compared to CAPS alone (90.8±35 s vs. 22.9±2 s respectively), however, these values did not reach significance (Figure 5-7 C). Mean time-to-peak of CAPS-evoked current was greater in IL-6 treated populations compared to CAPS alone (44.7±10 s vs. 2.8±0.4 s respectively). These data show that IL-6 significantly increased time-to-peak values of CAPS-evoked current (p=<0.05) (Figure 5-7 D). These data indicate that there is a trend towards IL-6 enhancement of CAPS-evoked total current.

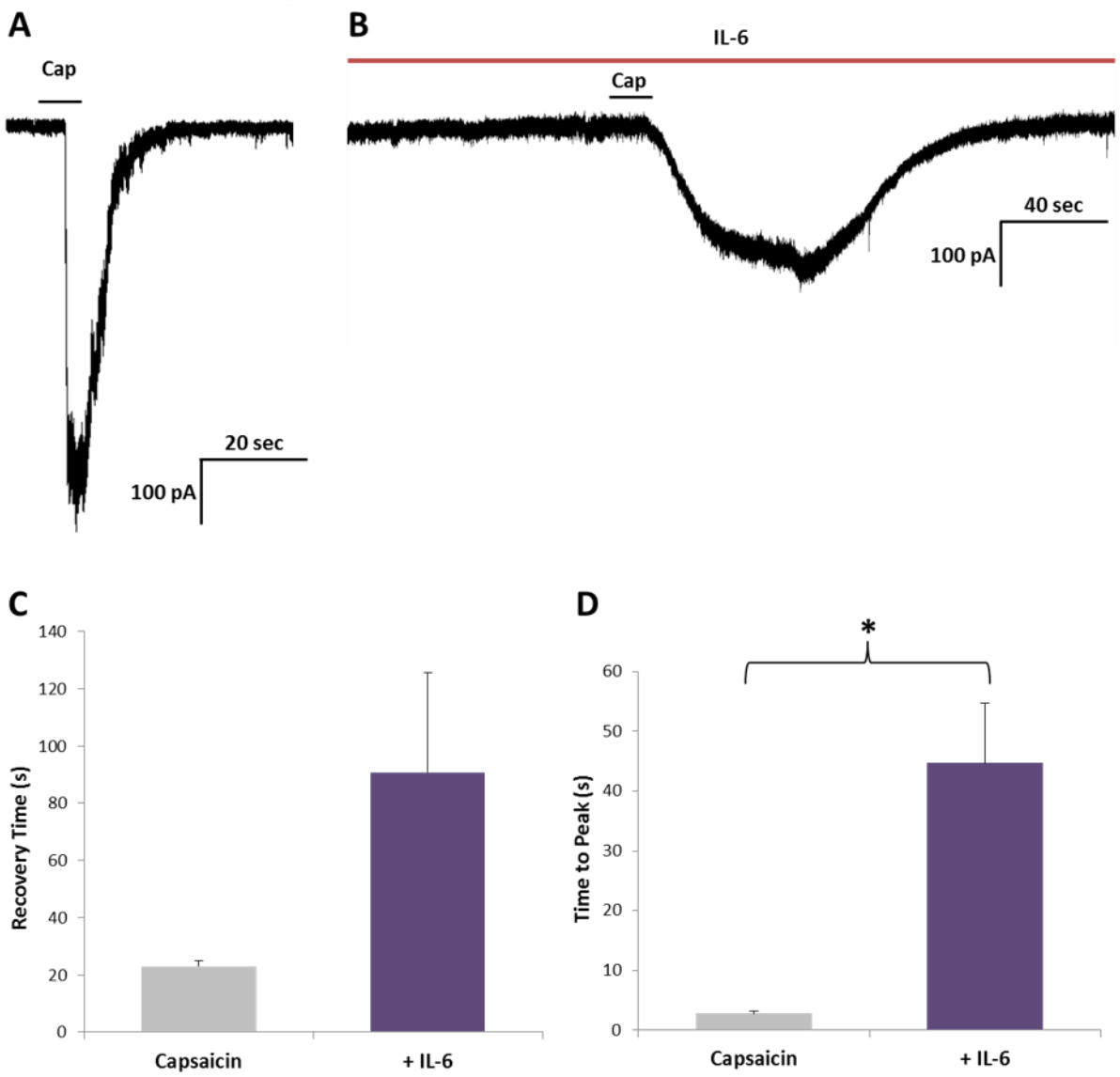

Figure 5-7: Effect of IL-6 on CAPS-evoked current kinetics. (**A**) Typical trace from a CAPS-responsive cell. (**B**) Typical trace from a CAPS-responsive cell in the presence of IL-6. (**C**) Mean recovery time for CAPS and IL-6+CAPS responses was 22.9±2 s and 90.8±35 s respectively. There was no significant difference between these values. (**D**) Mean time to peak for CAPS and IL-6+CAPS responses were 2.8±0.4 s and 44.7±10 s respectively. There was a significant increase in time to peak values in the presence of IL-6 (p=<0.05). Bars = +SEM.

5.3.3. Summary of results

- The levels of CAPS-evoked CGRP release were analysed in the presence or absence of TNFα. TNFα was found to enhance CAPS-evoked CGRP release by >200% (Figure 5-2 A-B).

- The levels of CAPS-evoked CGRP release were analysed in the presence or absence of IL-6±IL-6Rα and in the presence or absence of the PKCδ inhibitor Rottlerin. No effect was seen upon CAPS-evoked CGRP release (Figure 5-2 C-D).

- The mean cell size of CAPS-responding cells was found to be significantly smaller than non-responding cells (p=<0.05). There was a complete absence of CAPS-responding cells within the large cell size range (Figure 5-4 A-B).

- Successive CAPS applications resulted in tachyphylaxis in CAPS-responding cells with a decrease in mean CAPS current from 721 pA to 8 pA over 6 successive CAPS applications (Figure 5-5 A-C).

- IL-6 appeared to have no significant effect on CAPS-induced tachyphylaxis (Figure 5-6 A-B).

- Time-to-peak of CAPS-evoked responses were significantly extended in the presence of IL-6 (p=<0.05). Furthermore, there was a trend towards prolonged recovery time of CAPS-evoked responses in the presence of IL-6. Overall our results demonstrate a significant augmentation of CAPS-evoked current kinetics in the presence of IL-6 (Figure 5-7 A-D).

5.4. Discussion

There is a growing body of evidence to suggest a major role for IL-6 in the development and maintenance of hyperalgesia and chronic pain. Indeed, a correlation has been found between the up-regulation of IL-6 and rising pain intensity in a variety of inflammatory pain states (Verri *et al.*, 2006a, Wang *et al.*, 2009c, Rincon, 2012). IL-6 activates cells by binding to its cognate receptor IL-6Rα and subsequent association with its signal transducing receptor component gp130 (see Heinrich *et al.*, 1998). We have for the first time demonstrated that gp130 receptor protein is ubiquitously expressed throughout the rat TG (see Chapter 3). In addition, we have shown that IL-6 activates the JAK/STAT signalling pathway within subpopulations of TG neuronal cells. Indeed, our data has shown that IL-6 is preferentially activating STAT3 within the NF200+ population of TG neurons (see Chapter 4). One possibility to explain these findings is that although gp130 is ubiquitously expressed, its levels of expression may not be uniformly distributed across all populations of neuronal cells. Alternatively, IL-6 may be activating other signalling cascades within the NF200-negative population, which would require a different outcome measure to STAT3 phosphorylation to be quantified, such as transducer sensitisation.

The cellular mechanisms underlying TRPV1 sensitisation by inflammatory mediators remain unclear, however, a key mediator in the potentiation of TRPV1 activity is thought to be the phosphorylation of serines S502 and S801 on TRPV1 by protein kinase C (PKC) (Vellani *et al.*, 2001, Bhave *et al.*, 2003, Honan and McNaughton, 2007, Studer and McNaughton, 2010). Interestingly, a particular isoenzyme of PKC, PKCδ, has been demonstrated to have a regulatory role in IL-6 signalling via the

JAK/STAT pathway. For instance, PKCδ has been shown to enhance STAT3 dimerisation and nuclear translocation and to maximise transcriptional activity (Schuringa *et al.*, 2001, Novotny-Diermayr *et al.*, 2002, Wallerstedt *et al.*, 2010). Although, one study has suggested a negative regulatory role for PKCδ in inhibiting STAT3 DNA binding and transcriptional activity (Jain *et al.*, 1999). Furthermore, there is evidence to suggest a link between IL-6 evoked activation of PKCδ and sensitisation of TRPV1. For instance, PKCδ was demonstrated to have a key role in enhancing heat hyperalgesia (Obreja *et al.*, 2005). Moreover, a further study has suggested a novel pathway for TRPV1 sensitisation by IL-6 signalling, via cross-talk between PI3K and PKCδ and subsequent phosphorylation of TRPV1 (Andratsch *et al.*, 2009).

We have previously shown that IL-6 is preferentially activating the JAK/STAT signalling pathway in the NF200+ population of TG neurons. Furthermore, we have previously shown that in the TG, TRPV1 expressing neurons are almost entirely NF200-negative (see Chapter 3). Therefore, by investigating the sensitisation of TRPV1 responses, this permits us to analyse functional activation of other signalling pathways by IL-6 in the TRPV1+ (NF200-negative) cell population. We have therefore analysed two potential outcome measurements of the sensitisation of the TRPV1 transducer following cytokine application *in vitro*. First, we have investigated the effect of IL-6 on CAPS-evoked CGRP release as a measure of TRPV1 sensitisation by analysing CGRP levels in supernatant by enzyme immunoassay. In addition, we have investigated a possible role for PKCδ in TRPV1 sensitisation, by including in our experimental protocol the PKCδ inhibitor, Rottlerin. Previous *in vitro* studies have determined TRPV1 sensitisation by inflammatory mediators such as TNFα, BDNF and GDNF, by demonstrating increased release of CGRP following exposure of neurons to the TRPV1 agonist CAPS (Price *et al.*, 2005, Khan *et al.*,

2008, Schmutzler *et al.*, 2009). To our knowledge, only one previous study has investigated the *in vitro* effects of IL-6 on CAPS-evoked CGRP release in neuronal cells. Their results demonstrated a significant augmentation of CAPS-evoked CGRP release in the presence of IL-6 in rat DRG (Vardanyan *et al.*, 2010). Therefore, as far as we are aware, ours is the first study to investigate the effect of IL-6 on CAPS-evoked CGRP release within the rat TG.

Second, we have performed electrophysiological studies to examine the effect of IL-6 on CAPS-evoked responses in rat TG neuronal cells. These studies enabled us examine a further outcome measure and in addition, to incorporate the majority of the TRPV1+ population of TG neuronal cells in our investigation, including those which were CGRP-negative. Previous electrophysiological studies on rat and mice DRG neuronal cells have demonstrated that the presence of IL-6 resulted in the potentiation of heat-evoked and CAPS-evoked inward currents and led to a shift in activation thresholds towards lower temperatures (Obreja *et al.*, 2005, Andratsch *et al.*, 2009). Therefore, to our knowledge, ours is the first electrophysiological study to investigate the effect of IL-6 on CAPS-evoked responses within the rat TG.

Our study on the effect of IL-6 on CAPS-evoked CGRP release, showed that treatment of neuronal cells with CAPS alone resulted in a significant increase in CGRP release above basal levels. However, CAPS-evoked CGRP release was not significantly altered in the presence of IL-6±IL-6Rα or following the inclusion of Rottlerin (Figure 5-2, C, D). IL-6 has been shown previously to augment CAPS-evoked CGRP release *in vitro* in rat DRG (Vardanyan *et al.*, 2010). One hypothesis from our findings is that IL-6 may be activating alternative signalling pathways within the trigeminal nervous system. However, a further possibility to explain the contrasting results could be that in the study on rat DRG, the neuronal cells were

cultured for 4 days as opposed to <24 hours in our study. This may have led to an alteration in neuronal phenotype and possibly an up-regulation of TRPV1 expression due to the presence of growth factors within the media (Bonnington and McNaughton, 2003b) resulting in enhanced CGRP-release. Of interest to our study was their finding that the enhanced release of CGRP by IL-6 did not require the presence of the soluble IL-6Rα (Vardanyan *et al.*, 2010). This is in line with the results from our *in vitro* experiments and would suggest that the soluble receptor was already present under our experimental conditions. This could possibly be due to shedding of the soluble IL-6Rα from satellite glial cells present in the culture (Dubovy *et al.*, 2010). Interestingly, a previous *in vitro* study in mice DRG investigating the effect of IL-6 on CAPS-evoked inward current, also found that the soluble IL-6Rα was not required for the sensitisation of TRPV1 to occur. This is in contrast however, to other behavioural and *in vitro* studies in rat, again using different methodologies to those performed here, which have shown that the presence of the soluble IL-6Rα was required for the TRPV1 sensitisation effects of IL-6 to occur (Oprée and Kress, 2000, Obreja *et al.*, 2005). However, somewhat surprisingly, one study showed that IL-6Rα alone significantly augmented heat-induced CGRP release to the same level as when IL-6 was included in the treatment (Obreja *et al.*, 2002). As mentioned previously, to our knowledge, ours is the first *in vitro* study to investigate the effect of IL-6 on CAPS-evoked CGRP release on rat TG neurons. Clearly more studies need to be undertaken to elucidate the underlying mechanisms by which IL-6 influences neuronal cells both within the somatosensory system and within the trigeminal nervous system. Taken together with previous data, our results suggest an hypothesis, that the effects of inflammatory mediators may differ between the TG and DRG.

Indeed, the results from our electrophysiological experiments go some way towards supporting this hypothesis. As a measure of control, cell size areas were calculated from membrane capacitance values and confirmed the findings of our *in vivo* TRPV1 expression data, in that those cells responding to CAPS, and presumably expressing TRPV1, were limited to the small to medium cell size ranges (see Chapter 3). Furthermore, when analysing mean cell size areas, we found that non-responding cells were significantly larger. Although we were unable to show any significant effect of IL-6 on CAPS-evoked tachyphylaxis, our results do suggest a trend towards unusual tachyphylaxis in the presence of IL-6. We have further examined the effect of IL-6 on CAPS-evoked current kinetics. Interestingly, we found that in the presence of IL-6, CAPS-evoked inward current was significantly prolonged. Whilst previous electrophysiological studies on somatosensory neurons have shown transient potentiation of CAPS-evoked currents (Obreja *et al.*, 2005, Andratsch *et al.*, 2009), our data appear to suggest that within the trigeminal nervous system, IL-6 leads to sensitisation of TRPV1 in a manner that alters the gating properties of this transducer, prolonging the opening time of the channel. These results give weight to our hypothesis that the effects of IL-6 may differ between the somatosensory and trigeminal nervous systems. Indeed, in their behavioural studies, Cuellar and colleagues (2010) found that trigeminal thermonociceptors were distinct from somatic thermonociceptors both in their conduction velocities and thresholds.

There is now a consensus regarding the central role of TRPV1 in mediating thermal hyperalgesia (Rueff and Mendell, 1996, Bennett *et al.*, 1998(a), Caterina *et al.*, 2000, Shu and Mendell, 2001, Bonnington and McNaughton, 2003b, Lewin *et al.*, 2004, Woodbury *et al.*, 2004, Pogatzki-Zahn *et al.*, 2005, Zhang *et al.*, 2005, Yu *et al.*, 2008, Walder *et al.*, 2012, Barcena de Arellano *et al.*, 2013). With this in mind, our data would suggest that IL-6 may be influencing TRPV1+ TG neuronal cells via

alternative signalling pathways to the JAK/STAT pathway such as the MAPK/ERK1/2 or PI3K/Akt pathways. The outcome of which is the sensitisation of TRPV1, enhancing the ability of TG neurons to respond to thermal stimuli. Indeed, an increase in thermal sensitivity has been shown in patients with pulpitis and oral cancer (Hahn *et al.*, 1993, Khabbaz *et al.*, 2000, Nagamine *et al.*, 2006). Furthermore, an upregulation in the expression of TRPV1 has been demonstrated during pulpitis, which would have the effect of exacerbating thermal hyperalgesia (Chung *et al.*, 2011). In addition, the potentiation of TRPV1 activation by IL-6 which we have demonstrated, may contribute to central sensitisation and the development of allodynia.

6. Discussion

The question of how the sensory nervous system interprets the constant barrage of diverse stimuli into clear and discriminatory percepts, has long captivated the interest of many scientific disciplines (Romo and de Lafuente, 2013). In an attempt to help clarify this question, two main theories have been proposed. The specificity theory, originating from studies by German neurophysiologists in the 19th century, suggests that a percept is generated by the activation of specific neuronal pathways, with each sensory modality being processed along fixed specific labelled lines from the periphery to the brain (see Belmonte and Viana, 2008, Ma, 2010). The pattern theory, as exemplified in the gate control theory of pain (Melzack and Wall, 1962, 1965), advocates against specific labelled lines, and in contrast suggests that the ultimate percept results from modulation within the brain of input from a variety of afferent neurons which respond to a multitude of different stimuli (see Ma, 2010).

In an attempt to specify a line-labelled system in primary afferent neurons, it has been the tradition in the field of sensory neurobiology, to classify sensory neurons into functional sub-populations using certain neurochemical, physiological and phenotypic characteristics (see Priestley, 2009). More recently, molecular and transgenic studies have aided in the process of classifying sensory neurons into functionally distinct sub-populations. However, it is now recognised that the use of these classifications as a way of conferring modality specificity is an oversimplification and that the classification of sensory neurons is far more complex than previously thought. Evidence now suggests that a specific repertoire of characteristics and receptor expression patterns, may be a more accurate method of describing modality specificity and to predicting expected percepts following

activation of sensory neurons. Indeed, considering the labile nature of the sensory nervous system, and the formation of transduction complexes which confer considerable plasticity to the sensory neuron (see Frings, 2009), one may question the motivation behind attempting to classify sensory neurons to a specific modality.

Furthermore, large variations between species have been observed in many of the characteristics used to define sensory neuron modality (see Ringkamp and Meyer, 2009). This may have a bigger impact on our understanding of pain mechanisms, since the majority of our knowledge has been derived from studies on the spinal sensory system in rat models. However, an increasing number of studies are using transgenic mice models to investigate mRNA or genes related to pain mechanisms. This will obviously have implications as to the applicability of findings from these studies to those of previous and current studies in rat models. In addition, it has recently been hypothesised that neuronal phenotype and modality may be regulated by the type of tissue being targeted, an hypothesis supported by studies which have observed phenotypic differences in sensory neurons depending on their target innervation (see Frings, 2009, Kiasalari *et al.*, 2010, Hargreaves, 2011).

However, notwithstanding these considerations, and in an attempt to expand the knowledge-base on sensory neurons within the rat trigeminal nervous system, we have carried out an in-depth *in vivo* study investigating neurochemical populations and cell size distributions of sensory neurons within the TG and compared our findings to those within the DRG. In addition, we have carried out a detailed *in vivo* analysis of expression patterns for receptor components of three important inflammatory mediators, NGF, TNFα and IL-6, along with the thermo-transducers TRPV1 and TRPM8. Here again, we have compared our findings from the TG to those from the DRG. Furthermore, we have performed several *in vitro* studies to

investigate the functional implications of IL-6-receptor-activated signalling in TG neuronal cells and the possible sensitisation of TRPV1 in these cells.

6.1. Defining neurochemical properties and functions of TG neurons

The neurofilament NF200 has traditionally been used to define a population of neurons which conduct in the Aα/β fibre range, have large cell bodies and function as non-nociceptors (Michael and Priestley, 1999). The results from our study on NF200 expression within the DRG concur with these accepted classifications. However, our results from the TG have questioned the applicability of these classifications to the trigeminal nervous system. Within the TG we have observed a significantly larger population of NF200+ neurons, and most interestingly, these neurons are enriched in the medium cell size range. The conclusions we can draw from these results are that within the TG, the majority of NF200+ neurons conduct in the Aδ fibre range and therefore, have a higher probability of functioning as nociceptors.

By way of explanation, we know that the tooth pulp is richly innervated in unmyelinated nerve fibres, and that pain is the predominant sensation evoked by pulpal stimuli (Brashear, 1935, Anderson *et al.*, 1970, Mumford and Bowsher, 1976, Johnsen and Johns, 1978, McGrath *et al.*, 1983, Sessle, 1986, Narhi *et al.*, 1994, Nair, 1995, Orchardson and Cadden, 2001, Narhi, 2005). Thus, tooth pulp was thought to be innervated by C fibre nociceptors. However, increasing evidence is suggesting that pulpal afferents originate from myelinated parent axons which taper and lose their myelination as they enter the pulp (Orchardson and Cadden, 2001). This hypothesis is supported by several *in vivo* and *in vitro* studies which have shown pulpal afferents to have larger cells bodies than expected and which are within the medium cell size range, that the parent axons are thinly myelinated Aδ fibres, and

that the conduction velocity of pulpal neurons increases as they leave the pulp and enter the alveolar nerve (Sugimoto *et al.*, 1988, Hildebrand *et al.*, 1995, Lazarov, 2002, Ichikawa *et al.*, 2006, Paik *et al.*, 2009, Fried *et al.*, 2011). Taken together with our results, we have described a novel population of NF200 expressing, Aδ fibre, possibly nociceptive neurons which are enriched within the TG. A proportion of this population may be those neurons with tapering axons and which are functionally adapted to the innervation of tooth pulp. In addition, this enriched population of TG neurons which display an unusual phenotype, may contribute to the distinct response patterns to tissue injury observed within the trigeminal nervous system (see Hargreaves, 2011).

The impact of these findings is even greater when considering our *in vitro* studies. We have shown that IL-6 is preferentially activating TG neuronal cells within the NF200+ population. In addition, we have shown a significantly larger population of NF200+ neurons in the TG compared to the DRG. Since IL-6 is now thought to have a crucial role in the development of mechanical hyperalgesia (Arruda *et al.*, 1998, Anderson and Rao, 2001, Verri *et al.*, 2006b, Manjavachi *et al.*, 2010), and that NF200+ neurons are generally thought to be mechanoreceptors (see McMahon and Priestley, 2005), these findings may in some way explain the prevalence of mechanical hyperalgesia and allodynia occurring in many orofacial pain conditions such as temporomandibular disorders (Anderson and Rao, 2001, Sessle, 2005, Takeda *et al.*, 2005(a), Takeda *et al.*, 2006, Morgan and Gebhart, 2008, Takeda *et al.*, 2008(a), Takeda *et al.*, 2008(b), Takeda *et al.*, 2008(c), Saloman *et al.*, 2013).

Another distinctive feature we have identified within the TG, is the unusual lack of co-expression of CGRP and TrkA. Within the DRG, TrkA and CGRP are almost exclusively co-expressed (Averill *et al.*, 1995, McMahon, 1996). Furthermore,

activation of TrkA by NGF is known to regulate the expression of neuropeptides (Pezet and McMahon, 2006). We have observed within the TG, that <50% of TrkA expressing neurons co-expressed CGRP and conversely, around 40% of CGRP+ neurons were TrkA-negative. These findings suggest that the pro-inflammatory effects following injury-induced upregulation of NGF and subsequent release of CGRP, would be significantly reduced within the trigeminal nervous system.

In addition, our observations would suggest that within the trigeminal nervous system, since we have shown that around half of the neurons expressing TrkA were CGRP-negative, that these neurons may be expressing other neuropeptides such as substance P (SP), somatostatin, vasoactive intestinal polypeptide and galanin (see Priestley, 2009). Possibly, these neuropeptides have a more important role during inflammatory conditions within the trigeminal nervous system than they do in the somatosensory system. Indeed, it has been shown that inflammation within the temporomandibular joint potentiates the excitability of Aβ-fibre neurons and that the resulting allodynia is dependent on the release of SP by TG neurons (Takeda *et al.*, 2005(a), Takeda *et al.*, 2005(b)). Furthermore, activation of TG nociceptors and subsequent release of SP within the VBSNC, has been shown to produce sustained excitation of VBSNC nociceptor terminals (see Sessle, 2000). This may possibly be a result of SP-induced glial cell activation within the VBSNC, which has been demonstrated to facilitate neuronal plasticity (Guo *et al.*, 2007). Further studies investigating co-expression of neurotrophin receptors and neuropeptides such as SP within the trigeminal nervous system, may help to elucidate the neuromodulatory role these molecules have in mediating persistent pain.

Furthermore, the lack of TrkA expression in a substantial proportion of CGRP+ neurons in the TG, seems to suggest that the expression of neuropeptides may be

regulated by a neurotrophin other than NGF in these neurons. One possible candidate would be the regulation of neuropeptide expression by GDNF. The findings from a previous *in vivo* study on rat molar pulp would support this proposal since the majority of pulpal TrkA+ neurons co-expressed GFRα1 (Yang *et al.*, 2006). Within the somatosensory system the populations of nociceptors which respond to NGF and GDNF (TrkA+ and GFRα1/Ret+ respectively) are thought to be distinct populations with different functional properties (Priestley *et al.*, 2002). Our results would suggest that within the trigeminal nervous system, these distinctions are less clear-cut, the functional consequences of which will require further investigation.

This lack of distinction in functional properties between peptidergic and non-peptidergic nociceptors within the TG, may have wider impact on the sensitisation of nociceptors within the trigeminal nervous system. Both NGF and GDNF have been shown to sensitise and increase expression of TRPV1 (see Priestley *et al.*, 2002, Priestley, 2009). In addition, CAPS-evoked responses in IB4+, presumably GDNF responsive neurons, are significantly larger, suggesting that TRPV1 has distinct functional properties within the IB4+ and IB4- populations of nociceptors in DRG (Priestley *et al.*, 2002). Therefore, if IB4+ and IB4- populations are less clearly defined within the TG, it would follow that the distinct functional properties of TRPV1 between neuronal populations observed in the DRG, would also be less clearly defined within the trigeminal nervous system.

These differences may have functional implications and lead to unusual response mechanisms following activation of these neurons by inflammatory mediators within the trigeminal nervous system. Indeed, since we have shown that within the TG a large proportion of neurons express p55 and all neurons express gp130, the downstream sensitisation of TRPV1 by TNFα and IL-6 might result in atypical

responses and pain perception. Furthermore, activation of TRPV1 has been shown to result in the increased release of both TNFα and IL-6 (Sooampon *et al.*, 2013, Yang *et al.*, 2013).

These findings pose an interesting scenario. TRPV1 has recently been shown to be intrinsically heat sensitive (Cao *et al.*, 2013), and is known to play a major role in the mediation of thermal hyperalgesia (Caterina *et al.*, 2000, Bonnington and McNaughton, 2003b). Furthermore, the oral cavity is frequently exposed to a barrage of thermal stressors recently shown to activate TRPV1 (Sooampon *et al.*, 2013). We could hypothesise therefore, that within the oral cavity there is an on-going thermally-induced activation of TRPV1 leading to an increase in the release of potent pro-inflammatory mediators, which in turn, further sensitise TRPV1, possibly via atypical mechanisms. Hence, thermal hyperalgesia within the oral cavity would be potentiated, possibly explaining the increase in thermal sensitivity in patients with conditions such as pulpitis and oral cancer (Hahn *et al.*, 1993, Khabbaz *et al.*, 2000, Nagamine *et al.*, 2006).

The concept of unusual TRPV1 response mechanisms occurring within the trigeminal nervous system, is supported by our *in vitro* investigations on IL-6 mediated TRPV1 sensitisation within TG neuronal cells. We observed significant effects mediated by IL-6 on CAPS-evoked current kinetics. Previous studies on somatosensory neurons observed a transient potentiation of CAPS-evoked currents in DRG cells when in the presence of IL-6 (Obreja *et al.*, 2005, Andratsch *et al.*, 2009). However, we found CAPS-evoked currents to be significantly prolonged, suggesting IL-6 sensitises TRPV1 in a manner that effects the gating properties and kinetics of this thermo-transducer within the trigeminal nervous system.

Taken together, our findings give weight to the recently emerging hypothesis of peripheral regulation of neuronal phenotype (see Hargreaves, 2011), since we have shown several significant differences in neuronal phenotype and function between the TG and DRG in a manner that may reflect the unique areas of innervation found within the orofacial region. The information obtained from our present study, may help to further elucidate the peripheral mechanisms of sensory integration and interpretation within the trigeminal nervous system and may help in the long-term development of more targeted and effective therapeutics for managing orofacial pain.

6.2. Future research plans

6.2.1. Characterisation of changes in neurochemical phenotype and nociceptive marker expression in a model of chronic orofacial hyperalgesia

Several animal models are now available for use in research studies investigating orofacial pain mechanisms. One frequently used orofacial neuropathic pain model is that of chronic constriction injury (CCI) to the infraorbital nerve. This involves tying a single or double ligature of chromic gut loosely around the superior branches of the infraorbital nerve, a procedure which mimics that of CCI to the sciatic nerve for somatosensory studies (Anderson and Rao, 2001, Shubayev and Myers, 2001, Latremoliere *et al.*, 2008). A model of injury to the dentin and pulp cavity allows for the investigation of response mechanisms in a specific subpopulation of trigeminal sensory neurons (Wheeler *et al.*, 1998, Yang *et al*., 2006). Several inflammatory orofacial pain models have been developed which involve the injection of various agents to induce an inflammatory response such as formalin (Lu *et al.*, 2009), turpentine oil (Neubert *et al.*, 2000) and IL-6 (Yan *et al.*, 2012). However, the majority of studies investigating chronic inflammatory mechanisms use complete

Freund's adjuvant (CFA) as a vehicle for inducing chronic inflammatory hyperalgesia. For example, CFA can be injected into the TMJ space (Takeda *et al.,* 2006, Wang *et al*., 2009), facial skin (Takeda *et al.*, 2008(b)) or right upper lip/whisker pad (Morgan and Gebhart, 2008) depending on the orofacial pain condition being studied. Since we wish to investigate the response mechanisms of trigeminal neurons to chronic inflammation, we have decided upon the latter model of CFA-induced chronic orofacial hyperalgesia.

All experiments would be carried out on adult male Sprague Dawley rats. Following sedation, rats would receive an injection of CFA or saline into the right upper lip/whisker pad, lateral to the nostrils (Morgan and Gebhart, 2008) or into the right hind paws (Amaya *et al.*, 2003). Twenty-four hours, 72 hours, 1 week and 2 weeks following treatment, 8 animals would be killed and transcardially perfused and fixed. TG and DRG would be rapidly dissected and prepared for cryosectioning. Indirect dual immunofluorescence to be carried out to investigate changes in expression and binding patterns of neurochemical markers NF200, CGRP and IB4 in TG and DRG in both CFA treated and sham treated animals. For the TG, expression data would be collected from each of the somatotopic areas within the TG corresponding to the ophthalmic, maxillary and mandibular branches of the trigeminal nerve. Following this, indirect dual or triple immunofluorescence would be used to determine changes in expression and co-expression levels of TrkA, p55, TRPV1 and TRPM8 within neurochemically defined neuronal subpopulations of TG and DRG in both CFA treated and sham treated animals. Data analysis would be performed to investigate whether chronic hyperalgesia alters neurochemical phenotype and/or increases or decreases expression levels of nociceptive markers. Comparisons in the responses to CFA would be made between TG and DRG to determine whether sensory neurons within the orofacial region respond differently to those of somatosensory neurons.

The findings from previous studies would suggest increases in expression of TrkA, p55 and TRPV1 may be observed following inflammation. Of particular interest to us in relation to the findings from our current study, is a significant increase observed in TRPV1 expression within the NF200+ subpopulation of DRG neurons following inflammation (Wheeler *et al.*, 1998, Amaya *et al.*, 2003, Sakuma *et al.*, 2007).

6.2.2. The role of neurotrophins NGF and GDNF in regulating neuropeptide expression within the trigeminal and somatosensory nervous systems

We have shown a lack of correlation in the co-expression of TrkA and CGRP in TG neurons. In order to investigate this further, we would carry out indirect dual immunofluorescence on adult male Sprague Dawley rats to analyse expression of the GDNF receptor components GFRα1/2 and Ret along with neuropeptides CGRP and SP within neurochemically defined subpopulations of both TG and DRG. Analysis would be undertaken in the naïve state and following induction of chronic hyperalgesia using CFA as described earlier.

To further analyse the regulation of neuropeptide expression within TG and DRG, primary cell culture of TG and DRG neuronal cells would be carried. Cells would be immunolabelled and sorted by fluorescence-activated cell sorting (FACS) into neurochemically defined subpopulations of NF200+, CGRP+ and IB4+ cells. Following this, cells would be treated with NGF or GDNF for 18 h, 1 day and 2 days post-plating. Analysis of neuropeptide synthesis would be investigated using RT-PCR to determine the regulatory effects of these neurotrophins on expression of CGRP and/or SP mRNA in TG and DRG neuronal cells. In addition, we could determine differential regulatory effects within each neurochemically defined subpopulation of neuronal cells.

In addition, NGF and GDNF have previously been shown to differentially regulate TRPV1 within TrkA+ and IB4+ subpopulations of DRG neuronal cells (Amaya *et al.*, 2004). We would extend this to the TG using FACS to sort primary cell cultures of TG and DRG neuronal cells into TrkA+, IB4+ and NF200+ populations. Following treatment of cells with NGF or GDNF, immunocytochemistry would be carried out to investigate whether exposure of neuronal cells to neurotrophins, changes the expression of TRPV1 preferentially within a particular subpopulation. Amaya *et al.* (2004) showed in DRG an upregulation in expression of TRPV1 by NGF in TrkA+ cells and by GDNF in IB4+ cells. However, since we have shown a lack of correlation of TrkA and neuropeptide expression in the TG, we could hypothesise that the effects of NGF and GDNF may be less clear cut within the trigeminal nervous system.

References

Abe J, Hosokawa H, Okazawa M, Kandachi M, Sawada Y, Yamanaka K, Matsumura K, Kobayashi S (2005) TRPM8 protein localization in trigeminal ganglion and taste papillae. Molecular Brain Research 136:91-98.

Akira S (1997) IL-6-regulated transcription factors. The International Journal of Biochemistry & Cell Biology 29:1401-1418.

Akopian AN, Ruparel NB, Patwardhan A, Hargreaves KM (2008) Cannabinoids Desensitize Capsaicin and Mustard Oil Responses in Sensory Neurons via TRPA1 Activation. J Neurosci 28:1064-1075.

Amaral FA, Sachs D, Costa VV, Fagundes CT, Cisalpino D, Cunha TM, Ferreira SH, Cunha FQ, Silva TA, Nicoli JR, Vieira LQ, Souza DG, Teixeira MM (2008) Commensal microbiota is fundamental for the development of inflammatory pain. Proceedings of the National Academy of Sciences 105:2193-2197.

Amaya F, Oh-hashi K, Naruse Y, Iijima N, Ueda M, Shimosato G, Tominage M, Tanaka Y, Tanaka M (2003) Local inflammation increases vanilloid receptor 1 expression within distinct subgroups of DRG neurons. Brain Research

Amaya F, Shimosato G, Nagano M, Ueda M, Hashimoto S, Tanaka Y, Suzuki H, Tanaka M (2004) NGF and GDNF differentially regulate TRPV1 expression that contributes to development of inflammatory thermal hyperalgesia. European Journal of Neuroscience 20:2303-2310.963: 190-196

Anderson DJ, Hannam AG, Mathews B (1970) Sensory mechanisms in mammalian teeth and their supporting structures. Physiology Reviews 50:171-195.

Anderson LC, Rao RD (2001) Interleukin-6 and nerve growth factor levels in peripheral nerve and brainstem after trigeminal nerve injury in the rat. Archives of Oral Biology 46:633-640.

Andratsch M, Mair N, Constantin CE, Scherbakov N, Benetti C, Quarta S, Vogl C, Sailer CA, Uceyler N, Brockhaus J, Martini R, Sommer C, Zeilhofer HU, Muller

W, Kuner R, Davis JB, Rose-John S, Kress M (2009) A key role for gp130 expressed on peripheral sensory nerves in pathological pain. The Journal of Neuroscience 29:13473-13483.

Arruda JL, Colburn RW, Rickman AJ, Rutkowski MD, DeLeo JA (1998) Increase of interleukin-6 mRNA in the spinal cord following peripheral nerve injury in the rat: potential role of IL-6 in neuropathic pain. Molecular Brain Research 62:228-235.

Austin PJ, Moalem-Taylor G (2010) The neuro-immune balance in neuropathic pain: Involvement of inflammatory immune cells, immune-like glial cells and cytokines. Journal of Neuroimmunology 229:26-50.

Averill S, McMahon SB, Clary DO, Reichardt LF, Priestley JV (1995) Immunocytochemical localisation of TrkA receptors in chemically identified subgroups of adult-rat sensory neurons. European Journal of Neuroscience 7:1484-1494.

Babes A, Ciobanu AC, Neacsu C, Babes R-M (2011) TRPM8, a sensor for mild cooling in mammalian sensory nerve endings. Current Pharmaceutical Biotechnology 12:78-88.

Bae YC, Oh JM, Hwang SJ, Shigenaga Y, Valtschanoff JG (2004) Expression of vanilloid receptor TRPV1 in the rat trigeminal sensory nuclei. The Journal of Comparative Neurology 478:62-71.

Barcena de Arellano ML, Pauly N, Schneider A, Mechsner S (2013) TRPV1-dependent hyperalgesia in peritoneal endometriosis. Brain, Behavior, and Immunity 29, Supplement:S2-S3.

Baron R, Wasner G, Binder A (2012) Chronic pain: genes, plasticity, and phenotypes. The Lancet Neurology 11:19-21.

Basbaum AI, Bautista DM, Scherrer G, Julius D (2009) Cellular and Molecular Mechanisms of Pain. Cell 139:267-284.

Belmonte C, Garcia-Hirschfeld J, Gallar J (1996) Neurobiology of ocular pain. Progress in retina and eye research 16(1): 117-156

Belmonte C, Viana F (2008) Molecular and cellular limits to somatosensory specificity. Molecular Pain 4.

Benarroch EE (2011) CGRP Sensory neuropeptide with multiple neurologic implications. Neurology 77:281-287.

Bennett DLH, Koltzenburg M, Priestley JV, Shelton DL, McMahon SB (1998(a)) Endogenous nerve growth factor regulates the sensitivity of nociceptors in the adult rat. European Journal of Neuroscience 10:1282-1291.

Bennett DLH, Michael GJ, Ramachandran N, Munson JB, Averill S, Yan Q, McMahon SB, Priestley JV (1998(b)) A Distinct Subgroup of Small DRG Cells Express GDNF Receptor Components and GDNF Is Protective for These Neurons after Nerve Injury. J Neurosci 18:3059-3072.

Bereiter DA, Hirata H, Hu JW (2000) Trigeminal subnucleus caudalis: beyond homologies with the spinal dorsal horn. PAIN 88:221-224.

Bereiter DA, Hargreaves KM, Hu JW (2009) Trigeminal mechanisms of nociception: peripheral and brainstem organisation. In: Science of Pain(Basbaum AI and Bushnell MC, eds), pp 435-460 Oxford: Elsevier.

Bergdahl M, Bergdahl J (1999) Burning mouth syndrome: prevalence and associated factors. Journal of Oral Pathology and Medicine 28: 35-354

Bhave G, Hu H-J, Glauner KS, Zhu W, Wang H, Brasier DJ, Oxford G, S., Gereau IV RW (2003) Protein kinase C phosphorylation sensitizes but does not activate the capsaicin receptor transient receptor potential vanilloid 1 (TRPV1). Proceedings of the National Academy of Sciences 100:12480-12485.

Blentic A, Chambers D, Skinner A, Begbie J, Graham A (2010) The formation of the cranial ganglia by placodally-derived sensory neuronal precursors. Molecular and Cellular Neuroscience In Press, Accepted Manuscript.

Bonnington JK, McNaughton PA (2003a) Signalling pathways involved in the senseitisation of mouse nociceptive neurons by nerve growth factor. Journal of Physiology 551:433-446.

Bonnington JK, McNaughton PA (2003b) Signalling pathways involved in the sensitisation of mouse nociceptive neurones by nerve growth factor. The Journal of Physiology 551:433-446.

Bosco R, Alvarado S, Quiroz D, Eblan-Zajjur A (2010) Digital Morphometric Characterization of Lumbar Dorsal Root Ganglion Neurons in Rats. The Journal of Histotechnology 33:113-118.

Bowen EJ, Schmidt TW, Firm CS, Russo AF, Durham PL (2005) Tumor necrosis factor alpha stimulation of calcitonin gene-related peptide expression and secretion from rat trigeminal ganglion neurons. Journal of Neurochemistry 96:65-77.

Brashear AD (1935) The innervation of the teeth. Analysis of nerve fiber components of the pulp and peridental tissues and their probable significance. Journal of Comparative Neurology 64:169-185.

Bullitt E (1991) Somatotopy of spinal nociceptive processing. Journal of Comparative Neurology 312:279-290.

Burton MD, Sparkman NL, Johnson RW (2011) Inhibition of interleukin-6 trans-signaling in the brain inhibits lipopolysaccharide-induced sickness behavior. Brain, Behavior, and Immunity 25:S179-S242.

Cadden SW, Orchardson R (2001) The Neural Mechanisms of Oral and Facial Pain. Dental Update 28:359-367.

Cady RJ, Glenn JR, Smith KM, Durham PL (2011) Calcitonin Gene-Related Peptide promotes cellular changes in trigeminal neurons and glia implicated in peripheral and central sensitization. Molecular Pain 7.

Calvo M, Dawes JM, Bennett DLH (2012) The role of the immune system in the generation of neuropathic pain. The Lancet 11:629-642.

Caminero A, Comabella M, Montalban X (2011) Tumor necrosis factor alpha (TNF-[alpha]), anti-TNF-[alpha] and demyelination revisited: An ongoing story. Journal of Neuroimmunology 234:1-6.

Cao E, Cordero-Morales Julio F, Liu B, Qin F, Julius D (2013) TRPV1 Channels Are Intrinsically Heat Sensitive and Negatively Regulated by Phosphoinositide Lipids. Neuron 77:667-679.

Caterina MJ, Rosen TA, Tominaga M, Brake AJ, Julius D (1999) A capsaicin-receptor homologue with a high threshold for noxious heat. Nature 398:436-441.

Caterina MJ, Leffler A, Malmberg AB, Martin WJ, Trafton J, Petersen-Zeitz KR, Koltzenburg M, Basbaum AI, Julius D (2000) Impaired nociception and pain sensation in mice lacking the capsaicin receptor. Science 288:306-313.

Caterina MJ, Julius D (2001) The vanilloid receptor: a molecular gateway to the pain pathway. Annual Review of Neuroscience 24:487-517.

Ceruti S, Villa G, Fumagalli M, Colombo L, Magni G, Zanardelli M, Fabbretti E, Verderio C, Maagdenberg vdAMJM, Nistri A, Abbracchio MP (2011) Calcitonin gene-related peptide-mediated enhancement of purinergic neuron/glia communication by the algogenic factor bradykinin in mouse trigeminal ganglia from wild-type and R192Q Ca 2.1 knock-in mice: implications for basic mechanisms of migraine pain. The Journal of Neuroscience 31:3638-3649.

Chalaris A, Garbers C, Rabe B, Rose-John S, Scheller J (2011) The soluble Interleukin 6 receptor: Generation and role in inflammation and cancer. European Journal of Cell Biology 90:484-494.

Chaudhary P, Martenson ME, Baumann TK (2001) Vanilloid Receptor Expression and Capsaicin Excitation of Rat Dental Primary Afferent Neurons. Journal of Dental Research 80:1518-1523.

Chen J, Joshi SK, DiDomenico S, Perner RJ, Mikusa JP, Gauvin DM, Segreti JA, Han P, Zhang X-F, Niforatos W, Bianchi BR, Baker SJ, Zhong C, Simler GH, McDonald HA, Schmidt RG, McGaraughty SP, Chu KL, Faltynek CR, Kort ME, Reilly RM, Kym PR (2011) Selective blockade of TRPA1 channel attenuates pathological pain without altering noxious cold sensation or body temperature regulation. PAIN 152:1165-1172.

Cho H-J, Staikopoulos V, Ivanusic JJ, Jennings EA (2009a) Hyperpolarization-activated cyclic-nucleotide gated 4 (HCN4) protein is expressed in a subset of rat dorsal root and trigeminal ganglion neurons. Cell and Tissue Research 338:171-177.

Cho H-J, Staikopoulos V, Furness JB, Jennings EA (2009b) Inflammation-induced increase in hyperpolarization-activated, cyclic nucleotide-gated channel protein in trigeminal ganglion neurons and the effect of buprenorphine. Neuroscience 162:453-461.

Chung M-K, Lee J, Duraes G, Ro JY (2011) Lipopolysaccharide-induced Pulpitis Up-regulates TRPV1 in Trigeminal Ganglia. Journal of Dental Research 90:1103-1107.

Chung YL, Lee MY, Wang AJ, Yao LF (2003) A therapeutic strategy uses histone deacetylase inhibitors to modulate the expression of genes involved in the pathogenesis of rheumatoid arthritis. Molecular Therapy 8:707-717.

Colvin L (2006) Theories of Pain. In: Anaesthesia Science(Webster NR and Galley HF, eds), pp 343-362 Aberdeen: Blackwell Publishing.

Costigan M, Woolf CJ (2000) Pain: Molecular Mechanisms. The Journal of Pain 1:35-44.

Costigan M (2012) Pain's peptide signature. PAIN 153:509-510.

Coutaux A, Adam F, Willer J-C, Bars DL (2005) Hyperalgesia and allodynia: peripheral mechanisms. Joint Bone Spine 72:359-371.

Craig AD (2003) Pain mechanisms: labeled lines versus convergence in central processing. The Annual Review of Neuroscience 26:1-30.

Cuellar J, Manering N, Klukinov M, Nemenov M, Yeomans D (2010) Thermal nociceptive properties of trigeminal afferent neurons in rats. Molecular Pain 6:39.

Cunha FQ (1992) The pivotal role of tumour necrosis factor alpha in the development of inflammatory hyperalgesia. British Journal of Pharmacology 107:660.

Cunha TM, Verri Jr WA, Valério DA, Guerrero AT, Nogueira LG, Vieira SM, Souza DG, Teixeira MM, Poole S, Ferreira SH, Cunha FQ (2008) Role of cytokines in mediating mechanical hypernociception in a model of delayed-type hypersensitivity in mice. European Journal of Pain 12:1059-1068.

D'Amico-Martel A, Noden DM (1983) Contributions of placodal and neural crest cells to avian cranial peripheral ganglia. American Journal of Anatomy 166:445-468.

De Simone R, Alleva E, Tirassa P, Aloe L (1990) Nerve growth factor released into the bloodstream following intraspecific fighting induces mast cell degranulation in adult male mice. Brain, Behavior, and Immunity 4:74-81.

del Camino D, Murphy S, Heiry M, Barrett LB, Earley TJ, Cook CA, Petrus MJ, Zhao M, D'Amours M, Deering N, Brenner GJ, Costigan M, Hayward NJ, Chong JA, Fanger CM, Woolf CJ, Patapoutian A, Moran MM (2010) TRPA1 Contributes to Cold Hypersensitivity. The Journal of Neuroscience 30:15165-15174.

Dhaka A, Earley TJ, Watson J, Patapoutian A (2008) Visualizing Cold Spots: TRPM8-Expressing Sensory Neurons and Their Projections. The Journal of Neuroscience 28:566-575.

Djouhri L, Lawson SN (2004) A[beta]-fiber nociceptive primary afferent neurons: a review of incidence and properties in relation to other afferent A-fiber neurons in mammals. Brain Research Reviews 46:131-145.

Dmitrieva N, McMahon SB (1996) Sensitisation of visceral afferents by nerve growth factor in the adult rat. International Association for the Study of Pain 66:87-97.

Dray A (2005) Pharmacology of Inflammatory Pain. In: The Paths of Pain(Merskey H, Loeser, J.D. and Dubner, R, ed), pp 177-190 Seattle: IASP.

Drummond HA, Furtado MM, Myers S, Grifoni S, Parker KA, Hoover A, Stec DE (2006) ENaC proteins are required for NGF-induced neurite growth. American Journal of Physiology - Cell Physiology 290:C404-C410.

Dubovy P, Klusakova I, Svizenska I, Brazda V (2012) Satellite glial cells express IL-6 and corresponding signal-transducing receptors in the dorsal root ganglia of rat neuropathic pain model. Neuron Glia Biology 6(1): 73-83

Duncan D (1934) A relation between axone diameter and myelination determined by measurement of myelinated spinal root fibers. The Journal of Comparative Neurology 60:437-471.

Eftekhari S, Salvatore CA, Calamari A, Kane SA, Tajti J, Edvinsson L (2010) Differential distribution of calcitonin gene-related peptide and its receptor components in the human trigeminal ganglion. Neuroscience 169:683-696.

Fang X, McMullan S, Lawson SN, Djouhri L (2005) Electrophysiological differences between nociceptive and non-nociceptive dorsal root ganglion neurones in the rat in vivo. The Journal of Physiology 565:927-943.

Fang X, Djouhri L, McMullan S, Berry C, Waxman SG, Okuse K, Lawson SN (2006) Intense Isolectin-B4 Binding in Rat Dorsal Root Ganglion Neurons Distinguishes C-Fiber Nociceptors with Broad Action Potentials and High Nav1.9 Expression. J Neurosci 26:7281-7292.

Fehrenbacher JC, Sun XX, Locke EE, Henry MA, Hargreaves KM (2009) Capsaicin-evoked iCGRP release from human dental pulp: a model system fro the study of peripheral neuropeptide secretion in normal healthy tissue. PAIN 144:253-261.

Fernandes ES, Fernandes MA, Keeble JE (2012) The functions of TRPA1 and TRPV1: moving away from sensory nerves. British Journal of Pharmacology 166:510-521.

Flores CM, Leong AS, O. Dussor G, Catherine H-R, Hargreaves KM, Kilo S (2001) Capsaicin-evoked CGRP release from rat buccal mucosa: development of a model system for studying trigeminal mechanisms of neurogenic inflammation. vol. 14, pp 1113-1120: Blackwell Science Ltd.

Fried K, Sessle BJ, Devor M (2011) The paradox of pain from tooth pulp: Low-threshold “algoneurons”? PAIN 152:2685-2689.

Frings S (2009) Primary processes in sensory cells: current advances. Journal of Comparative Physiology A 195:1-19.

Fristad I, Berggreen E, Haug SR (2006) Delta ([delta]) opioid receptors in small and medium-sized trigeminal neurons supporting the dental pulp of rats. Archives of Oral Biology 51:273-281.

Gadient RA, Patterson PH (1999) Leukemia Inhibitory Factor, Interleukin 6, and Other Cytokines Using the GP130 Transducing Receptor: Roles in Inflammation and Injury. Stem Cells 17:127-137.

Gardiner NJ, Cafferty WBJ, Slack SE, Thompson SWN (2002) Expression of gp130 leukaemia inhibitory factor receptor subunits in adult rat sensory neurones: regulation by nerve injury. Journal of Neurochemistry 83:100-109.

Gaspersic R, Kovacic U, Cör A, Skaleric U (2007) Expression of TrkA receptor for neurotrophins in trigeminal neurons innervating the rat gingivomucosal tissue. Neuroscience Letters 418:253-256.

Gerhold KA, Bautista DM (2009) Molecular and Cellular Mechanisms of Trigeminal Chemosensation. Annals of the New York Academy of Sciences 1170:184-189.

Gibbs JL, Melnyk JL, Basbaum AI (2011) Differential TRPV1 and TRPV2 Channel Expression in Dental Pulp. Journal of Dental Research 90:765-770.

Glauben R, Batra A, Fedke I, Zeitz M, Lehr HA, Leoni F, Mascagni P, Fantuzzi G, Dinarello CA, Siegmund B (2006) Histone hyperacetylation is associated with amelioration of experimental colitis in mice. Journal of Immunology 176:5015-5022.

Gold MS, Gebhart GF (2010) Nociceptor sensitization in pain pathogenesis. Nature Medicine 16:1248-1257.

Gould HJ, Gould TN, England JD, Paul D, Liu ZP, Levinson SR (2000) A possible role for nerve growth factor in the augmentation of sodium channels in models of chronic pain. Brain Research 854:19-29.

Gschwendt M, Muller HJ, Kielbassa K, Zang R, Kittstein W, Rincke G, Marks F (1994) Rottlerin, a Novel Protein Kinase Inhibitor. Biochemical and Biophysical Research Communications 199:93-98.

Guo A, Vulchanova L, Wang J, Li X, Elde R (1999) Immunocytochemical localization of the vanilloid receptor 1 (VR1): relationship to neuropeptides, the P2X₃ purinoceptor and IB4 binding sites. European Journal of Neuroscience 11:946 -958.

Guo J, Qiang M, Ludueña RF (2011) The distribution of β-tubulin isotypes in cultured neurons from embryonic, newborn, and adult mouse brains. Brain Research 1420:8-18.

Guo LH, Schluesener HJ (2007) The innate immunity of the central nervous system in chronic pain: the role of Toll-like receptors. Cellular and Molecular Life Sciences 64:1128-1136.

Guo W, Wang H, Watanabe M, Shimizu K, Zou S, LaGraize SC, Wei F, Dubner R, Ren K (2007) Glial-Cytokine-Neuronal Interactions Underlying the Mechanisms of Persistent Pain. J Neurosci 27:6006-6018.

Hahn CL, Falkler WAJ, Minah GE (1993) Correlation between thermal sensitivity and microorganisms isolated from deep carious dentin. Journal of Endodontics 19:26-30.

Hakim AW, Dong X-D, Svensson P, Kumar U, Cairns BE (2009) TNF alpha mechanically sensitizes masseter muscle afferent fibers of male rats. Journal of Neurophysiology 102:1551-1559.

Halliday DA, Zettler C, Rush RA, Scicchitano R, McNeil JD (1998) Elevated nerve growth factor levels in the synovial fluid of patients with inflammatory joint disease. Neurochemical Research 23:919-922.

Hargreaves KM (2011) Orofacial pain. PAIN 152:S25-S32.

Harper AA, Lawson SN (1985) Conduction velocity is related to morphological cell type in rat dorsal root ganglion neurones. The Journal of Physiology 359:31-46.

Harrington AM, Hughes PA, Martin CM, Yang J, Castro J, Isaacs NJ, Blackshaw LA, Brierley SM (2011) A novel role for TRPM8 in visceral afferent function. PAIN 152:1459-1468.

Hayashi T, Kondo T, Ishimatsu M, Yamada S, Nakamura K-i, Matsuoka K, Akasu T (2009) Expression of the TRPM8-immunoreactivity in dorsal root ganglion neurons innervating the rat urinary bladder. Neuroscience Research 65:245-251.

Heijmans-Antonissen C, Wesseldijk F, Munnikes RJ, Huygen FJ, van der Meijden P, Hop WCJ, Hooijkaas H, Zijlstra FJ (2006) Multiplex Bead Array Assay for Detection of 25 Soluble Cytokines in Blister Fluid of Patients with Complex Regional Pain Syndrome Type 1. Mediators of Inflammation 2006.

Heinrich PC, Behrmann I, Müller-Newen G, Schaper F, Graeve L (1998) Interleukin-6-type cytokine signalling through the gp130/Jak/STAT pathway. Biochem J 334:297-314.

Heinrich PC, Behrmann I, Haan S, Hermanns H, M., Muller-Newen G, Schaper F (2003) Principles of interleukin (IL)-6-type cytokine signalling and its regulation. Biochem J 15:1-20.

Henry M, Luo S, Levinson S (2012) Unmyelinated nerve fibers in the human dental pulp express markers for myelinated fibers and show sodium channel accumulations. BMC Neuroscience 13:29.

Hildebrand C, Fried K, Tuisku F, Johansson CS (1995) Teeth and tooth nerves. Progress in Neurobiology 45:165-222.

Hill RG (2001) Molecular basis for the perception of pain. The Neuroscientist 7:282-292.

Hoffman EM, Schechter R, Miller KE (2010) Fixative Composition Alters Distributions of Immunoreactivity for Glutaminase and Two Markers of Nociceptive Neurons, Nav1.8 and TRPV1, in the Rat Dorsal Root Ganglion. J Histochem Cytochem 58:329-344.

Honan SA, McNaughton PA (2007) Sensitisation of TRPV1 in rat sensory neurones by activation of SNSRs. Neuroscience Letters 422:1-6.

Huang J, Zhang X, McNaughton PA (2006a) Inflammatory pain: the cellular basis of heat hyperalgesia. Current Neuropharmacology 4:197-206.

Huang J, Zhang X, McNaughton PA (2006b) Modulation of temperature-sensitive TRP channels. Cell & Developmental Biology 17:638-645.

Hughes JP, Chessell I, Malamut R, Perkins M, Bačkonja M, Baron R, Farrar JT, Field MJ, Gereau RW, Gilron I, McMahon SB, Porreca F, Rappaport BA, Rice F, Richman LK, Segerdahl M, Seminowicz DA, Watkins LR, Waxman SG, Wiech K, Woolf C (2012) Understanding chronic inflammatory and neuropathic pain. Annals of the New York Academy of Sciences 1255:30-44.

Hwang SJ, Min Oh J, Valtschanoff JG (2005) Expression of the vanilloid receptor TRPV1 in rat dorsal root ganglion neurons supports different roles of the receptor in visceral and cutaneous afferents. Brain Research 1047:261-266.

Ichikawa H, Sugimoto T (2001) VR1-immunoreactive primary sensory neurons in the rat trigeminal ganglion. Brain Research 890:184-188.

Ichikawa H, Gouty S, Regalia J, Helke CJ, Sugimoto T (2004) Ca2+/calmodulin-dependent protein kinase II in the rat cranial sensory ganglia. Brain Research 1005:36-43.

Ichikawa H, Yabuuchi T, Jin HW, Terayama R, Yamaai T, Deguchi T, Kamioka H, Takano-Yamamoto T, Sugimoto T (2006) Brain-derived neurotrophic factor-immunoreactive primary sensory neurons in the rat trigeminal ganglion and trigeminal sensory nuclei. Brain Research 1081:113-118.

Ip NY, Nye SH, Boulton TG, Davis S, Taga T, Li Y, Birren SJ, Yasukawa K, Kishimoto T, Anderson DJ (1992) CNTF and LIF act on neuronal cells via shared signaling pathways that involve the IL-6 signal transducing receptor component gp130. Cell 69:1121-1132.

Jääskeläinen SK (2011) Pathophysiology of primary burning mouth syndrome. Clinical Neurophysiology.

Jacobs JS, Miller MW (1999) Expression of nerve growth factor, p75, and the high affinity neurotrophin receptors in the adult rat trigeminal system: evidence for multiple trophic support systems. Journal of Neurocytology 28:571-595.

Jain N, Zhang T, Kee WH, Li W, Cao X (1999) Protein kinase C-delta associates with the phosphorylates Stat3 in an interleukin-6-dependent manner. The Journal of Biological Chemistry 274:24392-24400.

Jeske NA, Diogenes A, Ruparel NB, Fehrenbacher JC, Henry M, Akopian AN, Hargreaves KM (2008) A-kinase anchoring protein mediates TRPV1 thermal hyperalgesia through PKA phosphorylation of TRPV1. PAIN 138:604-616.

Johnsen D, Johns S (1978) Quantitation of nerve fibres in the primary and permanent canine and incisor teeth in man. Archives in Oral Biology 23:825-829.

Jones GW, McLoughlin RM, V.J. H, Parker CR, Williams JD, Malhotra R, Scheller J, Williams AS, Rose-John S, Topley N, Jones SA (2010) Loss of CD4+ T cell IL-6R expression during inflammation underlines a role for IL-6 trans signalling in the local maintenance of Th17 cells. Journal of Immunology 184:2130-2139.

Kasai M, Kumazawa T, Mizumura K (1998) Nerve growth factor increases sensitivity to bradykinin mediated through B2 receptors, in capsaicin-sensitive small neurons cultured from rat dorsal root ganglia. Neuroscience Research 32:231-239.

Kashiba H, Uchida Y, Senba E (2001) Difference in binding by isolectin B4 to trkA and c-ret mRNA-expressing neurons in rat sensory ganglia. Molecular Brain Research 95:18-26.

Kawakami T, Ishihara M, Mihara M (2001) Distribution density of intraepidermal nerve fibers in normal human skin. Journal of Dermatology 28:63-70.

Khabbaz MG, Anastasiadis PL, Sykaras SN (2000) Determination of endotoxins in caries: association with pulpal pain. International Endodontic Journal 33:132-137.

Khan AA, Diogenes A, Jeske NA, Henry MA, Akopian A, Hargreaves KM (2008) Tumor necrosis factor-alpha enhances the sensitivity of rat trigeminal neurons to capsaicin. Neuroscience 155:503-509.

Kiasalari Z, Salehi I, Zhong Y, McMahon SB, Michael-Titus AT, Michael GJ (2010) Identification of perineal sensory neurons activated by innocuous heat. The Journal of Comparative Neurology 518:137-162.

Kim HY, Kim K, Li HY, Chung G, Park C-K, Kim JS, Jung SJ, Lee MK, Ahn DK, Hwang SJ, Kang Y, Binshtok AM, Bean BP, Woolf CJ, Oh SB (2010) Selectively targeting pain in the trigeminal system. PAIN 150:29-40.

Knowlton WM, McKemy DD (2011) TRPM8: from cold to cancer, peppermint to pain. Current Pharmaceutical Biotechnology 12:68-77.

Knowlton WM, Palkar R, Lippoldt EK, McCoy DD, Baluch F, Chen J, McKemy DD (2013) A Sensory-Labeled Line for Cold: TRPM8-Expressing Sensory Neurons Define the Cellular Basis for Cold, Cold Pain, and Cooling-Mediated Analgesia. The Journal Of Neuroscience: The Official Journal Of The Society For Neuroscience 33:2837-2848.

Kobayashi K, Fukuoka T, Obata K, Yamanaka H, Dai Y, Tokunaga A, Noguchi K (2005) Distinct expression of TRPM8, TRPA1, and TRPV1 mRNAs in rat primary afferent neurons with adelta/c-fibers and colocalization with trk receptors. The Journal of Comparative Neurology 493:596-606.

Kobierski LA, Srivastava S, Borsook D (2000) Systemic lipopolysaccharide and interleukin-1[beta] activate the interleukin 6: STAT intracellular signaling pathway in neurons of mouse trigeminal ganglion. Neuroscience Letters 281:61-64.

Krol KM, Stein EJ, Elliott J, Kawaja MD (2001) TrkA-expressing trigeminal sensory neurons display both neurochemical and structural plasticity despite a loss of p75^{NTR} function: responses to normal and elevated levels of nerve growth factor. European Journal of Neuroscience 13:35-47.

Kruger L, Young RF (1981) Specialized features of the trigeminal nerve and its central connections. In: The cranial nerves(Samii M and Jannetta PJ, eds), pp 273-301 Berlin: Springer-Verlag.

Lai HH, Qiu C-S, Crock LW, Morales MEP, Ness TJ, Gereau Iv RW (2011) Activation of spinal extracellular signal-regulated kinases (ERK) 1/2 is associated with the development of visceral hyperalgesia of the bladder. PAIN 152:2117-2124.

Lallemend F, Ernfors P (2012) Molecular interactions underlying the specification of sensory neurons. Trends in neurosciences 35:373-381.

Lam DK, Sessle BJ, Hu JW (2009) Glutamate and capsaicin effects on trigeminal nociception I: Activation and peripheral sensitization of deep craniofacial nociceptive afferents. Brain Research 1251:130-139.

Lane NE, Schnitzer TJ, Birbara CA, Mokhtarani M, Shelton DI, Smith MD, Brown MT (2010) Tanezumab for the treatment of pain from osteoarthritis of the knee. New England Journal of Medicine 363:1521-1531.

Latorre R, Brauchi S, Orta G, Zaelzer C, Vargas G (2007) ThermoTRP channels as modular proteins with allosteric gating. Cell Calcium 42:427-438.

Latremoliere A, Mauborgne A, Masson J, Bourgoin S, Kayser V, Hamon M, Pohl M (2008) Differential implication of proinflammatory sytokine interleukin-6 in the development of cephalic versus extracephalic neuropathic pain in rats. Neurobiology of Disease 28:8489-8501.

Lawson SN, Waddell PJ (1991) Soma neurofilament immunoreactivity is related to cell size and fibre conduction velocity in rat primary sensory neurons. The Journal of Physiology 435:41-63.

Lawson SL (2002) Phenotype and Function of Somatic Primary Afferent Nociceptive Neurones with C-, A delta- or A alpha/beta-Fibres. Experimental Physiology 87:239-244.

Lazarov NE (2002) Comparative analysis of the chemical neuroanatomy of the mammalian trigeminal ganglion and mesencephalic trigeminal nucleus. Progress in Neurobiology 66:19-59.

Lechner SG, Siemens J (2011) Sensory transduction, the gateway to perception: mechanisms and pathology. EMBO Rep 12:292-295.

Lennerz JK, Ruhle V, Ceppa EP, Neuhuber WL, Bunnett NW, Grady EF, Messlinger K (2008) Calcitonin receptor-like receptor (CLR), receptor activity-modifying protein 1 (RAMP1), and calcitonin gene-related peptide (CGRP) immunoreactivity in the rat trigeminovascular system: differences between

peripheral and central CGRP receptor distribution. The Journal of Comparative Neurology 507:1277-1299.

Leoni F, Zaliani A, Bertolini G, Porro G, Pagini P, Pozzi P, Dona G, Fossati G, Sozzani S, Azam T (2002) The antitumor histone deacetylase inhibitor suberoylanilide hydroxamic acid exhibits anti-inflammatory properties via suppression of cytokines. Proceedings of the National Academy of Sciences 99.

Leoni F, Fossati G, Lewis EC, Lee JK, Porro G, Pagini P, Modena D, Moras ML, Pozzi P, Reznikov LL (2005) The histone deacetylase inhibitor ITF2357 reduces production of pro-inflammatory cytokines in vitro and systemic inflammation in vivo. Molecular Medicine 11:1-15.

LeResche L, Drangsholt M (2008) Epidemiology of orofacial pain: prevalence, incidence, and risk factors. In: Orofacial pain: from basic science to clinical management (Sessle BJ, Lavigne GJ, Lund JP, Dubner R, eds) p 13-18 Quintessence Publishing Co Inc: USA.

Lewin GR, Mendell LM (1993) Nerve growth factor and nociception. Trends in neurosciences 16:353-359.

Lewin GR, Lu Y, Park TJ (2004) A plethora of painful molecules. Current Opinion in Neurobiology 14:443-449.

Li Y, Ji A, Weihe E, Schafer MK-H (2004) Cell specific expression and lipopolysaccharide-induced regulation of tumor necrosis factor alpha and TNF receptors in rat dorsal root ganglion. The Journal of Neuroscience 24:9623-9631.

Lindenlaub T, Sommer C (2003) Cytokines in sural nerve biopsies from inflammatory and non-inflammatory neuropathies. Acta Neuropathologica 105:593-602.

Liu M, Oh U, Wood JN (2011a) From transduction to pain sensation: Defining genes, cells, and circuits. PAIN 152:S16-S19.

Liu Y, Ma Q (2011b) Generation of somatic sensory neuron diversity and implications on sensory coding. Current Opinion in Neurobiology 21:52-60.

Lowe EM, Anand P, Terenghi G, Williams-Chestnut RE, Sinicropi DV, Osborne JL (1997) Increased nerve growth factor levels in the urinary bladder of women with idiopathic sensory urgency and interstitial cystitis. British Journal of Urology 79:572-577.

Loyd DR, Sun XX, Locke EE, Salas MM, Hargreaves KM (2012) Sex differences in serotonin enhancement of capsaicin-evoked calcitonin gene-related peptide release from human dental pulp. PAIN 153:2061-2067.

Lu X, Geng X, Zhang L, Zeng Y, Dong H, Yu H (2009) Substance P expression in the distal cerebrospinal fluid-contacting neurons and spinal trigeminal nucleus in formalin-induced orofacial inflammatory pain in rats. Brain Research Bulletin 78:139-144

Lumpkin EA, Caterina MJ (2007) Mechanisms of sensory transduction in the skin. Nature 445:858-865.

Ma Q (2010) Labeled lines meet and talk: population coding of somatic sensations. The Journal of Clinical Investigation 120:3773-3778.

Madrid R, de la Pena E, Donovan-Rodriguez T, Belmonte C, Viana F (2009) Variable Threshold of Trigeminal Cold-Thermosensitive Neurons Is Determined by a Balance between TRPM8 and Kv1 Potassium Channels. The Journal of Neuroscience 29:3120-3131.

Malin SA, Davis BM, Molliver DC (2007) Production of dissociated sensory neuron cultures and considerations for their use in studying neuronal function and plasticity. Nat Protocols 2:152-160.

Manjavachi MN, Motta EM, Marotta DM, Leite DFP, Calixto JB (2010) Mechanisms involved in IL-6-induced muscular mechanical hyperalgesia in mice. PAIN 151:345-355.

Matsuo S, Ichikawa H, Henderson TA, Silos-Santiago I, Barbacid M, Arends JJA, Jacquin MF (2001) trkA modulation of developing somatosensory neurons in oro-facial tissues: tooth pulp fibers are absent in trkA knockout mice. Neuroscience 105:747-760.

Mc Guire C, Beyaert R, van Loo G (2011) Death receptor signalling in central nervous system inflammation and demyelination. Trends in neurosciences 34:619-628.

McGlone F, Reilly D (2010) The cutaneous sensory system. Neuroscience & Biobehavioral Reviews 34:148-159.

McGrath PA, Gracely RH, Dubner R, Heft MW (1983) Non-pain and pain sensations evoked by tooth pulp stimulation. PAIN 15:377-388.

McKemy DD, Neuhausser WM, Julius D (2002) Identification of a cold receptor reveals a general role for TRP channels in thermosensation. Nature 416:52-58.

McMahon SB (1996) NGF as a mediator of inflammatory pain. Philosophical Transactions of the Royal Society 351:431-440.

McMahon SB, Priestley JV (2005) Nociceptor plasticity. In: The Neurobiology of Pain(Hunt S and Koltzenburg M, eds) Oxford: Oxford University Press.

McMahon SB, Malcangio M (2009) Current Challenges in Glia-Pain Biology. Neuron 64:46-54.

Melzack R, Wall PD (1962) On nature of cutaneous sensory mechanisms. Brain 85:331.

Melzack R, Wall PD (1965) Pain Mechanisms: a new theory. Science 150:971-979.

Meng J, Ovsepian SV, Wang J, Pickering M, Sasse A, Aoki KR, Lawrence GW, Dolly JO (2009) Activation of TRPV1 mediates calcitonin gene-related peptide release, which excites trigeminal sensory neurons and is attenuated by a

retargeted botulinum toxin with anti-nociceptive potential. The Journal of Neuroscience 29:4981-4992.

Mense S (2009) Anatomy of Nociceptors. In: Science of Pain(Basbaum AI and Bushnell MC, eds), pp 11-41 Oxford: Academic Press.

Michael GJ, Priestley JV (1999) Differential expression of the mRNA for the vanilloid receptor subtype 1 in cells of the adult rat dorsal root and nodose ganglia and its downregulation by axotomy. Journal of Neuroscience 19:1844-1854.

Michael GJ, Doufexi D (2000) Small bright VR1 cells define a distinct population of sensory neurones in the rat. European Journal of Neuroscience 12:190-208.

Miller RJ, Jung H, Bhangoo SK, White FA (2009) Cytokine and chemokine regulation of sensory neuron function. Handb Exp Pharmacol 194:417-449.

Mizuno M, Kondo E, Nishimura M, Ueda Y, Yoshiya I, Tohyama M, Kiyama H (1997) Localization of molecules involved in cytokine receptor signaling in the rat trigeminal ganglion. Molecular Brain Research 44:163-166.

Moalem G, Tracey DJ (2006) Immune and inflammatory mechanisms in neuropathic pain. Brain Research Reviews 51:240-264.

Molander C, Grant G (1990) On the organisation of cutaneous and muscle nerve projections in the rat lumbar dorsal horn. In: The primary afferent neuron A survey of recent morpho-functional aspects(Zenker W and Neuhuber WL, eds), pp 161-172 New York: Plenum.

Morgan JR, Gebhart GF (2008) Characterization of a Model of Chronic Orofacial Hyperalgesia in the Rat: Contribution of NAV 1.8. The Journal of Pain 9:522-531.

Mori H, Ishida-Yamamoto A, Senba E, Ueda Y, Tohyama M (1990) Calcitonin gene-related peptide containing sensory neurons innervating tooth pulp and buccal mucosa of the rat: an immunohistochemical analysis. Journal of Chemical Neuroanatomy 3:155-163.

Mosconi T, Snider WD, Jacquin MF (2001) Neurotrophin receptor expression in retrogradely labeled trigeminal nociceptors - comparisons with spinal nociceptors. Somatosensory & Motor Research 18:312-321.

Mumford JM, Bowsher D (1976) Pain and protopathic sensibility. A review with particular reference to the teeth. PAIN 2:223-243.

Murata Y, Masuko S (2006) Peripheral and central distribution of TRPV1, substance P and CGRP of rat corneal neurons. Brain Research 1085:87-94.

Nagamine K, Ozaki N, Shinoda M, Asai H, Nishiguchi H, Mitsudo K, Tohnai I, Ueda M, Sugiura Y (2006) Mechanical Allodynia and Thermal Hyperalgesia Induced by Experimental Squamous Cell Carcinoma of the Lower Gingiva in Rats. The Journal of Pain 7:659-670.

Nair PN (1995) Neural elements in dental pulp and dentin. Oral Surgery, Oral Medicine, Oral Pathology, Oral Radiology, and Endodontology 80:710-719.

Narhi M, Yamamoto H, Ngassapa D, Hirvonen T (1994) The neurophysiological basis and the role of inflammatory reactions in dentine hypersensitivity. Archives of Oral Biology 23:23-30.

Narhi MVO (2005) Nociceptors in the Dental Pulp. In: Encyclopedia of Pain(Schmidt RF and Willis WD, eds), pp 1418-1420 New York: Springer.

Neubert JK, Maidment NT, Matsuka Y, Adelson DW, Kruger L, Spigelman I (2000) Inflammation-induced changes in primary afferent-evoked release of substance P within trigeminal ganglia in vivo. Brain Research 871:181-191

Nicholas RS, Winter J, Wren P, Bergmann R, Woolf CJ (1999) Peripheral inflammation increases the capsaicin sensitivity of dorsal root ganglion neurons in a nerve growth factor-dependent manner. Neuroscience 91:1425-1433.

Nicol GD, Lopshire JC, Pafford CM (1997) Tumor Necrosis Factor Enhances the Capsaicin Sensitivity of Rat Sensory Neurons. The Journal of Neuroscience 17:975-982.

Norrsell U, Finger S, Lajonchere C (1999) Cutaneous sensory spots and the “law of specific nerve energies”: history and development of ideas. Brain Research Bulletin 48:457-465.

Novotny-Diermayr V, Zhang T, Gu L, Cao X (2002) Protein kinase C-delta associates with the interleukin-6 receptor subunit glycoprotein (gp) 130 via Stat3 and enhances Stat3-gp130 interaction. The Journal of Biological Chemistry 277:49134-49142.

Numazaki M, Tominaga T, Toyooka H, Tominaga M (2002) Direct phosphorylation of capsaicin receptor VR1 by protein kinase C epsilon and identification fo two target serine residues. The Journal of Biological Chemistry 277:13375-13378.

Obreja O, Schmelz M, Poole S, Kress M (2002) Interleukin-6 in combination with its soluble IL-6 receptor sensitises rat skin nociceptors to heat, in vivo. PAIN 96:57-62.

Obreja O, Biasio W, Andratsch M, Lips KS, Rathee PK, Ludwig A, Rose-John S, Kress M (2005) Fast modulation of heat-activated ionic current by proinfalmmatory interleukin 6 in rat sensory neurons. Brain 128:1634-1641.

Obreja O, Ringkamp M, Turnquist B, Hirth M, Forsch E, Rukwied R, Petersen M, Schmelz M (2011) Nerve growth factor selectively decreases activity-dependent conduction slowing in mechano-insensitive C-nociceptors. PAIN 152:2138-2146.

Oddiah D, Anand P, McMahon SB, Rattray M (1998) Rapid increase of NGF, BDNF and NT-3 mRNAs in inflamed bladder. Neuroreport 9:1455-1458.

Oprée A, Kress M (2000) Involvement of the Proinflammatory Cytokines Tumor Necrosis Factor-α, IL-1β, and IL-6 But Not IL-8 in the Development of Heat

Hyperalgesia: Effects on Heat-Evoked Calcitonin Gene-Related Peptide Release from Rat Skin. The Journal of Neuroscience 20:6289-6293.

Orchardson R, Cadden SW (2001) An update on the physiology of the dentine-pulp complex. Dental Update 28:200-209.

Paik SK, Park KP, Lee SK, Ma SK, Cho YS, Kim YK, Rhyu IJ, Ahn DK, Yoshida A, Bae YC (2009) Light and electron microscopic analysis of the somata and parent axons innervating the rat upper molar and lower incisor pulp. Neuroscience 162:1279-1286.

Pan M, Naftel JP, Wheeler EF (2000) Effects of deprivation of neonatal nerve growth factor on the expression of neurotrophin receptors and brain-derived neurotrophic factor by dental pulp afferents of the adult rat. Archives of Oral Biology 45:387-399.

Patapoutian A, Tate S, Woolf CJ (2009) Transient receptor potential channels: targeting pain at the source. Nature Reviews 8:55-68.

Pei L, Lin C-Y, Dai J-P, Yin G-F (2007) Facial pain induces the alteration of transient receptor potential vanilloid receptor 1 expression in rat trigeminal ganglion. Neuroscience Bulletin 23:92-100.

Peier AM, Moqrich A, Hergarden AC, Reeve AJ, Andersson DA, Story GM, Earley TJ, Dragoni I, McIntyre P, Bevan S, Patapoutian A (2002) A TRP channel that senses cold stimuli and menthol. Cell 108:705-715.

Perl ER (1992) Function of dorsal root ganglion neurons: an overview. In: Sensory neurons: Diversity, Development and Plasticity(Scott SA, ed), pp 3-23 New York: Oxford University Press.

Perl ER (2011) Pain mechanisms: A commentary on concepts and issues. Progress in Neurobiology 94:20-38.

Pezet S, McMahon SB (2006) Neurotrophins: mediators and modulators of pain. Annual Review of Neuroscience 29:507-538.

Pogatzki-Zahn EM, Shimizu I, Caterina M, Raja SN (2005) Heat hyperalgesia after incision requires TRPV1 and is distinct from pure inflammatory pain. PAIN 115:296-307.

Pover CM, Marshall H, Orr J, Coggeshall RE (1992) A method for producing unbiased histograms of neuronal profile sizes. Journal of Neuroscience Methods 49:123-131.

Prescott SA, Ratté S (2012) Pain processing by spinal microcircuits: afferent combinatorics. Current Opinion in Neurobiology 22:631-639.

Price T, Louria M, Candelario-Soto D, Dussor G, Jeske N, Patwardhan A, Diogenes A, Trott A, Hargreaves K, Flores C (2005) Treatment of trigeminal ganglion neurons in vitro with NGF, GDNF or BDNF: effects on neuronal survival, neurochemical properties and TRPV1-mediated neuropeptide secretion. BMC Neuroscience 6:4.

Price TJ, Flores CM (2007) Critical Evaluation of the Colocalization Between Calcitonin Gene-Related Peptide, Substance P, Transient Receptor Potential Vanilloid Subfamily Type 1 Immunoreactivities, and Isolectin B4 Binding in Primary Afferent Neurons of the Rat and Mouse. The Journal of Pain 8:263-272.

Priestley JV, Michael GJ, Averill S, Liu M, Willmott N (2002) Regulation of nociceptive neurons by nerve growth factor and glial cell line derived neurotrophic factor. Canadian Journal Of Physiology And Pharmacology 80:495-505.

Priestley JV (2009) Trophic Factors and their Receptors in Pain Pathways. In: Synaptic Plasticity in Pain (Malcangio M, ed), pp 21-45 London: Springer.

Quarta S, Vogl C, Constantin CE, Ueceyler N, Sommer C, Kress M (2011) Genetic evidence for an essential role of neuronally expressed IL-6 signal transducer gp130 in the induction and maintenance of experimentally induced mechanical hypersensitivity in vivo and in vitro. Molecular Pain 7(1):73

Reichardt LF (2006) Neurotrophin-regulated signalling pathways. Philosophical Transactions of the Royal Society 361:1545-1564.

Reichling DB, Levine JD (2009) Critical role of nociceptor plasticity in chronic pain. Trends in neurosciences 32:611-618.

Reid G, Flonta M (2001) Cold transduction by inhibition of a background potassium conductance in rat primary sensory neurones. Neuroscience Letters 297:171-174.

Rincon M (2012) Interleukin-6: from an inflammatory marker to a target for inflammatory diseases. Trends in Immunology 33:571-577.

Ringkamp M, Meyer RA (2009) Physiology of Nociceptors In: Science of Pain(Basbaum AI and Bushnell MC, eds), pp 97-114 Oxford: Elsevier.

Ritter AM, Lewin GR, Kremer NE, Mendell LM (1991) Requirement for nerve growth factor in the development of myelinated nociceptors in vivo. Nature 350:500-502.

Romo R, de Lafuente V (2013) Conversion of sensory signals into perceptual decisions. Progress in Neurobiology 103:41-75.

Rose-John S (2012) IL-6 trans-signalling via the soluble IL-6 receptor: importance for the pro-inflammatory activities of IL-6. International Journal of Biological Sciences 8(9): 1237-1247

Rueff A, Mendell LM (1996) Nerve growth factor and NT-5 induce increased thermal sensitivity of cutaneous nocicieptors in vitro. Journal of Neurophysiology 76:3593-3596.

Sabsovich I, Guo T-Z, Wei T, Zhao R, Li X, Clark DJ, Geis C, Sommer C, Kingery WS (2008) TNF signaling contributes to the development of nociceptive sensitization in a tibia fracture model of complex regional pain syndrome type I. PAIN 137:507-519.

Sakuma Y, Ohtori S, Miyagi M, Ishikawa T, Inoue G, Doya H, Koshi T, Ito T, Yamashita M, Yamauchi K, Suzuki M, Moriya H, Takahashi K (2007) Up-regulation of p55 TNF alpha-receptor in dorsal root ganglia neurons following lumbar facet joint injury in rats. European Spine Journal 16:1273-1278.

Saloman JL, Chung MK, Ro JY (2013) P2X3 and TRPV1 functionally interact and mediate sensitization of trigeminal sensory neurons. Neuroscience 232:226-238.

Sandkühler J, Gruber-Schoffnegger D (2012) Hyperalgesia by synaptic long-term potentiation (LTP): an update. Current Opinion in Pharmacology 12:18-27.

Sarria I, Ling J, Xu G-Y, Gu JG (2012) Sensory discrimination between innocuous and noxious cold by TRPM8-expressing DRG neurons in rat. Molecular Pain 8.

Schäfers M, Sommer C, Geis C, Hagenacker T, Vandenabeele P, Sorkin LS (2008) Selective stimulation of either tumor necrosis factor receptor differentially induces pain behavior in vivo and ectopic activity in sensory neurons in vitro. Neuroscience 157:414-423.

Schäfers M, Svensson CI, Sommer C, Sorkin LS (2003) Tumor Necrosis Factor-α Induces Mechanical Allodynia after Spinal Nerve Ligation by Activation of p38 MAPK in Primary Sensory Neurons. The Journal of Neuroscience 23:2517-2521.

Scheller J, Chalaris A, Garbers C, Rose-John S (2011(a)) ADAM17: a molecular switch to control inflammation and tissue regeneration. Trends in Immunology 32:380-387.

Scheller J, Chalaris A, Schmidt-Arras D, Rose-John S (2011(b)) The pro- and anti-inflammatory properties of the cytokine interleukin-6. Biochimica et Biophysica Acta (BBA) - Molecular Cell Research 1813:878-888.

Schmutzler BS, Roy S, Hingtgen CM (2009) Glial cell line-derived neurotrophic factor family ligands enhance capsaicin-stimulated release of calcitonin gene-related peptide from sensory neurons. Neuroscience 161:148-156.

Schuringa J-J, Dekker LV, Vellenga E, Kruijer W (2001) Sequential activation of Rac-1, SEK-1/MKK-4, and protein kinase C-delta is required for interleukin-6-induced STAT3 ser-727 phosphorylation and transactivation. The Journal of Biological Chemistry 276:27709-27715.

Schuringa J-J, Jonk L, J.C., Dokter WHA, Vellenga E, Kruijer W (2000) Interleukin-6-induced STAT3 transactivation and Ser727 phosphorylation involves Vav, Rac-1 and the kinase SEK-1/MKK-4 as signal transduction components. Biochem J 347:89-96.

Scully C (2008) Pain. In: Oral and Maxilloficial Medicine London: Elsevier Limited.

Sessle BJ (1986) The Neurobiology of Facial and Dental Pain: Present Knowledge, Future Directions. Journal of Dental Research 66:962-981.

Sessle BJ (2000) Acute and chronic craniofacial pain: brainstem mechanisms of nociceptive transmission and neuroplasticity, and their clinical correlates. Critical Reviews in Oral Biology & Medicine 11:57-91.

Sessle BJ (2005) Orofacial Pain. In: The Paths of Pain(Merskey H, Loeser, J.D. and Dubner, R, ed), pp 131-150 Seattle: IASP.

Sessle BJ, Iwata K, Dubner R (2008) Central nociceptive pathways. In: Orofacial pain: from basic science to clinical management (Sessle BJ, Lavigne GJ, Lund JP, Dubner R, eds) p 35-43 Quintessence Publishing Co Inc: USA.

Shellhammer SB, Gowgiel JM, Gaik GC, Weine FS (1984) Somatotopic organization and trasmedian pathways of the rat trigeminal ganglion. Journal of Dental Research 63:1289-1292.

Sherrington CS (1906) The integrative action of the nervous system. Cambridge: Cambridge University Press.

Shimizu T, Toriumi H, Sato H, Shibata M, Nagata E, Gotoh K, Suzuki N (2007) Distribution and origin of TRPV1 receptor-containing nerve fibers in the dura mater of rat. Brain Research 1173:84-91.

Shinoda M, Asano M, Omagari D, Honda K, Hitomi S, Katagiri A, Iwata K (2011) Nerve growth factor contribution via transient receptor potential vanilloid 1 to ectopic orofacial pain. The Journal of Neuroscience 31:7145-7155.

Shu X, Mendell LM (1999) Nerve growth factor acutely sensitizes the response of adult rat sensory neurons to capsaicin. Neuroscience Letters 274:159-162.

Shu X, Mendell LM (2001) Acute sensitization by NGF of the response of small-diameter sensory neurons to capsaicin. Journal of Neurophysiology 86:2931-2938.

Shubayev VI, Myers RR (2001) Axonal transport of TNF-α in painful neuropathy: distribution of ligand tracer and TNF receptors. Journal of Neuroimmunology 114:48-56

Siemionow M, Gharb BB, Rampazzo A (2011) The Face as a Sensory Organ. Plastic and Reconstructive Surgery Journal 127:652-662.

Simonetti M, Fabbro A, D'Arco M, Zweyer M, Nistri A, Giniatullin R, Fabbretti E (2006) Comparison of P2X and TRPV1 receptors in ganglia or primary culture of trigeminal neurons and their modulation by NGF or serotonin. Molecular Pain 2.

Sixt M-L, Messlinger K, Fischer MJM (2009) Calcitonin gene-related peptide receptor antagonist olcegepant acts in the spinal trigeminal nucleus. Brain 132:3134-3141.

Sommer C, Schmidt C, George A (1998) Hyperalgesia in Experimental Neuropathy Is Dependent on the TNF Receptor 1. Experimental Neurology 151:138-142.

Sooampon S, Phoolcharoen W, Pavasant P (2013) Thermal stimulation of TRPV1 up-regulates TNFα expression in human periodontal ligament cells. Archives of Oral Biology.

Sorkin LS, Xiao WH, Wagner R, Myers RR (1997) Tumour necrosis factor-[alpha] induces ectopic activity in nociceptive primary afferent fibres. Neuroscience 81:255-262.

Spicarova D, Palecek J (2010) Tumor necrosis factor alpha sensitizes spinal cord TRPV1 receptors to the endogenous agonist N-oleoyldopamine. Journal of Neuroinflammation 7.

Stenholm E, Bongenhielm U, Ahlquist M, Fried K (2002) VR1- and VRL-1-like immunoreactivity in normal and injured trigeminal dental primary sensory neurons of the rat. Acta Odontologica Scandinavica 60:72-79.

Story GM, Peier AM, Reeve AJ, Eid SR, Mosbacher J, Hricik TR, Earley TJ, Hergarden AC, Andersson DA, Hwang SW, McIntyre P, Jegla T, Bevan S, Patapoutian A (2003) ANKTM1, a TRP-like channel expressed in nociceptive neurons, is activated by cold temperatures. Cell 112:819-829.

Studer M, McNaughton PA (2010) Modulation of single-channel properties of TRPV1 by phosphorylation. The Journal of Physiology 588:3743-3756.

Su L, Wang C, Yu Y-h, Ren Y-y, Xie K-l, Wang G-l (2011) Role of TRPM8 in dorsal root ganglion in nerve injury-induced chronic pain. BMC Neuroscience 12:120.

Sugimoto T, Takemura M, Wakisaka S (1988) Cell size analysis of primary neurons innervating the cornea and tooth pulp of the rat. PAIN 32:375-381.

Suh K-I, Kim Y-K, Kho H-S (2009) Salivary levels of IL-1[beta], IL-6, IL-8, and TNF-[alpha] in patients with burning mouth syndrome. Archives of Oral Biology 54:797-802.

Svensson P, Wang MW, Dong X-D, Kumar U, Cairns BE (2010) Human nerve growth factor sensitizes masseter muscle nociceptors in female rats. PAIN In Press, Corrected Proof.

Takashima Y, Daniels RL, Knowlton W, Teng J, Liman ER, McKemy DD (2007) Diversity in the neural circuitry of cold sensing revealed by genetic axonal labeling of transient receptor potential melastatin 8 neurons. J Neurosci 27:14147-14157.

Takeda M, Tanimoto T, Nasu M, Ikeda M, Kadoi J, Matsumoto S (2005(a)) Activation of NK1 receptor of trigeminal root ganglion via substance P paracrine mechanism contributes to the mechanical allodynia in the temporomandibular joint inflammation in rats. PAIN 116:375-385.

Takeda M, Tanimoto T, Ikeda M, Nasu M, Kadoi J, Shima Y, Ohta H, Matsumoto S (2005(b)) Temporomandibular joint potentiates the excitabilities of trigeminal root ganglion neurons innervating the facial skin in rats. Journal of Neurophysiology 93:2723-2738.

Takeda M, Tanimoto T, Ikeda M, Nasu M, Kadoi J, Yoshida S, Matsumoto S (2006) Enhanced excitability of rat trigeminal root ganglion neurons via decrease in A-type potassium currents following temporomandibular joint inflammation. Neuroscience 138:621-630.

Takeda M, Kitagawa J, Takahashi M, Matsumoto S (2008(a)) Activation of interleukin-1[beta] receptor suppresses the voltage-gated potassium currents in the small-diameter trigeminal ganglion neurons following peripheral inflammation. PAIN 139:594-602.

Takeda M, Takahashi M, Matsumoto S (2008(b)) Contribution of activated interleukin receptors in trigeminal ganglion neurons to hyperalgesia via satellite glial interleukin-1[beta] paracrine mechanism. Brain, Behavior, and Immunity 22:1016-1023.

Takeda M, Tanimoto T, Nasu M, Matsumoto S (2008(c)) Temporomandibular joint inflammation decreases the voltage-gated K+ channel subtype 1.4-

immunoreactivity of trigeminal ganglion neurons in rats. European Journal of Pain 12:189-195.

Tanimoto T, Takeda M, Nasu M, Kadoi J, Matsumoto S (2005) Immunohistochemical co-expression of carbonic anhydrawe II with Kv1.4 and TRPV1 in rat small-diameter trigeminal ganglion neurons. Brain Research 1044:262-265.

Thompson SWN (2009) Windup in the Spinal Cord. In: Synaptic plasticity in pain (Malcangio M, ed), pp 255-267 London: Springer.

Tominaga M, Caterina MJ (2004) Thermosensation and Pain. Wiley Periodicals Inc 3-12.

Tracey I, Bushnell MC (2009) How Neuroimaging Studies Have Challenged Us to Rethink: Is Chronic Pain a Disease? The Journal of Pain 10:1113-1120.

Vardanyan M, Melemedjian OK, Price TJ, Ossipov MH, Lai J, Roberts E, Boos TL, Deschamps JR, Jacobson AE, Rice KC, Porreca F (2010) Reversal of pancreatitis-induced pain by an orally available, small molecule interleukin-6 receptor antagonist. PAIN 151:257-265.

Vellani V, Mapplebeck S, Moriondo A, Davis JB, McNaughton PA (2001) Protein kinase C activation potentiates gating of the vanilloid receptor VR1 by capsaicin, protons, heat and anandamide. Journal of Physiology 534:813-825.

Verri JWA, Cunha TM, Parada CA, Poole S, Cunha FQ, Ferreira SH (2006a) Hypernociceptive role of cytokines and chemokines: Targets for analgesic drug development? Pharmacology & Therapeutics 112:116-138.

Verri WA, Cunha TM, Parada CA, Wei X-q, Ferreira SrH, Liew FY, Cunha FQ (2006b) IL-15 mediates immune inflammatory hypernociception by triggering a sequential release of IFN-Î³, endothelin, and prostaglandin. Proceedings of the National Academy of Sciences 103:9721-9725.

Vulchanova L, Olson TH, Stone LS, Riedl MS, Elde R, Honda CN (2001) Cytotoxic targeting of isolectin IB4-binding sensory neurons. Neuroscience 108:143-155.

Walder RY, Radhakrishnan R, Loo L, Rasmussen LA, Mohapatra DP, Wilson SP, Sluka KA (2012) TRPV1 is important for mechanical and heat sensitivity in uninjured animals and development of heat hypersensitivity after muscle inflammation. PAIN 153:1664-1672.

Wallerstedt E, Smith U, Andersson CX (2010) Protein kinase C-delta is involved in the inflammatory effect of IL-6 in mouse adipose cells. Diabetologia 53:946-954.

Wang S, Lim G, Mao J, Sung B, Mao J (2009a) Regulation of the trigeminal NR1 subunit expression induced by inflammation of the temporamandibular joint region in rats. PAIN 141:97-102.

Wang S, Lim G, Mao J, Sung B, Mao J (2009b) Regulation of the trigeminal NR1 subunit expression induced by inflammation of the temporomandibular joint region in rats. PAIN 141:97-103.

Wang X-M, Hamza M, Wu T-X, Dionne RA (2009c) Upregulation of IL-6, IL-8 and CCL2 gene expression after acute inflammation: Correlation to clinical pain. PAIN 142:275-283.

Watanabe D, Yoshimura R, Khalil M, Yoshida K, Kishimoto T, Taga T, Kiyama H (1996) Characteristic localization of gp130 (the signal-transducing receptor component used in common for IL-6/IL-11/CNTF/LIF/OSM) in the rat brain. The European Journal of Neuroscience 8:1630-1640.

Weigelt A, Terekhin P, Kemppainen P, Dörfler A, Forster C (2010) The representation of experimental tooth pain from upper and lower jaws in the human trigeminal pathway. PAIN 149:529-538.

Wetmore C, Olson L (1995) Neuronal and nonneuronal expression of neurotrophins and their receptors in sensory and sympathetic ganglia suggest new intercellular trophic interactions. The Journal of Comparative Neurology 353:143-159.

Wheeler EF, Naftel JP, Pan M, von Bartheld CS, Byers MR (1998) Neurotrophin receptor expression is induced in a subpopulation of trigeminal neurons that label by retrograde transport of NGF or Fluoro-gold following tooth injury. Molecular Brain Research 61:23-38.

White FA, Bhangoo SK, Miller RJ (2005) Chemokines: integrators of pain and inflammation. Nat Rev Drug Discov 4:834-844.

Woodbury CJ, Zwick M, Wang S, Lawson JJ, Caterina MJ, Koltzenburg M, Albers KM, Koerber HR, Davis BM (2004) Nociceptors Lacking TRPV1 and TRPV2 Have Normal Heat Responses. J Neurosci 24:6410-6415.

Woolf CJ, Safich-Garabedian B, Ma QP, Crilly P, Winter J (1994) Nerve growth factor contributes to the generation of inflammatory sensory hypersensitivity. Neuroscience 62:327-331.

Woolf CJ, Bennett GJ, Doherty M, Dubner R, Kidd B, Koltzenburg M, Lipton R, Loeser JD, Payne R, Torebjork E (1998) Towards a mechanism-based classification of pain? PAIN 77:227-229.

Woolf CJ, Costigan M (1999(a)) Transcriptional and posttranslational plasticity and the generation of inflammatory pain. Proc Natl Acad Sci 96:7723-7730.

Woolf CJ, Mannion RJ (1999(b)) Neuropathic pain: aetiology, symptoms, mechanisms and management. The Lancet 353:1959-1964.

Woolf CJ (2004) Pain: moving from symptom control toward mechanism-specific pharmacologic management. Physiology in Medicine 140.

Woolf CJ, Ma QP (2007) Nociceptors - noxious stimulus detectors. Neuron 55:353-364.

Woolf CJ (2011) Central sensitization: implications for the diagnosis and treatment of pain. Pain 152:S2-S15

Wotherspoon G, Priestley JV (1999) Expression of the 5-HT1B receptor by subtypes of rat trigeminal ganglion cells. Neuroscience 95:465-471.

Xu J-T, Xin W-J, Zang Y, Wu C-Y, Liu X-G (2006) The role of tumour necrosis factor-alpha in the neuropathic pain induced by lumbar 5 ventral root transection in rat. PAIN 123:306-321.

Yamazaki Y, Ren K, Shimada M, Iwata K (2008) Modulation of paratrigeminal nociceptive neurons following temporomandibular joint inflammation in rats. Experimental Neurology 214:209-218.

Yan J, Melemedjian O, Price T, Dussor G (2012) Sensitization of dural afferents underlies migraine-related behavior following meningeal application of interleukin-6 (IL-6). Molecular Pain 8:6.

Yang H, Bernanke JM, Naftel JP (2006) Immunocytochemical evidence that most sensory neurons of the rat molar pulp express receptors for both glial cell line-derived neurotrophic factor and nerve growth factor. Archives of Oral Biology 51:69-78.

Yang Y, Yang H, Wang Z, Mergler S, Wolosin JM, Reinach PS (2013) Functional TRPV1 expression in human corneal fibroblasts. Experimental Eye Research 107:121-129.

Yilmaz Z, Renton T, Yiangou Y, Zakrzewska J, Chessell IP, Bountra C, Anand P (2007) Burning mouth syndrome as a trigeminal small fibre neuropathy: Increased heat and capsaicin receptor TRPV1 in nerve fibres correlates with pain score. Journal of Clinical Neuroscience 14:864-871.

Yu L, Yang F, Lou H, Liu F-Y, Han J-S, Xing G-G, Wan Y (2008) The role of TRPV1 in different subtypes of dorsal root ganglion neurons in rat chronic inflammatory nociception induced by complete Freund's adjuvant. Molecular Pain 4:61-71.

Zakrzewska JM (2007) Diagnosis and management of non-dental orofacial pain. Dental Update 34:134-139.

Zakrzewska JM (2010) Orofacial pain. British Journal of Anaesthesia 105(2):241-242

Zanjani TM, Sabetkasaei M, Karimian B, Labibi F, Farokhi B, Mossafa N (2010) The attenuation of pain behaviour and serum interleukin-6 concentration by nimesulide in a rat model of neuropathic pain. Scandinavian Journal of Pain 1:229-234.

Zhang X, Blenis J, Li H-C, Schindler C, Chen-Kiang S (1995) Requirement for serine phosphorylation for formation of STAT-promoter complexes. Science 267:1990-1994.

Zhang X, Huang J, McNaughton PA (2005) NGF rapidly increases membrane expression of TRPV1 heat-gated ion channels. The EMBO Journal 24:4211-4223.

Zhang X, McNaughton PA (2006) Why pain gets worse: the mechanism of heat hyperalgesia. Journal of General Physiology 128:491-493.

Zhang X, Kainz V, Burstein R, Levy D (2011) Tumor necrosis factor-[alpha] induces sensitization of meningeal nociceptors mediated via local COX and p38 MAP kinase actions. PAIN 152:140-149.

Zhu W, Oxford GS (2007) Phosphoinositide-3-kinase and mitogen activated protein kinase signalling pathways mediate acute NGF sensitization of TRPV1. Molecular and Cellular Neuroscience 34:689-700.

Zotterman Y (1939) Touch, pain and tickling: an electrophysiological investigation on cutaneous sensory nerves. Journal of Physiology 95:1-28.

Zylka MJ, Rice FL, Anderson DJ (2005) Topographically Distinct Epidermal Nociceptive Circuits Revealed by Axonal Tracers Targeted to Mrgprd. Neuron 45:17-25.